

UCSF

UC San Francisco Electronic Theses and Dissertations

Title

Chemical genetic approaches to study protein kinase signaling pathways

Permalink

<https://escholarship.org/uc/item/0sn1j4nk>

Author

Hertz, Nicholas T.

Publication Date

2013

Peer reviewed|Thesis/dissertation

Chemical genetic approaches to study protein kinase signaling pathways

by

Nicholas T. Hertz

DISSERTATION

Submitted in partial satisfaction of the requirements for the degree of

DOCTOR OF PHILOSOPHY

in

Chemistry and Chemical Biology

in the

GRADUATE DIVISION

of the

UNIVERSITY OF CALIFORNIA, SAN FRANCISCO

Copyright 2013

by

Nicholas T. Hertz

Acknowledgements

I would like to thank Kevan for his support, insight, encouragement and enthusiasm for science. I would also like to thank Al for all of his support and encouragement. My parents were instrumental in me getting to this point and I want to thank them for their continued support and my wife Janel for everything.

Part of this thesis is a reproduction of material previously published, and contains contributions from collaborators listed therein. Chapter 1 is reproduced in part with permission from: Hertz, N.T., Wang, B.T., Allen, J.J., Zhang, C., Dar, A.C., Burlingame, A.L., and Shokat, K.M., Chemical genetic approach for kinase-substrate mapping by covalent capture of thiophosphopeptides and analysis by mass spectrometry, *Current Protocols in Chemical Biology*. 2010, February; 2:(15-36). Chapter 2 is reproduced in part with permission from: Ultanir, S.K.*, Hertz, N.T.*, Li, G., Ge1, W.P., Burlingame, A.L., Pleasure, S.J., Shokat, K.M., Jan, L.Y., and Jan, Y., Chemical genetic identification of NDR1/2 kinase substrates AAK1 and Rabin8 uncovers their roles in controlling dendrite arborization and synapse maturation. *Neuron*. 2012, March 22; 73:1127-42. Chapter 3 is reproduced in part with permission from: Hengeveld, R.C.C.*, Hertz, N.T.*, Vromans, M.J.M., Zhang, C., Burlingame, A.L., Shokat, K.M., Lens, S.M.A., Development of a chemical genetic approach for human Aurora B kinase identifies novel substrates of the chromosomal passenger complex. *Molecular and Cellular Proteomics*. 2012, May 1; 11:47-59. Chapter 4 is reproduced in part with permission from: Hertz, N.T., Berthet, B., Sos, M.L., Thorn, K.S., Burlingame, A.L., Nakamura, K., Shokat, K.M., A neo-substrate that amplifies catalytic activity of Parkinson's disease related kinase PINK1, *Cell*. 2013, August 15; 154:737-747

Chemical genetic approaches to study protein kinase signaling pathways

Nicholas T. Hertz

Kevan M. Shokat

Alma L. Burlingame

Abstract

Protein kinase signaling is fundamental to regulating cellular homeostasis in the in every aspect of life. Protein kinases act by placing a phosphate group on a very specific subset of cellular proteins. The addition of a negative charged group on the surface of a protein can dramatically affect the folding, subcellular localization and activity of substrate proteins. Understanding the kinase responsible for a specific phosphorylation event has proven difficult as there are more than 500 mammalian kinases and greater than 50,000 phospho sites. The Shokat lab has pioneered a technique in which a particular kinase is engineered to accept either a specific inhibitor or modified substrate, which is normally not used by any other kinase. In this thesis we demonstrate the utility of this technique, by demonstrating its application to two important kinases. One of these kinases, NDR, is shown to be important in normal brain development, and we identify novel substrates that act directly downstream of NDR. Additionally, we identify novel targets of the kinase Aurora B, a kinase that is critical to normal chromosome segregation during cell division.

In addition to these well-behaved kinases, we investigate a kinase, PINK1, that proves an exception to normal kinases. We show that PINK1 has the ability to utilize a

kinetin triphosphate (KTP) catalytically better than its endogenous substrate, which we therefore call a neo-substrate. The development of a neo-substrate or new substrate for the kinase PINK1 enhances the cellular activity of the disease-associated allele of PINK1 (G309D), effectively reversing the deleterious effect of the mutation. Since PINK1 is a key element in protection against mitochondrial damage and is genetically linked to Parkinson's Disease, our approach also has immediate therapeutic implications. Typically, overactive kinases such as oncogenic kinases provide the only opportunity for drug development because inhibitors of kinases are the only modality available for regulation of kinases. Therefore we believe this may represent a novel modality to regulate the activity of kinases.

Table of Contents

Chapter 1: Chemical genetic approach for kinase-substrate mapping by covalent capture of thiophosphopeptides and analysis by mass spectrometry

1.1 Abstract	2
1.2 Introduction	2
1.3 Strategic Planning	6
1.3.1 Engineering the kinase	6
1.3.2 Lysate optimization	9
1.3.3 Generating positive control peptides and protein	11
1.6 Commentary	13
1.6.1 Background information	13
1.6.2 Critical parameters	14
1.6.3 Troubleshooting	17
1.6.4 Anticipated results	17
1.6.5 Time considerations	17

Chapter 2: Chemical genetic identification of NDR1/2 kinase substrates AAK1 and Rabin8 uncovers their roles in controlling dendrite arborization and synapse maturation

2.1 Abstract	19
2.2 Introduction	19

2.3 Results	23
2.3.1 NDR1/2 are necessary and sufficient to reduce dendrite branching	23
2.3.2 NDR1/2 control dendritic spine maturation	24
2.3.3 Development and characterization of an analog specific NDR1 construct	28
2.3.4 Chemical genetic identification of NDR1 substrates	31
2.3.5 AAK1 controls dendrite branching in a similar way to NDR1/2	35
2.3.3 Rabin8 is necessary for spine maturation	37
2.4 Discussion	39
2.4.1 NDR1/2, dendrite pruning and tumor-suppressors	40
2.4.2 AAK1 phosphorylation regulates dendrite branching and length	41
2.4.3 Rab8 GEF Rabin8 regulates spine morphogenesis	43
2.4.4 Other candidate substrates of NDR1/2	44
2.4.5 Chemical genetics for kinase substrate identification	45
2.5 Experimental procedures	45
2.5.1 Kinase assays and covalent capture for phosphorylation site ID	45

Chapter 3: Development of a chemical genetic approach for human Aurora B kinase identifies novel substrates of the chromosomal passenger complex

3.1 Abstract	48
3.2 Introduction	49
3.3 Results	52
3.3.1 Human Aurora B does not tolerate mutation of the Leucine 154 gatekeeper	52
3.3.2 Identification of a unique second-site suppressor for the human as Aurora B	54

3.3.3 as-Aurora B mutants are inhibited by low concentrations of NA-PP1 in cells	57
3.3.4 as-Aurora B mutant can thiophosphorylate multiple proteins in cell extracts	59
3.3.5 Identification of Aurora substrates and site of phosphorylation in cell extracts	61
3.3.6 HMGN2 is a mitotic substrate of Aurora B	65
3.3.7 Nuclear excluded Aurora B to identify additional mitotic substrates:	67
4.4 Discussion	70

Chapter 4: A neo-substrate that amplifies catalytic activity of Parkinson's disease related kinase PINK1

4.1 Abstract	76
4.2 Introduction	76
4.3 Results	84
4.3.1 PINK1 accepts N6 modified ATP analog kinetin triphosphate (KTP)	84
4.3.2 KTP is produced in human cells upon treatment with KTP precursor kinetin	88
4.3.3 Kinetin increases phosphorylation of PINK1 substrate anti-apoptotic Bcl-xL	90
4.3.4 Kinetin accelerates Parkin recruitment to depolarized mitochondria	92
4.3.5 Kinetin blocks mitochondrial motility in axons in a PINK1 dependent manner	96
4.3.6 Kinetin decreases apoptosis due to oxidative stress in human derived neurons	98
4.4 Discussion	102
4.5 Experimental Procedures	106
4.5.1 Western blot analysis	106
4.5.2 Expression, purification and enzymatic characterization of PINK1	106
4.5.3 Identification of PINK1 autophosphorylation site by LC/MS/MS	106

4.5.4 Enzymatic production of KMP in vitro	107
4.5.5 HPLC analysis for KTP production in cells	107
4.5.6 Parkin mitochondrial translocation assay	108
4.5.7 Details on automated quantitation of Parkin mitochondrial translocation	108
4.5.8 Mitochondrial motility assay	109
4.5.9 PINK1 shRNA production	110
4.5.10 Dopamine neuron cultures	110
4.5.11 Apoptosis assays and phospho S62 Bcl-xL immunoblot analysis	110

Chapter 5:

5.1 All references in alphabetical order	141
--	-----

List of Figures

Figure 1.1 Thiophosphopeptide purification scheme	4
Figure 1.2 Lysate labeling schematic	7
Figure 1.3 Analog specific allele generality	10
Figure 1.4 Generating and testing positive control peptide	12
Figure 1.5 Kinome wide kinase engineering	15
Figure 2.1 NDR1/2 regulates dendritic branching and arborization	21
Figure 2.2 NDR1/2's role on dendritic spine development	25
Figure 2.3 Design and analysis of NDR AS mutants	27
Figure 2.4 Identification of NDR1's phosphorylation targets by chemical genetics	30
Figure 2.5 Spectra of as-NDR specific phosphopeptides	34
Figure 2.6 Validation of AAK1 and Rabin8 NDR1 phosphorylation sites	36
Figure 2.7 AAK1 affects dendrite branching and length in hippocampal neurons	38
Figure 2.8 Rabin8 affects spine morphogenesis in dissociated hippocampal neurons	42
Figure 3.1 The H250Y mutation rescues kinase activity of Aurora B as mutants	50
Figure 3.2 The as Aurora B mutants are inhibited by PP1 and utilize N6 modified ATP	53
Figure 3.3 Identification of putative Aurora B substrates by covalent capture	56
Figure 3.4 Analysis of the resulting peptides identified by mass spectrometry	58
Figure 3.5 Validation of potential Aurora B phosphorylation sites and substrate	64
Figure 3.6 Scheme for nuclear excluded Aurora B	66
Figure 3.7 Validation of INCENP expression for nuclear excluded Aurora B	68
Figure 4.1 Alignment of PINK1 to typical kinases reveals several large inserts	77

Figure 4.2 Neo-substrate KTP amplifies kinase activity in-vitro	79
Figure 4.3 Optimized PINK1 expression constructs used to express PINK1	81
Figure 4.4 Enzymatic characterization of PINK1 catalytic activity with KTP	83
Figure 4.5 Neo-substrate precursor kinetin can be ribosylated in vitro	85
Figure 4.6 Neo-substrate precursor kinetin is converted to KTP in human cells	87
Figure 4.7 Kinetin stimulates Bcl-xL phosphorylation in a PINK1 dependent manner	89
Figure 4.8 Analysis in HeLa cells reveals kinetin accelerates Parkin recruitment	91
Figure 4.9 Quantitative analysis of Parkin recruitment in HeLa cells	93
Figure 4.10 Automated quantitation reveals kinetin accelerates Parkin recruitment	95
Figure 4.11 Kinetin stimulates PINK1 dependent phosphorylation of Parkin	97
Figure 4.12 Kinetin halts axonal mitochondrial motility in a PINK1 dep manner	99
Figure 4.13 Kinetin inhibits Caspase 3/7 cleavage in a PINK1 dep manner	101
Figure 4.14 Kinetin inhibits stress induced apoptosis in HeLa cells	103

List of Tables

Table 3.1 Overview of Aurora B specific phosphopeptides	60
Table 3.2 Novel putative Aurora B substrates	61

Appendix A

A.1.1 Basic Protocol: Digestion and Covalent Capture of Thiophosphorylated Peptides	112
A.1.1 Materials	112
A.1.2 Step 1. Digestion of labeled protein lysate	113
A.1.3 Covalent capture of thiophosphorylated peptides	116
A.2.1 Support protocols	18
A.2.1 Materials	120
A.2.2 Kinase reaction and western blot	122
A.2.3 Identification of optimal ATP analog	124
A.2.4 Thiophosphorylation of a candidate substrate	125
A.2.5 Making thiophosphorylated control protein/peptide	127
A.2.6 Anticipated results	129
A.2.7 Troubleshooting guide	131

Appendix B: Aurora B substrates

B. Aurora B substrates identified using nuclear excluded Aurora B	131
---	-----

Appendix C: Aurora B experimental procedures

C.1.1. Purification of recombinant proteins	137
C.1.2 Immunoprecipitation and in vitro kinase reactions	138
C.1.3 Western blotting	138
C.1.4 Isolation of thiophosphorylated peptides	139
C.1.5 Mass spectrometry	140

Chapter 1

Chemical genetic approach for kinase-substrate mapping by covalent capture of thiophosphopeptides and analysis by mass spectrometry

1.1 Abstract:

Mapping kinase-substrate interactions demands robust methods to rapidly and unequivocally identify substrates from complex protein mixtures. Towards this goal we present a method in which a kinase, engineered to utilize synthetic ATP γ S analogs, specifically thiophosphorylates its substrates in a complex lysate. The thiophosphate label provides a bio-orthogonal tag that can be used to affinity purify and identify labeled proteins. Following the labeling reaction proteins are digested with trypsin, thiol containing peptides are then covalently captured and non-thiol containing peptides are washed from the resin. Oxidation promoted hydrolysis, at sites of thiophosphorylation, releases phosphopeptides for analysis by tandem mass spectrometry. By incorporating two specificity gates: kinase engineering and peptide affinity purification, this method yields high confidence substrate identifications. This method gives both the identity of the substrates and phosphorylation site localization. With this information investigators can analyze the biological significance of the phosphorylation mark immediately following confirmation of the kinase-substrate relationship. Here we provide an optimized version of this technique to further enable widespread utilization of this technology.

1.2 Introduction

Members of the kinase superfamily are integral components of many signaling pathways. Kinases play pivotal roles in regulating growth and development and are misregulated in many diseases including cancer. Kinases transduce extracellular signals

by altering the functions of substrate proteins through phosphorylating specific sites on these proteins. It is estimated that a third of all proteins are phosphorylated, and therefore regulated by kinases, however there are only 518 known human kinases (Cohen, 2001; Manning et al., 2002). Therefore many kinases must phosphorylate multiple substrates. The mapping of these relationships is complicated by the shared enzymology of kinases and therefore it is extremely difficult to assign a phospho-site to a specific kinase.

We have developed bio-orthogonal chemical reactions that allow the assignment of a particular phospho-site to a specific kinase (Bishop et al., 2000a; Shah et al., 1997). In this approach the active site of the kinase of interest (KOI) is engineered by creating a new active site pocket that allows the kinase to accept a bulky ATP analog (Figure 1.1A). This engineered “lock and key” provides selectivity for the KOI, as the engineered kinase will accept the N⁶ substituted ATP analog whereas the vast majority of wild-type kinases cannot use these analogs (Figure 1.3A,B).

In order to identify the substrates of a particular enzyme, many of the most widespread proteomic methods rely on affinity-based approaches to enrich for proteins of interest. To apply this approach to kinase-substrate mapping, we developed a modified gamma-phosphate analog (thiophosphate) capture and release strategy for thiophosphate purification. The ATP analog used to identify direct kinase substrates is modified in two ways: a bulky group is added in the N⁶ position providing exclusive recognition by the engineered kinase of interest, and the gamma phosphate is replaced with a thiophosphate moiety (Figure 1.1A). The modified analog-specific (AS) kinase will use these analogs most efficiently, therefore the substrates of the AS kinase will be uniquely labeled with

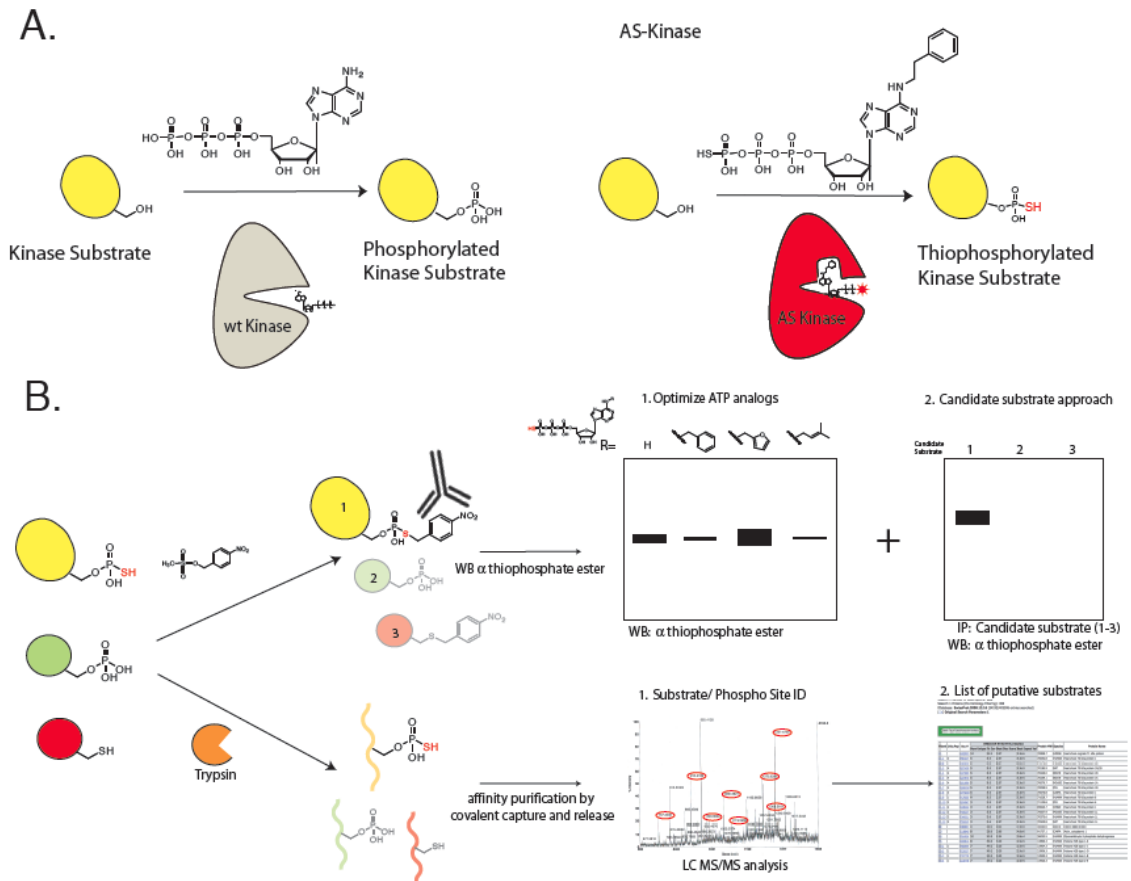


Figure 1.1 Thiophosphopeptide purification scheme. (A) Wild-type (wt) kinase utilizes ATP to phosphorylate its substrates. In contrast, an engineered analog-specific (AS) kinase has a new active-site pocket that allows it to accept an unnatural bulky ATP analog. This “lock and key” allows the AS kinase to transfer the thiophospho group to its substrates. (B) Detail of the two different affinity-purification methods. The thiophosphorylated substrates are found in a background of phosphorylated and unlabeled proteins. In the first technique, the thiophosphorylated proteins are reacted with a thiol-specific alkylating agent that generates a bio-orthogonal thiophosphate ester. Labeled proteins are detected by a thiophosphate ester-specific antibody. In the second approach, the lysate is first digested to generate tryptic peptides. Thiol-containing peptides are then captured by reaction with iodoacetyl agarose beads, and all non-thiol-containing peptides are washed away. The remaining peptides are treated with Oxone, which releases thiophosphate ester-linked peptides by spontaneous hydrolysis.

the thiophosphate affinity tag. This tag can then be used to purify and identify the tagged proteins (Figure 1.1B).

We have published two different approaches for the affinity purification of thiophosphorylated substrates (Allen et al., 2007; Blethrow et al., 2008). In this chapter I provide an updated protocol for the application of these techniques, and demonstrate how they can be used in a complementary manner to rapidly identify the substrates of one kinase from a complex protein mixture.

In the first technique we react the thiophosphorylated proteins with a thiol specific alkylating agent that generates a bio-orthogonal thiophosphate ester. We affinity purify the tagged proteins by using a thiophosphate ester specific antibody 51-8 (Allen et al., 2005; Allen et al., 2007) see Figure 1.2A. The antibody is able to distinguish between a thiophosphate ester and a cysteine thioether, and in this way we are able to specifically visualize and identify tagged substrates by immunoblotting (IB) and immunoprecipitation (IP). This approach cannot reliably allow for the identification of the site of phosphorylation because the para-nitrobenzyl moiety can prevent normal collision induced dissociation of the modified peptide. Given that it is difficult to produce the monoclonal antibody 51-8 in sufficient amounts for IP, we now routinely use this technique for two optimization steps. 1. To determine the optimal N⁶ substituted ATP γ S analog for a KOI and 2. To optimize N⁶ substituted ATP γ S, ATP, and GTP concentrations to achieve the lowest background labeling in cell lysates. Once labeling conditions are optimized, a candidate protein may also be verified as a KOI substrate by immunoprecipitating the candidate substrate and immunoblotting with monoclonal antibody 51-8 (Figure 1.1B).

After optimization of labeling conditions using the thiophosphate specific antibody, our second technique provides unambiguously assigned sites of modification on substrates of the engineered kinase. In this technique, the modified peptides are directly affinity purified, and then subjected to tandem mass spectrometry to identify the parent protein and to assign phosphorylation sites (Blethrow et al., 2008) and Figure 1.2.C. To accomplish the affinity purification, we first digest the labeled protein lysate and then covalently capture the peptides by reacting the digested peptides with iodoacetyl agarose beads, thus capturing all thiol containing peptides. Unbound peptides are washed away, and the beads are then treated with Oxone to oxidize the sulfur in the thiophosphate ester to a sulfoxide. The peptides linked by a thiophosphate ester bond to the agarose beads are then released by spontaneous hydrolysis, while those linked by a cysteine thioether are retained on the resin. In this chapter and Appendix A.1.1-1.3 I provide the most updated and optimized protocol for this technique. In Appendix A2.1-2.7 I provide detailed positive and negative controls to allow any lab to implement this technique.

1.3.1 Strategic Planning

1.3.2 Engineering the kinase of interest

To apply this method the KOI must be able to catalytically transfer thiophosphate to substrate proteins, and tolerate the mutation of the normally bulky gatekeeper to a smaller residue. In fact, along with other groups, we have generated 19 analog specific kinases (Figure 1.5), shown that they will tolerate gatekeeper mutations, and identified putative substrates. We believe most kinases will be able to use ATP γ S as a

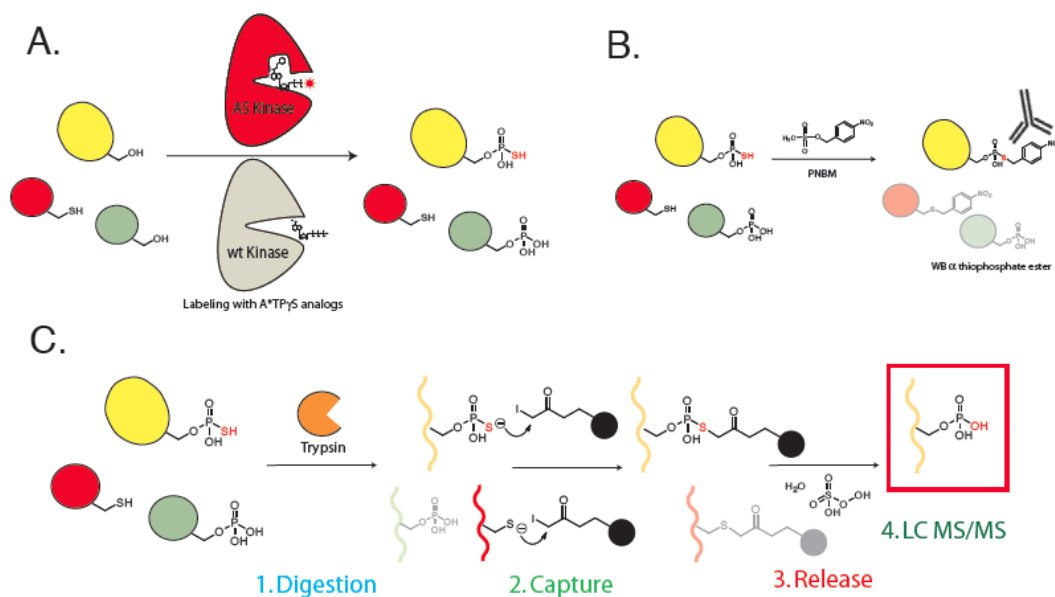


Figure 1.2 (A) Labeling of a cell lysate by incubating AS kinase and N6-substituted ATP γ S analogs generates thiophosphorylated and phosphorylated proteins. (B) Alkylating thiol-containing proteins generates the bio-orthogonal thiophosphate ester. Thiophosphate ester–labeled proteins are detected by a thiophosphate ester–specific antibody (clone 51-8). (C) Thiol-containing peptides are captured by reaction with iodoacetyl beads. During washing, all other non-thiol-containing peptides are washed away. The bound peptides are treated with Oxone to convert the thiol group to a sulfoxide. The presence of an electrophilic phosphoester in the thiophosphate ester-linked peptides catalyzes the spontaneous hydrolysis of these peptides and, after concentration, these peptides are analyzed by tandem LC-MS/MS.

phosphorylation cofactor; in preliminary experiments 13 out of 15 kinases were able to use ATP γ S to thiophosphorylate substrate proteins (Allen et al., 2007) and Figure 1.3A,B. To determine whether a KOI can transfer thiophosphate, the thiophosphate ester specific antibody is used to rapidly determine the thiophosphorylation state of a substrate protein after incubation with ATP γ S and the KOI. The first step is therefore to set up an *in vitro* kinase reaction with the KOI, substrate protein and ATP γ S followed by IB with the thiophosphate ester specific antibody (Appendix A.2.2). The bioinformatic technique for identifying the gatekeeper as well as the generation of an AS kinase have been described previously (Blethrow et al., 2004; Buzko and Shokat, 2002; Gregan et al., 2007). As described in (Buzko and Shokat, 2002), the kinase database is an online tool that can be used to easily find the gatekeeper residue for their kinase (<http://sequoia.ucsf.edu/ksd/>). After identifying the gatekeeper residue (equivalent to I338 in v-Src) conventional site directed mutagenesis techniques can be used to mutate the gatekeeper to either a glycine (analog sensitive-1, as1) or alanine (analog-sensitive-2, as2). These space creating mutations will allow the kinase to utilize bulky ATP analogs (Buzko and Shokat, 2002; Gregan et al., 2007) and Figure 1.3A,B.

Certain protein kinases lose catalytic activity upon mutation of their gatekeeper residue to Glycine or Alanine. In such cases, second-site mutations can be used to rescue activity of the kinase (Zhang et al., 2005). Identification of second-site suppressor mutations have been successfully executed through bioinformatic analysis or genetic selection. Mutations at a few positions were found to rescue activity in multiple kinases and thus can be considered as top candidate sites for rescue mutations [unpublished results]. For example, one position is immediately N-terminal from the conserved DFG

motif (DFG-1) and Ala was found beneficial for kinases activity this position. If the natural residue in a kinase is different from Ala at DFG-1, one can change it to Ala attempting to rescue activity of the kinase. Another position is typically 11 residues N-terminal from the DFG motif (DFG-11) and Leu was found beneficial for kinase activity in general here. If different from Leu, the residue at DFG-11 could be mutated to Leu for rescue of activity. It should be noted that successful rescue mutations varies from kinase to kinase and that there seems to be no universal rescue mutation as of now.

Once the AS kinase protein has been expressed and purified, the kinase assay is repeated to identify the N⁶ substituted ATP analog that is preferentially utilized by the AS-KOI (Appendix A.2.3 and Figure 1.1B).

1.3.2 Lysate Optimization

Optimization of N⁶ substituted ATP γ S analog concentration in each specific lysate is also required to ensure the lowest levels of background and therefore the highest confidence in the identified substrates. There are several different parameters required to optimize the labeling conditions. Although the N⁶ substituted ATP γ S analogs are preferentially used by the engineered AS kinase, at high enough concentrations other kinases can also utilize these analogs. Providing sufficient unmodified ATP and GTP ensure that these kinases are occupied and will therefore decrease the non-specific use of the N⁶ substituted ATP γ S analogs. In addition, each lysate will have a different N⁶ substituted ATP γ S analog that will produce the lowest level of background. The conditions that give the highest signal-to-noise should be determined empirically by varying the levels of AS kinase, N⁶ substituted ATP γ S analog, ATP, and GTP in the

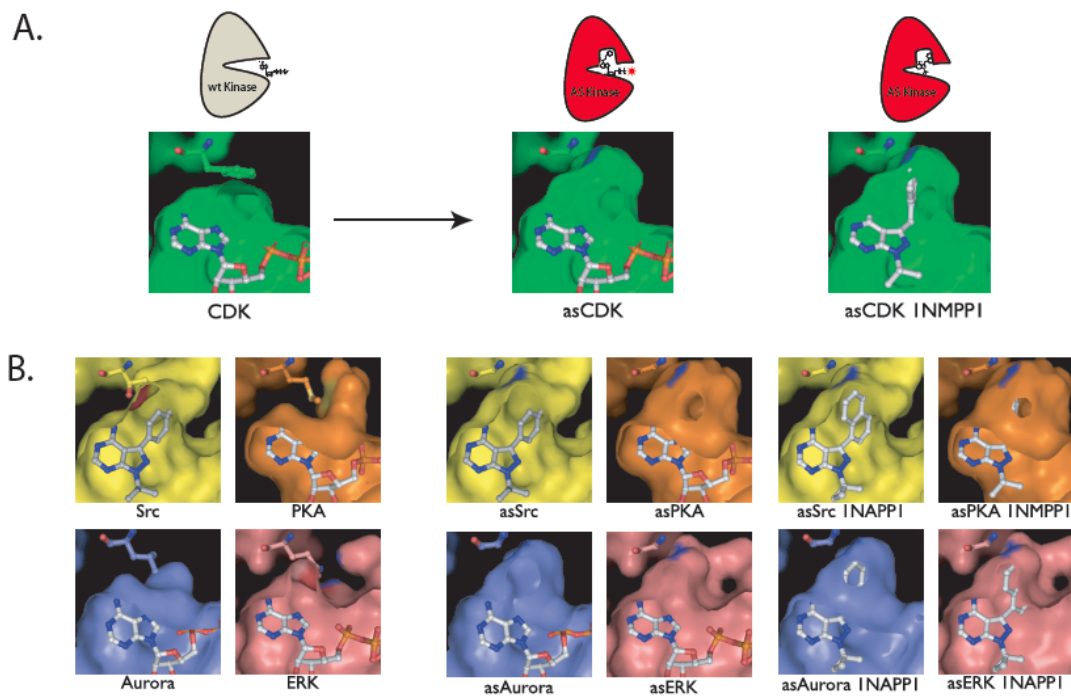


Figure 1.3 (A) The gatekeeper residue is shown in CDK1 as a phenylalanine above the bound ATP in the CDK1 active site. After mutation to the much smaller glycine, a pocket is opened that allows for a bulky substituent to bind (pictured as asCDK1). A “bumped” (N6-substituted) ATP analog or inhibitor (in this case 1NMPP1) can now bind to the engineered kinase by utilizing the extra space above the N7 position. (B) The active sites of SRC, PKA, aurora, and ERK are shown along with their gatekeeper residues and the successful mutation of these bulky residues to smaller ones. The mutation of the gatekeeper to a smaller residue creates a similar pocket in each of these four kinases. These kinases are shown with ATP bound or with bumped inhibitors that target these engineered kinases, but not the wild type. The similarity in the engineered pocket among disparate kinases demonstrates the wide applicability of this method.

presence of AS kinase and by testing for the phosphorylation of a candidate substrate in the complex mixture (See appendix A.2.4). Utilizing the thiophosphate ester specific antibody to detect background thiophosphorylated proteins is the best method for lysate optimization. The amount of kinase is critical to the efficiency of the labeling. When using a recombinant form of the AS kinase, up to 1% (by total weight) of the AS kinase can be added; For example 10 μg of AS kinase in 1 mg of total lysate (100 μl of 10 mg/mL lysate). If using a transfected cell then the level of kinase can be varied by using different expression vectors, but usually the highest level of expression is necessary to achieve the best signal to noise. Varying the levels of ATP (50-200 μM), GTP (1-3 μM), and N⁶ substituted ATP γ S analog (100-500 μM) should give an optimal set of specific conditions in which the lowest background and the highest levels of AS specific labeling is observed (Appendix A.2.4).

1.3.3 Generating positive control peptides and protein

We recommend generating a hyper-thiophosphorylated control protein (myelin basic protein (MBP)) and control peptide (GSK3 substrate peptide CREB) which can be accomplished using commercially available materials (Appendix A.2.5). The labeled protein will serve as a control for the retention of the thiophosphate modification during the digestion steps, and both controls will serve to ensure that the covalent capture, release, and mass spectrometric analysis of thiophosphorylated peptides are working properly. See Figure 1.1.4 for details.

During the labeling procedure two negative controls are essential; minus N⁶ substituted ATP γ S analog and minus AS kinase. These controls will provide information

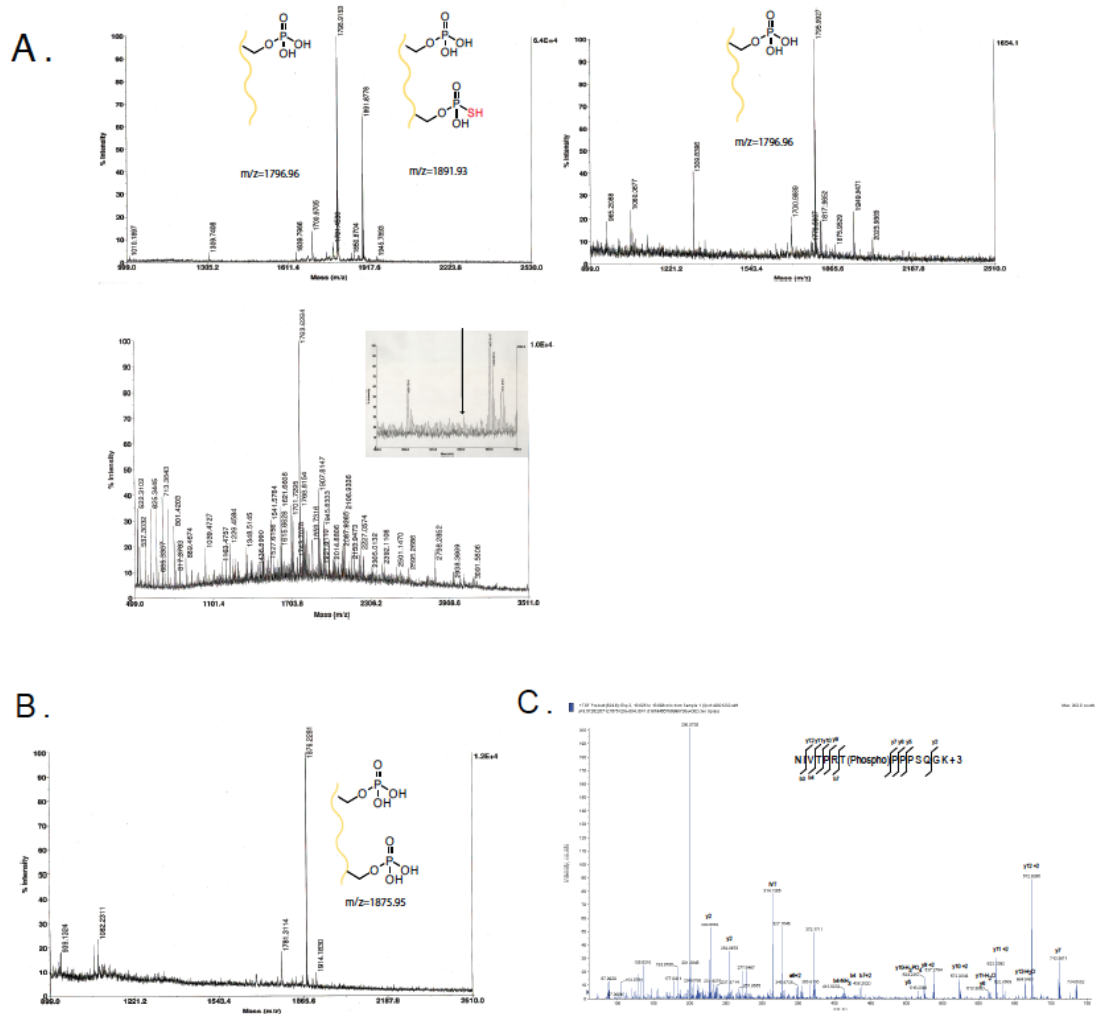


Figure 1.4 (A) Raw data showing an expected MALDI analysis of thiophosphorylated CREB peptide. Both the singly phosphorylated (KRREILSRRPS(p)YR) (1795.84 MH+) and the thiophosphorylated (KRREILS(thiophosphate)RRPS(p)YR) 1891.986 (MH+) peptide are shown in the first pane. Analysis of the flow-through after covalent capture with iodoacetyl agarose beads in the second pane shows the complete reaction of the thiophosphorylated (1891.986) peptide, but no reaction with the parent peptide (1795.84 MH+). Analysis of the flow-through with additional HeLa lysate after covalent capture with iodoacetyl agarose beads in the third pane shows many peptides, but the CREB peptide is not seen. (B) Following hydrolysis, the only peptide present is the double phosphorylated CREB peak at 1875.986 (MH+), demonstrating the specificity of the technique. (C) After the covalent capture reaction with digested thiophosphorylated myelin basic protein, only one peptide (NIVT(phospho)PRTPPPSQK) is observed. MS-MS analysis of the 1587.8001 (MH+), NIVT(phospho)PRTPPPSQK (seen as the triply phosphorylated peptide at 524.6 m/z) shows good sequence coverage of this peptide with loss of phosphate from the y10 ion.

about which background substrates are detected and therefore excluded from the list of identified substrates. Using these controls to troubleshoot and optimize each step of the procedure is critical to the success of the protocol.

1.6 Commentary

1.6.1 Background Information

Identifying the substrates of a kinase is a critical step towards understanding its biological role. Traditional approaches for kinase substrate mapping depend on knockout experiments followed by phosphopeptide enrichment and mass spectrometry. While useful, this method fails to identify all kinase substrates as there exists redundancy in which a single substrate may be phosphorylated by multiple kinases. Methods for phosphopeptide enrichment include metal affinity chromatography using titanium oxide columns (Trinidad et al., 2008) and identifying new phospho proteins by enriching thiophospho peptides (Kwon et al., 2003). A quantitative mass spectrometry approach can more precisely define the effects of stimulation or knockout of a particular kinase. In an application of this technique, a SILAC labeling approach followed by TiO₂ enrichment was used to determine the effects of growth factors on global phosphorylation status (Olsen et al., 2006). All of these approaches fail to specifically assign a phosphorylation site to a particular kinase but are useful for defining the global changes in phosphorylation and for mapping novel phosphorylation sites.

Our approach allows for the labeling of the substrates of a single kinase in a chemical genetic approach, and can therefore unambiguously assign kinase substrate

relationships. Originally the N⁶ modified ATP analogs were radioactively labeled in the gamma phosphate position. Putative substrates were then identified by coupling this approach with affinity tagged libraries. This approach was successfully used to identify Cdk1 and Pho 85 substrates in *S. cerevisiae* (Dephoure et al., 2005; Ubersax et al., 2003). Although this engineered “lock and key” provides selectivity for a single kinase, the transfer of a radioactively tagged phosphate by the N⁶ modified ATP substrate only assists in visualization and traditional biochemical purification of direct kinase substrates from tagged libraries that are not available in more complex eukaryotes.

Introduction of a bio-orthogonal tag onto the substrate proteins of a particular kinase simplifies the affinity purification and identification of the substrates of any protein kinase in a complex lysate. This approach relies on two separate specificity gates: the kinase is engineered to accept bulky ATP analogs, and the substrates are tagged with a bio-orthogonal phosphate analog. The affinity purification of the tagged substrates also depends on two specificity gates: only thiol containing peptides are pulled down, and of those peptides that are covalently bound to the affinity matrix, only those linked by thiophosphate ester bonds are cleaved off the resin. These specificity elements allow for the purification of very low abundance substrates, while also increasing the confidence in the identification of the identified substrates.

See Appendix A.1.1-A.1.3 for the detailed covalent capture protocol.

See Appendix A.2.1-A.2.5 for support protocols.

1.6.2 Critical Parameters

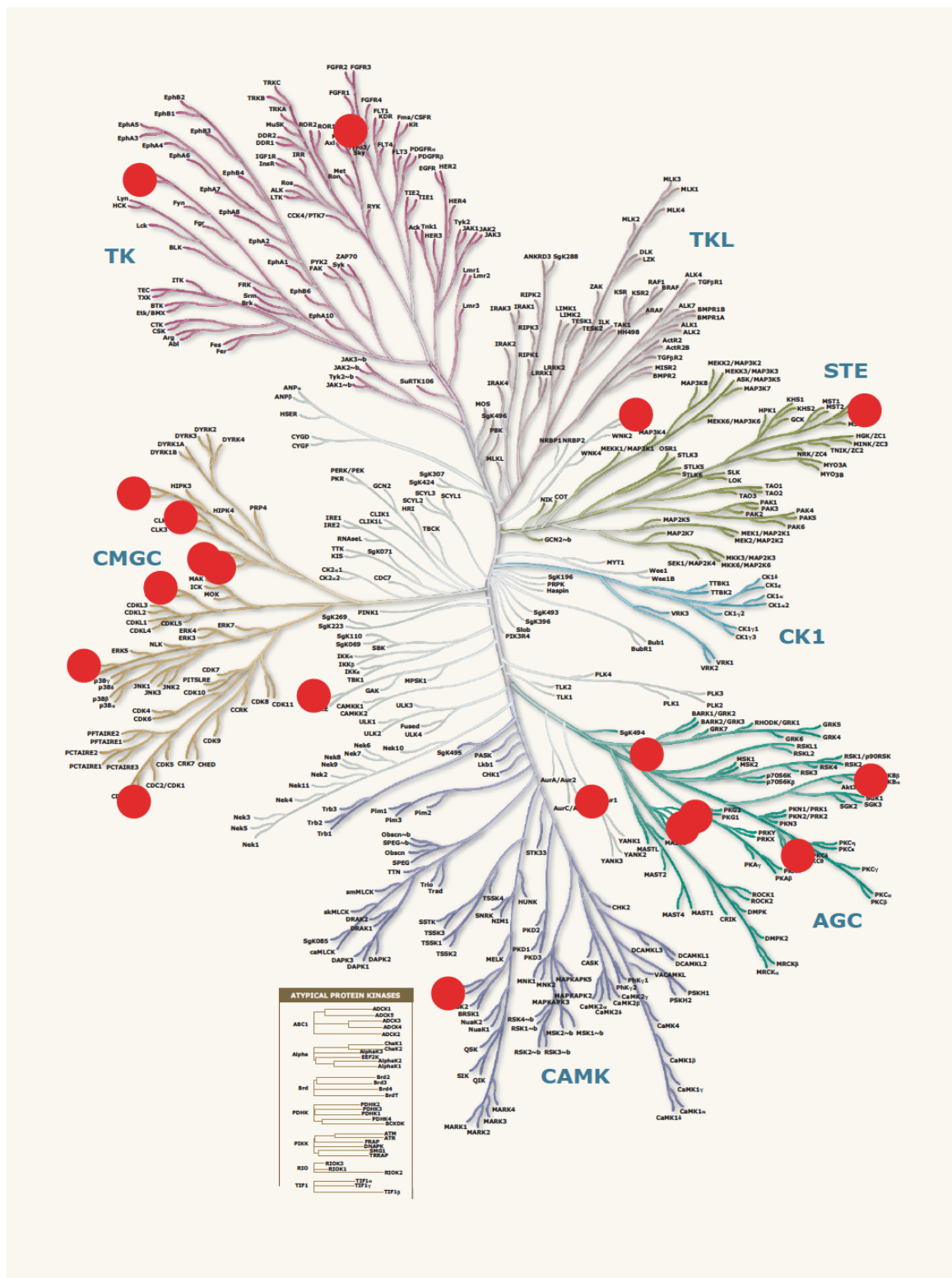


Figure 1.5 Kinases engineered by the author using the analog specific approach

Utilization of the N⁶ modified ATP analogs by other kinases can lead to false identification of kinase substrate relationships. It is therefore crucial to fully optimize the labeling reaction. Using a wide range of ATP, GTP, and N⁶ modified ATP analogs during the lysate optimization steps will provide the best conditions for these reactions. Nonspecific binding of peptides to the agarose beads can also lead to the false identification of substrate proteins. Generating several positive and negative control samples will help control for the non-specific purification of peptides.

Several controls are essential for distinguishing background from AS kinase specific labeling. First, it is essential to demonstrate the AS kinase dependence of purification of any phosphopeptides. When labeling is observed, or phosphopeptides are affinity purified from samples that do not contain AS kinase but do contain the N⁶ modified ATP analog, these proteins must be subtracted from any list of putative substrates. When non-phosphorylated peptides are identified in the absence of AS kinase it may indicate that the washing steps are not effective. Increasing the stringency of the wash steps by increasing the volume or incubating the washes for 10 minutes should lower background. Secondly, the positive control thiophosphorylated peptide and protein are very useful for diagnosing the digestion and affinity purification steps. In typical tryptic digests, complex lysates are reduced and alkylated before digestion to ensure the complete digestion of all proteins. The alkylation step with iodoacetamide is incompatible with our technique, thereby complicating the digestion of thiophosphorylated protein lysates. Also the thiophosphate mark is susceptible to acid promoted hydrolysis. It is therefore important to include the hyper-thiophosphorylated MBP as a digestion control to ensure the mark is retained on substrate proteins. A rapid

way to determine whether the covalent capture and release reaction is working is by including a separate covalent capture reaction with the CREB peptide followed by MALDI TOF analysis.

1.6.3 Troubleshooting

A trouble-shooting guide is presented in Appendix A.2.7

1.6.4 Anticipated results

Anticipated peptide m/z ratios are presented in Appendix A.2.6

1.6.5 Time considerations

A significant investment of time and resources is required for the design and production of an AS kinase. Once a kinase has been engineered, optimization of labeling conditions and identification of putative substrate proteins should be rapidly achieved in 1-2 weeks. Production of the labeled positive controls should take 1-2 days depending on how long the digestion of labeled MBP is permitted. Once comfortable with labeling, digestion and preparation of covalent capture reactions an experienced investigator should be able to prepare and process several samples in 2-3 days.

Chapter 2

Chemical genetic identification of NDR1/2 kinase substrates

AAK1 and Rabin8 uncovers their roles in controlling dendrite arborization and synapse maturation

2.1 Abstract

The development of the correct neuronal circuitry essential for normal brain function is dependent upon the controlled growth and pruning of dendritic networks leading to functional synaptic connections between neurons. Previous studies have identified homologs of the human kinases MST3 and NDR1/2 in worms and flies as key regulators of dendrite growth and morphology, however no direct substrates have been identified and their role in mammalian cells is unknown. Here we show expression of dominant negative NDR1/2 mutants or siRNA knockdown of these kinases increased dendrite length and proximal branching of mammalian neurons in vitro as well as in vivo, whereas expression of constitutively active NDR1/2 had the opposite effects. Furthermore, NDR1/2 also regulates spine maturation. To identify NDR kinase substrates responsible for these phenotypes, we employed chemical genetics and discovered two proteins involved in intracellular vesicle trafficking: AAK1 kinase associated with AP1/2 adaptors and Rabin8, a GDP exchange factor (GEF) of Rab8 GTPase. Our experiments show that AAK1 contributes to dendrite growth regulation and Rabin8 regulates spine maturation. In this study, we observed that the NDR1/2 kinases control the proper arborization of dendrites and formation of synaptic spines in mammalian cells and discovered the NDR substrates that mediate these phenotypes.

2.2 Introduction

Functional neural circuitry requires that developing neurons must first undergo dendritic arborization to evenly cover the sensory field with dendrites. To then produce

functional synapses, synaptic spines, micron-sized membrane protrusions that receive most excitatory synaptic inputs, must form along these dendrites.

NDR (nuclear Dbf2-related) kinases are a subclass of AGC group (protein kinase A(PKA)/PKG/PKC) of serine/threonine kinases. The NDR family kinases, which includes the tumor suppressor Lats1/2 (large tumor suppressor 1/2) (Hergovich et al., 2006), have important functions in neuronal morphogenesis in many different species. The NDR homologs (Cbk1p in yeast, SAX-1 in worms and Trc in fly) perform essential functions in regulating polarized cellular differentiation in various organisms, including bud formation in yeast (Nelson et al., 2003), epidermal hair tip and sensory bristle formation in *Drosophila* (Cong et al., 2001; Geng et al., 2000) and dendritic morphogenesis and tiling in worm and fly (Emoto et al., 2004; Emoto et al., 2006; Gallegos and Bargmann, 2004). Lats1/2 (wts) and its upstream kinase hippo are also necessary for maintenance of dendritic arbors (Emoto et al., 2006).

The two mammalian NDR kinases, NDR1 and NDR2 (referred to as NDR1/2) are 86% identical by sequence. Their biochemical activation mechanisms are well characterized and no differences between NDR1 and NDR2 are reported (Hergovich et al., 2006). (Add a sentence to explain activation mechanism). NDR1 and NDR2 are expressed in the mouse brain (Devroe et al., 2004; Stegert et al., 2004; Stork et al., 2004). Although NDR1/2 are expressed ubiquitously in the mammalian brain, no role has been shown for these kinases presumably because a knockout of NDR1 kinase is suppressed by compensatory expression of NDR2.

Despite the clear role for NDR proteins in polarized cell differentiation, few substrates of this kinase have been discovered. Other than two substrates for the NDR1/2

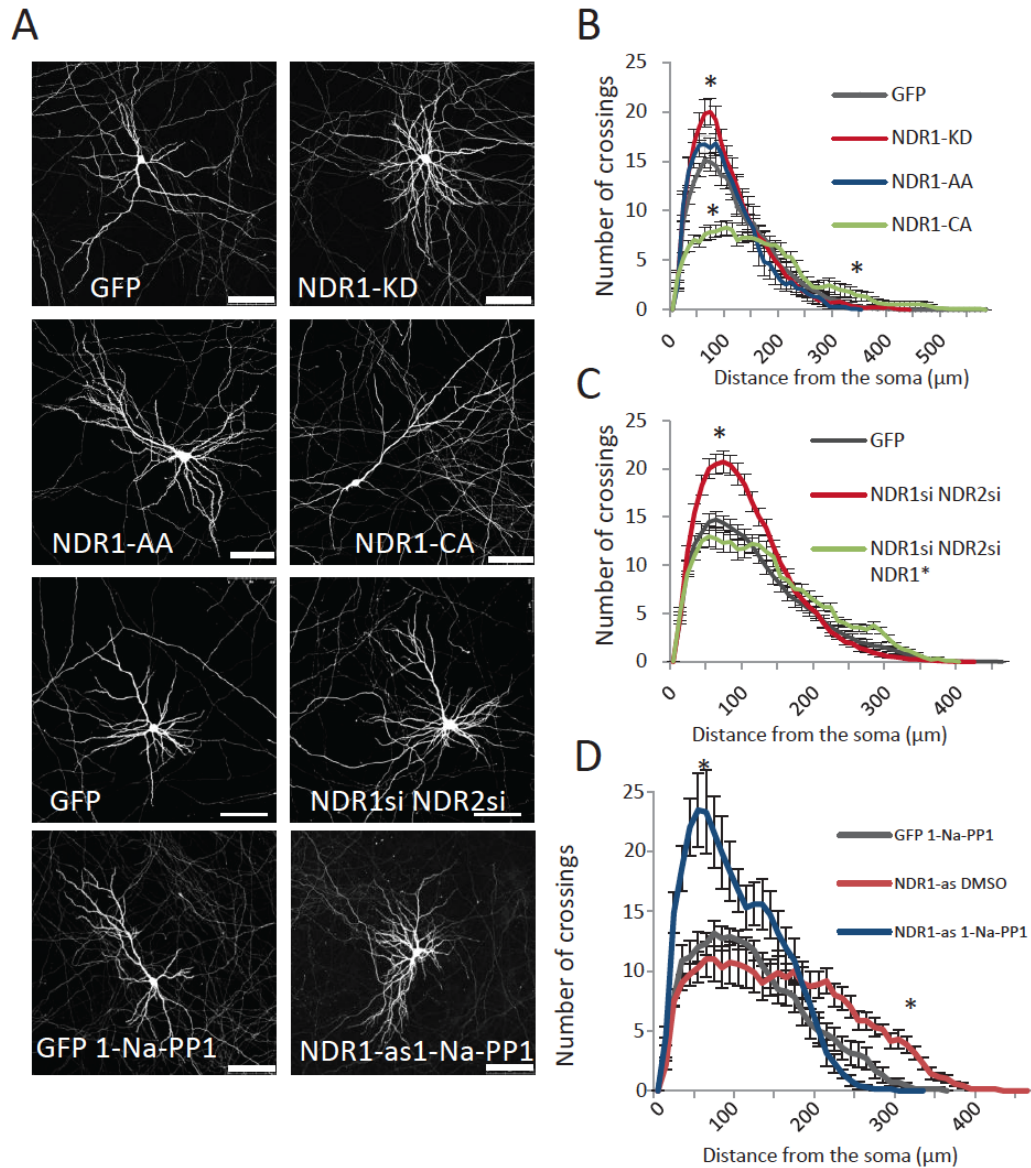


Figure 2.1 A. Hippocampal neurons expressing NDR1 mutants or siRNA together with GFP. Scale bars are 100 μm . B. Sholl graphs of dendrites of neurons transfected with GFP alone or GFP co-transfected with NDR1 mutants. C. Sholl graphs of neurons expressing GFP plasmid or GFP plasmid which also expresses siRNA. For dual NDR1 and NDR2 siRNA knockdown NDR1 siRNA and NDR2 siRNA plasmids were co-transfected. For rescue with siRNA resistant NDR1 (NDR1*), this plasmid was co-transfected with NDR1si and NDR2si. D. Sholl analysis for chemical genetic inhibition of analog sensitive NDR1-as by 1-Na-PP1 shows increased proximal branching with NDR1-as inhibition. * indicates $p < 0.05$, ** indicates $p < 0.01$, *** indicates $p < 0.001$ in all graphs in all figures assessed by Kruskal Wallis non-parametric test followed by dual test with Dunn's method in comparison with GFP control (unless otherwise indicated). Error bars are standard error of the mean in all.

yeast homolog *cbk1: sec2p* (Kurischko et al., 2008) and *ssd1p*, a non-conserved protein (Jansen et al., 2009) no substrates have been reported- what are these substrates. Identification of NDR family member *Lats1/2* phosphorylation targets in fly has elucidated its function as a tumor suppressor (Harvey et al., 2003; Huang et al., 2005; St John et al., 1999; Wu et al., 2003).

In this study, we investigated NDR1/2 function in cultured hippocampal neurons *in vitro* and in cortical neurons *in vivo* by perturbing its function via dominant negative and constitutively active NDR1/2 and siRNA expression. We found that NDR1/2 limits dendrite branching and length both *in vitro* and *in vivo*. NDR kinases were also required for mature spine synapse formation as NDR1/2 loss of function lead to more immature spines *in vitro*. Therefore we utilized chemical genetic techniques to engineer NDR1 kinase to uniquely accept a modified ATP analog and to transfer a thiophosphate to substrate proteins. We identified 5 potential NDR1 substrates in mouse brain. The two most prevalent substrates are: AP2 associated kinase-1 (AAK1) and Rab8 guanine exchange factor (GEF) Rabin8 (*sec2p* homolog) both known to function in intracellular vesicle trafficking. Using phosphomimetic and phosphomutant forms of AAK1 and Rabin8 we show that AAK1 phosphorylation is important in limiting dendritic branching whereas Rabin8 phosphorylation is important for spine maturation in cultured hippocampal neurons. Identification of two separate phosphorylation targets of Ndr1 mechanistically defines a role for Ndr1 kinase in both the process of dendritic arborization and synaptic spine formation in neurons.

2.3 Results

2.3.1 NDR1/2 are necessary and sufficient to reduce dendrite branching

The biochemical activation mechanism of NDR kinases has been established: MST3 kinase phosphorylates NDR1/2 at its C-terminal hydrophobic residue T444 to activate it (Stegert et al., 2005). NDR1/2 can be activated by okadaic acid (OA) via inhibition of protein phosphatase 2A, facilitating phosphorylation at T444 and the autophosphorylation at S281 (Stegert et al., 2005). MOB1/2 binding to N-terminal region of NDR kinases is required for the release of autoinhibition and maximal activity (Bichsel et al., 2004). Autophosphorylation site S281 is critical for NDR1/2 kinase activity. In order to test NDR1/2's role in dendrite development we first generated dominant negative and constitutively active NDR1 mutants. For dominant negative NDR1 we mutated Ser281 and Thr444 to Alanine (S281A; T444A, NDR1-AA) or catalytic lysine to alanine (K118A, NDR1-KD); both mutants have no kinase activity (Millward et al., 1999; Stegert et al., 2004). To obtain constitutively active NDR1, we replaced the C-terminal hydrophobic domain with that of PRK2 (PIFtide), similar to the generation of constitutively active NDR2 (Stegert et al., 2004).

Kinase activity levels of NDR1 kinase dead (NDR1-KD) and constitutively active (NDR1-CA) mutants was confirmed by *in vitro* kinase assay with immunoprecipitated NDR1 using an NDR1 substrate peptide as the kinase target (Stegert et al., 2005) (Figure 2.2E). We then expressed mutant NDR1 proteins together with GFP, to test for their effect on the morphology of cultured hippocampal neurons. Neurons were transfected at DIV6-8 to perturb NDR1/2 function during dendrite development and analyzed at DIV16. With low transfection efficiency it was possible to investigate the cell-

autonomous function of NDR1/2. We found that NDR1-KD resulted in increased proximal dendrite branching, whereas NDR1-CA caused a major reduction in proximal dendritic branching (Figure 2.1A,B). Total dendrite branch points were also increased in NDR1-AA and NDR1-KD and reduced in NDR1-CA (Figure 2.1,B) In addition, NDR1-CA resulted in a larger number of branch crossing at 340 μm in Sholl analysis (Figure 2.1B), indicating that NDR1 activity may produce longer main dendrites at the expense of proximal dendrite branches. These results indicate that NDR1 activity inhibits proximal dendrite branching and total length during development.

To corroborate these findings, we next used NDR1 and NDR2 siRNA to knockdown NDR1/2 function. We find that expression of NDR1 and NDR2 siRNA together (but not alone) increased proximal branching and total branch points as did dominant negative mutants (Figure 2.1C). This effect was rescued by co-expression of siRNA resistant NDR1 (NDR1*), indicating that the effect was indeed due to loss of NDR1/2 kinase function. Taken together with Trc's role on dendrite development of sensory neurons in fly, where *trc* mutants show increased branching and increased total length (Emoto et al., 2004), our findings reveal an evolutionarily conserved function of NDR1/2 in dendrite morphogenesis.

2.3.2 NDR1/2 control dendritic spine maturation

NDR kinases have important roles in polarized growth, however their function in synaptic development has not been investigated. To examine NDR1/2's role on synaptic development we first analyzed dendritic spine morphologies in neurons expressing dominant negative or constitutively active NDR1, or siRNA. Dendritic spines can be

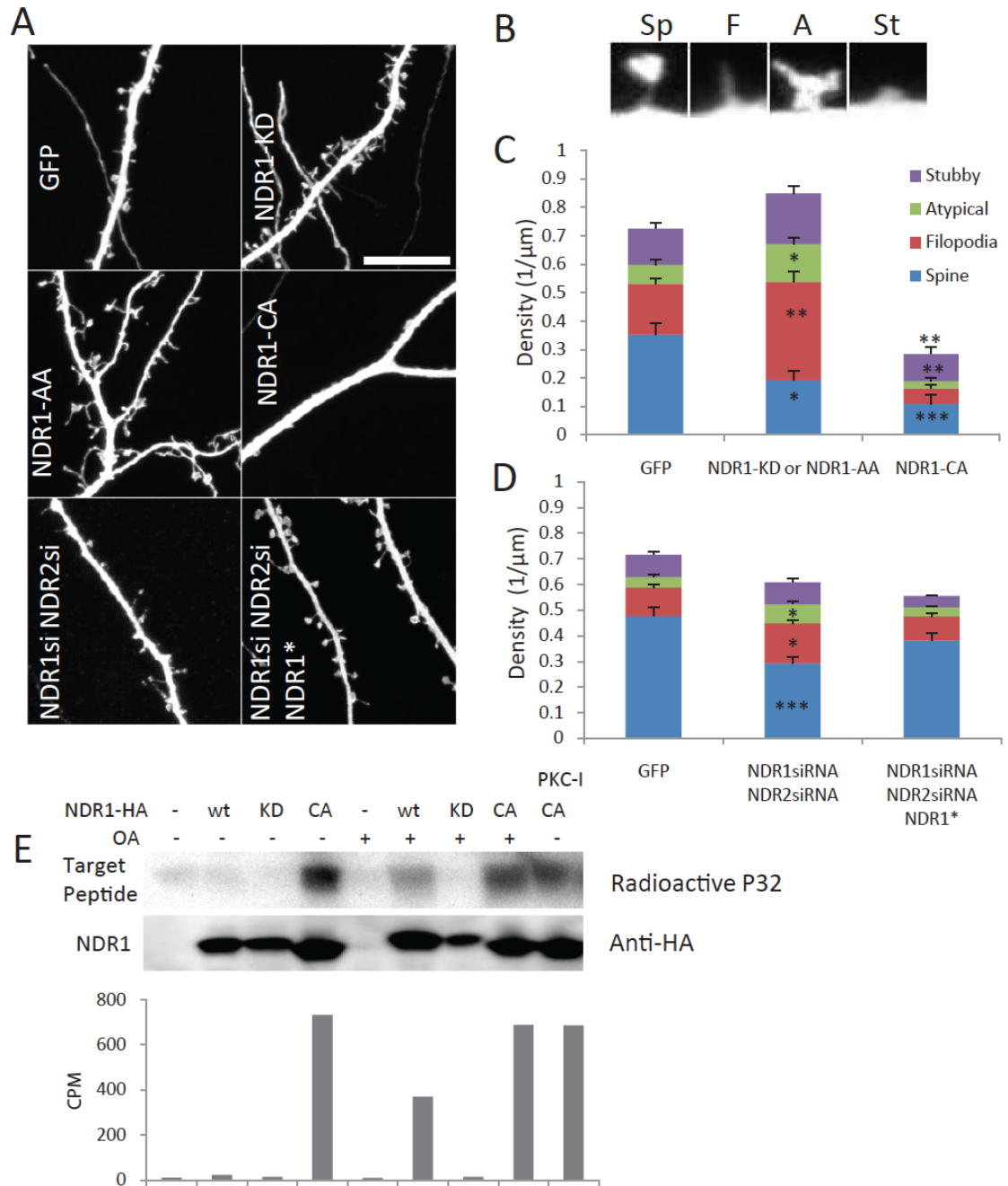


Figure 2.2 NDR1/2's role on dendritic spine development A. Dendritic spines of transfected neurons are shown, scale bar is 10 μm . B. Dendritic spine categories Sp: mushroom spine, F: filopodia, A: atypical, St: Stubby. C. Effect of NDR1 dominant negative and constitutively active expression on different categories of dendritic spine densities. D. Effect of NDR1 and NDR2 knockdown by siRNA on dendritic spines. E. HA tagged NDR1 is expressed in COS-7 cells, immunoprecipitated and reacted with NDR target peptide. NDR1 wild type can be activated by 30 min treatment of 0.5 μM okadaic acid (OA), NDR1-KD is inactive and NDR1-CA is active without OA shown by radioactive kinase assay using radioactive ATP-[^{32}P]. PKC inhibitor (PKC-I) does not affect NDR1 kinase activity. Anti-HA immunoblot shows total expressed NDR1. Graph shows data from liquid scintillation counting.

categorized according to their morphology (Harris, 1999; Yuste and Bonhoeffer, 2004). To evaluate the effect of NDR1/2 on developmental maturation of spines, we divided spines into 4 categories (Konur and Yuste, 2004): Mushroom spines: protrusions with a head and a neck, filopodia: thin protrusions without a discernable spine head, atypical: protrusions with irregular shape and stubby: short protrusions without a discernable spine neck (Figure 2.2B). Spine morphology is correlated with synaptic function, where mushroom shaped spines contain AMPA receptors in proportion to the size of spine's head while filopodia mostly lack these receptors (Matsuzaki et al., 2001). Spine morphologies are especially diverse during early development (Fiala et al., 1998; Konur and Yuste, 2004). Atypical and stubby protrusions are more common in developing tissue, but dendrites contain mostly mushroom spines representing mature synapses later in development (Harris, 1999).

We transfected neurons at DIV6-8 and analyzed them at DIV16. Expression of dominant negative NDR1 (NDR1-KD or NDR1-AA) caused a robust increase of filopodia and atypical protrusion density together with a reduction in mushroom spine density (Figure 2.2A,C), indicating that NDR1 function is necessary for mature spine formation. In contrast, NDR1-CA drastically reduced the total dendritic protrusion density, as a result of significant reduction in mushroom spines and filopodia (Figure 2.2A,C). Robust inhibition of dendritic protrusions by NDR1-CA suggests that excessive NDR1 activity reduces all actin-rich dendritic protrusions. Similar to the dominant negative effects of NDR1 mutants, NDR1siRNA + NDR2siRNA also resulted in increased filopodia and decreased mushroom spine densities, which was rescued by co-expression of siRNA resistant NDR1 (NDR1*) (Figure 2.2A,D). The difference in the extent of

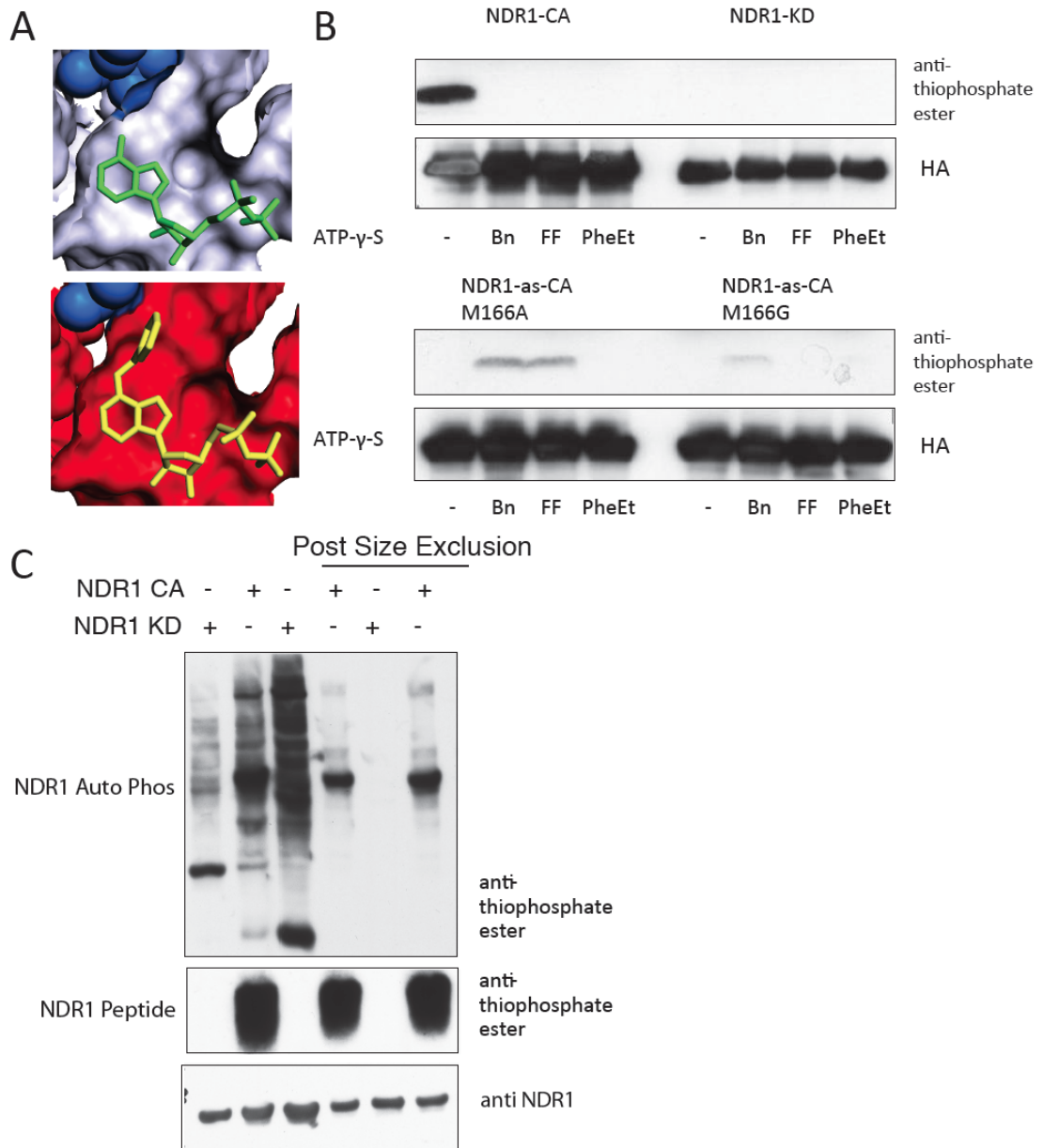


Figure 2.3 Design and analysis of NDR analog specific mutants. A. Depiction of ATP binding site of wild type Src kinase with ATP (green) (top) and as-Src with Benzyl-ATP- γ -S (yellow) (bottom). Mutation in gatekeeper residue (blue) resulted in an affinity pocket where bulky ATP can bind. B. Three bulky ATP analogs (Benzyl (Bn), Furfuryl (FF) & Phen-ethyl (PheEt)) were tested for usage by NDR1-as kinases. Kinases expressed in COS-7 cells are immunoprecipitated and reacted with NDR target peptide. Thiophosphorylation is detected by anti-thiophosphate ester antibody. M166A NDR1-as-CA uses Bn at highest efficiency. However a huge loss in activity directed us towards identifying additional suppressive mutations that could increase the activity of as-NDR. C. Expression of as-NDR in SF21 cells by infection with a baculovirus with NDR inserted at the polyhedrin promotor. NDR was purified by Ni column (Lane 1-3) followed by a size exclusion column to purify NDR. Activity is only see with as-NDR constitutively active (CA) not kinase dead (KD)

filopodia/atypical protrusion increase between dominant negative mutants and siRNA might be due to incomplete knockdown by siRNAs. In addition, the total number of dendritic protrusions were not rescued completely with NDR1*, suggesting a small non-specific effect of siRNA expression. These data indicate that NDR1/2 are required for efficient formation and/or maturation of mushroom spines. Expression of NDR2-KD and NDR2-CA yielded alterations similar to the corresponding NDR1 mutants (data not shown).

Our data revealed that both loss and gain of function of NDR1/2 altered spine morphogenesis. NDR1/2 loss of function reduced mushroom spines and increased filopodia and atypical protrusions, indicating that NDR1/2 are required for mature mushroom spine formation. The reduction in mature spines is reflected in reduced mEPSC frequency. On the other hand, uncontrolled NDR1-CA activity lead to retraction of all dendritic protrusions, most likely via a separate mechanism different from the process for spine maturation. Notwithstanding the likely involvement of processes that impact immature dendritic protrusions to different extent, it appears that strictly controlled NDR1/2 activity is required for spine maturation.

2.3.3 Development and characterization of an analog specific NDR1 construct

To analyze the direct effect of NDR1 activity on dendritic branching, we sought to generate an analog specific NDR1 construct. To do this we identified the gatekeeper residue and mutated this residue (Methionine 166) to Alanine (M166A) to make an analog-sensitive NDR1 (NDR1-as), which can utilize bulky ATP analogs instead of ATP and can be blocked by kinase inhibitors such as 1-Na-PP1 (Bishop et al., 2000b) (Figure

2.3A). We analyzed NDR1 activity by an *in vitro* kinase reaction with these mutants using NDR1's target peptide as described previously (Stegert et al., 2005). The thiophosphorylated substrate peptide was detected by anti-thiophosphate ester antibody on western blot after esterification by p-nitro mesylate (PNBM) (Allen et al., 2007). Similar to Aurora B, this mutation abolished kinase activity (Figure 2.3B and 2.4A). In order to rescue the activity of NDR1 we sought to identify second site suppressive mutations that we could make to recover the activity of NDR1. We identified these residues as Methionine 152 and Serine 229 and mutated these to several residues in an attempt to rescue the lost activity. We found that generating the mutations M152L and S229A together dramatically increased the activity of NDR1 to that of wt NDR1 (M166G) or even higher activity (M166A) (Figure 2.4A) (Zhang et al., 2005). We generated two analog sensitive NDR1-CA's (M166A and M166G).

To directly test whether inhibition of NDR1 was responsible for the dramatic phenotype we observed in dendrite branching, we transfected neurons with activated NDR1-as at DIV8 and investigated the effect of NDR1 on dendrite development with or without 1-Na-PP1 inhibition from DIV8 to DIV16. We found that addition of asNDR specific inhibitor 1-Na-PP1 resulted in increased proximal branching (50 μ m), total branch points and total length (Figure 2.1D), likely due to a dominant negative effect. Activated NDR1-as treated with the vehicle DMSO resulted in larger dendrite arbor with greater number of branch crossings at 340 μ m in Sholl analysis (Figure 2.1D). Although M166A gatekeeper mutation resulted in reduced ATP- γ -S usage (Figure 2.4A), M152L and S229A rescue mutations lead to recovery of ATP- γ -S usage albeit at a lower level than Benzyl-ATP- γ -S as expected (Figure 2.4A). These results further confirm that

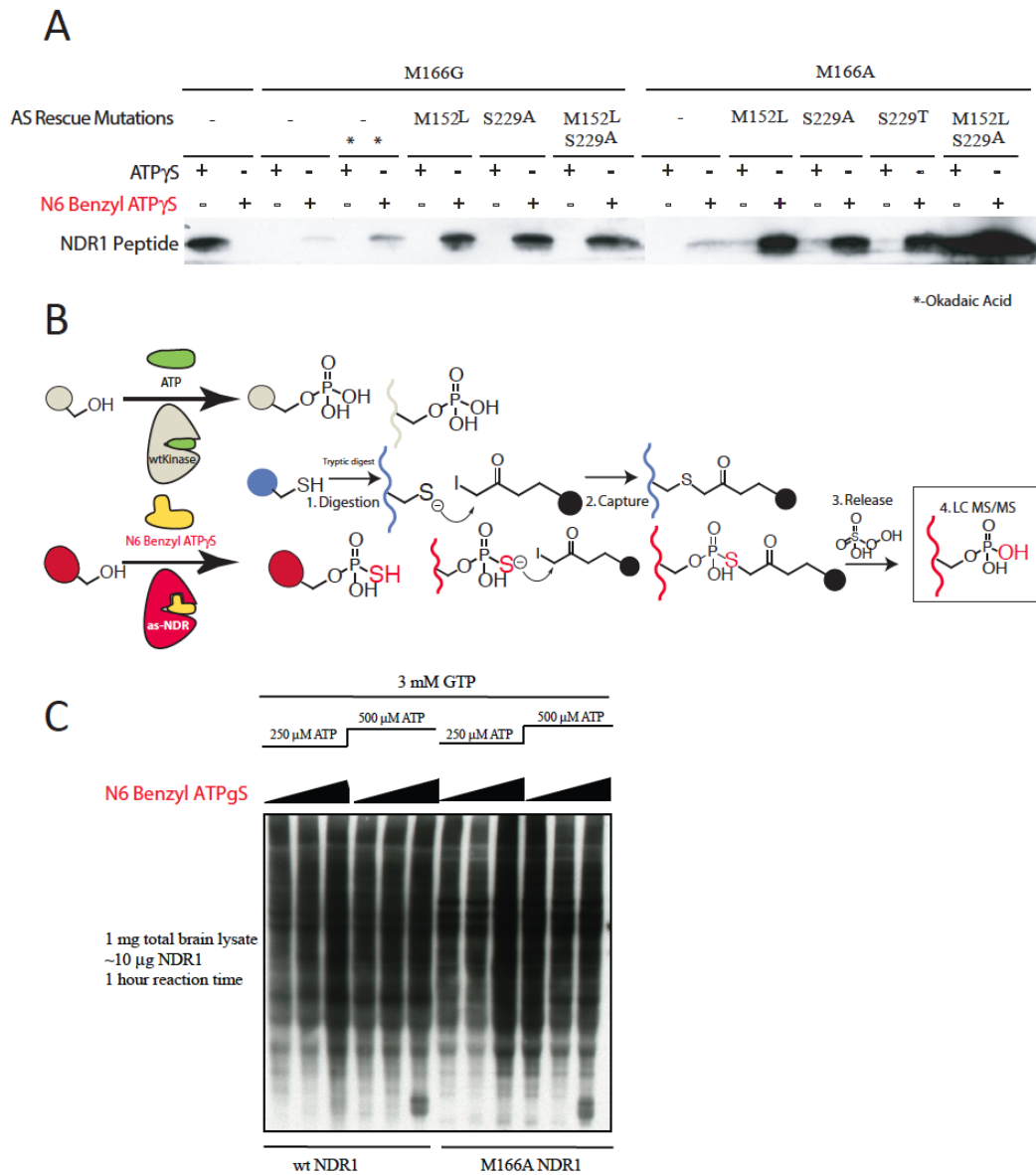


Figure 2.4 Identification of NDR1's phosphorylation targets by chemical genetics. A. NDR1-as mutants (M166A and M166G) in NDR1-CA use Benzyl-ATP- γ -S and their efficiency is increased by two point mutations in the kinase domain M152L and S229A/T. HA tagged kinase was expressed and purified from COS-7 cells using HA tag. Kinase reaction was done using NDR substrate peptide. Thiophosphorylation was detected by anti-thiophosphate ester antibody. B. D. Covalent capture method for kinase substrate identification. A protein phosphorylated by endogenous kinases is depicted in gray. A protein thiophosphorylated by NDR1-as is depicted in red. Blue depicts a protein which contains a cysteine. C. Addition of either wildtype or analog specific SF21 expressed NDR to whole brain lysate to analyze labeling by anti-thiophosphate antibody. Very few additional bands are seen with as-NDR, and addition of different concentrations of ATP do not appear to decrease non-specific labeling.

NDR1 function is necessary to reduce proximal dendrite branching and NDR1 activity may in turn facilitate dendrite arbor expansion distally. Additionally, the generation of NDR1 analog specific construct allowed us to directly test the effect of NDR1 inhibition on dendritic branching, and to identify substrates of NDR1.

2.3.4 Chemical genetic identification of NDR1 kinase substrates reveals multiple targets in vesicle trafficking

Having found NDR1/2 function important for dendrite arborization and synaptic maturation, we next looked into the cellular mechanisms by which NDR1/2 regulates dendrite morphogenesis and spine maturation. Since there are no known substrates of NDR1/2, we utilized the chemical genetic substrate identification method by covalent capture reviewed in Chapter 1 and (Blethrow et al., 2008) to identify NDR1 substrates.

Initially we utilized NDR1 immunoprecipitated from COS-7 cells to perform labeling reactions in whole brain lysates. In these reactions there was a paucity of specific labeling with the addition of as-NDR1, therefore we generated a baculovirus expression construct to allow us to make larger and more pure quantities of NDR1. We utilized the pFastbac HTA construct to generate a baculovirus capable of infecting SF21 insect cells. We purified the His tagged as-NDR1 construct as either the constitutively active or kinase dead form (Figure 2.3C). In order to phosphorylate NDR1 substrates with Benzyl-ATP- γ -S we reacted 10 μ g of purified kinase with 1 mg brain lysate protein. We were unable to visually see a dramatic number of new bands upon addition of as-NDR1 to brain lysate, but proceeded to analyze these samples by covalent capture followed by mass spectrometry. Briefly, labeled protein lysate was digested by trypsin, then thiol containing

peptides (including thiophosphorylated substrates and cysteine containing peptides) were captured by thiol reactive resin while non-thiol containing peptides are washed away. In the third step, beads are treated with Oxone to oxidize sulphur and elute phosphopeptides by spontaneous hydrolysis of thiophosphate linkage, whereas cysteine containing peptides remain attached to the beads by thioether bonds. Finally, the eluted peptides are analyzed by LC/MSMS to identify not only the substrates but also the phosphorylation sites, which is a major advantage of the method (Figure 2.4B).

In each experiment, we included two negative controls (lysate alone and lysate reacted with NDR1-KD) in parallel, with these controls we could disregard abundant proteins that are detected non-specifically. We carried out substrate labeling from brain lysates 8 times using P3 (2X), P8 (5X) and P13 (1X) brains, to identify potential NDR1 targets. In a typical brain lysate labeling experiment, approximately 750 different peptides (~80% phospho-peptides) belonging to ~270 proteins are detected. Of these, ~20 proteins were specific to the sample containing NDR1-as-CA. We identified 5 phospho-proteins that are specific to NDR1-as-CA and are detected in more than one experiment. Strikingly, 4 of these contained the consensus sequence for the NDR1 homolog Cbk1p (HXRRXS/T) (Mazanka et al., 2008). In addition, we cultured dissociated cortical neurons on transwell insert culture dishes in order to harvest neuronal processes but not cell bodies to simplify total protein content. We identified one additional candidate with Cbk1p consensus site: Rab11fip5 (Rab11 family interacting protein 5) which could also regulate intracellular trafficking. Proteins without the Cbk1p consensus sequence were not included in the table for this experiment.

Phosphopeptides belonging to AAK1 and Rabin8 were identified in brain lysate treated with as-NDR1 (Figure 2.5A,B). Therefore we believe that we have identified as putative NDR1 substrates AAK1 (AP-2 associated kinase 1) and Rabin8 (Rab8-GEF), which are known to function in vesicle trafficking (Henderson and Conner, 2007). Additionally we identified phosphopeptides belonging to PI4Kbeta (Phosphatidyl inositol 4 kinase beta), which catalyzes the formation of phosphatidyl inositol 4 phosphate that can give rise to other phosphatidyl inositols (De Matteis et al., 2005), Pannexin-2, a large pore ion channel expressed in the brain (MacVicar and Thompson, 2010) and Rab11fip5 which regulates Rab11 (Horgan and McCaffrey, 2009). Given the high sequence homology especially in the kinase domain and indistinguishable biochemical properties, taken together with the ability of NDR1 to rescue for NDR1/2 reduction, NDR1 and NDR2 probably have common substrates.

We were particularly interested in the two most prevalent candidates AAK1 and Rabin8 because both function in intracellular vesicle trafficking (Figure 2.5A,B). AAK1 was identified in 7 out of 8 experiments and Rabin8 was identified in 3 out of 8 experiments. Moreover, the yeast Rabin8 homolog Sec2p is phosphorylated by yeast NDR kinase Cbk1p (Kurischko et al., 2008) indicating that this kinase regulation could be evolutionarily conserved. We confirmed that AAK1 and Rabin8 were indeed phosphorylated by NDR1 by using direct kinase assay (Figure 2.6A,B). We reacted purified NDR1-as-CA with purified substrate proteins using Benzyl-ATP- γ -S and detected phosphorylation by anti-thiophosphate ester antibody after esterification with PNBM (Figure 2.6A,B), a method that avoids the background caused by AAK1 autophosphorylation when using radioactive ATP for detection. We confirmed that the

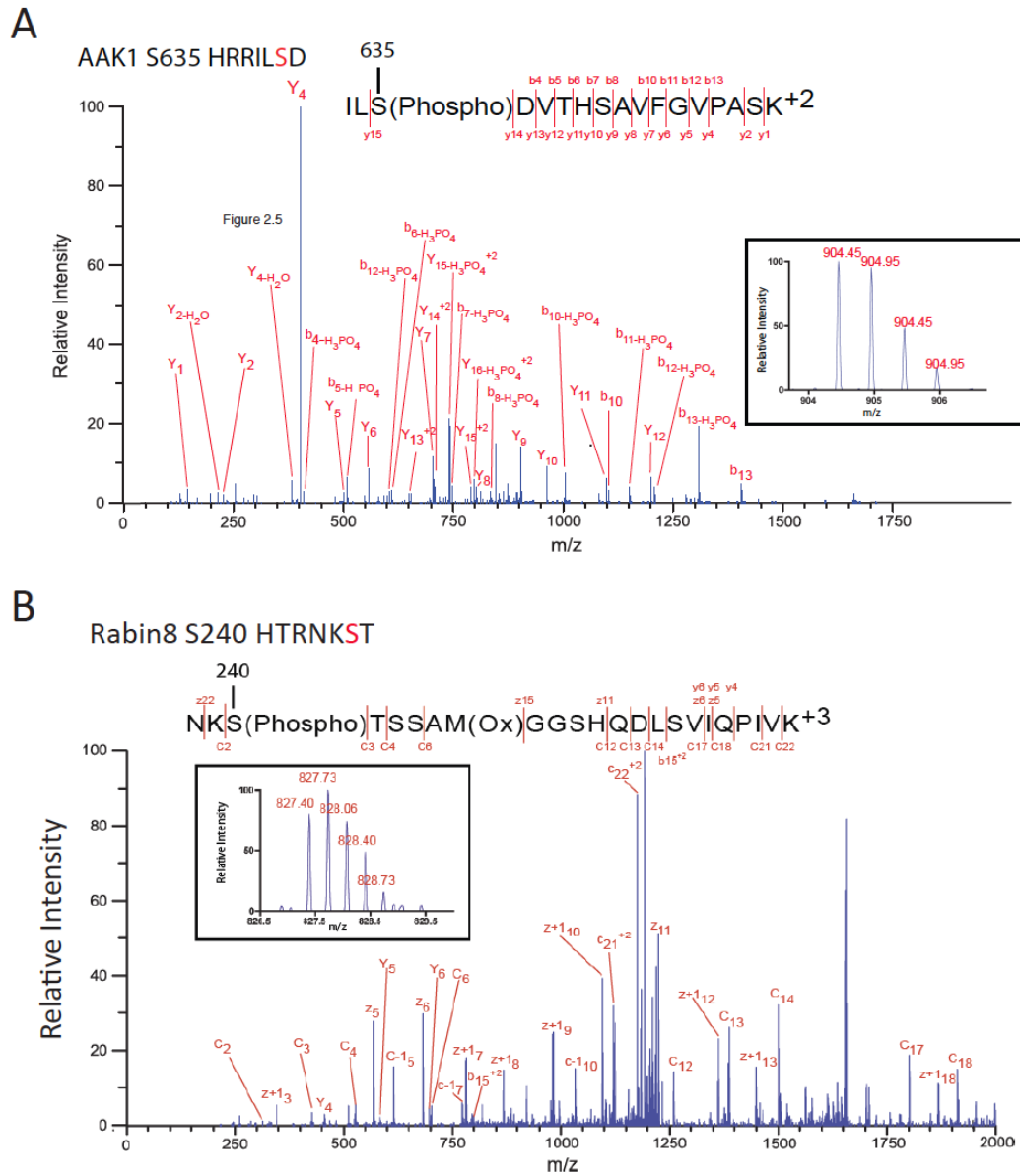


Figure 2.5 Spectra of as-NDR specific phosphopeptides. A. Mass spectroscopy identification of AAK1 phosphorylation by HCD (higher energy C-trap dissociation) spectra analysis of AAK1 derived peptide containing phosphorylated S635. B. ETD (Electron-transfer dissociation) spectra of Rabin8 derived peptide containing phosphorylated S240 is shown.

AAK1 phosphorylation site was indeed S635 (Figure 2.5A) since S635A mutant was not phosphorylated (Figure 2.6A and C). Rabin8 was phosphorylated by NDR1 at S240 (Figure 2.5B). However, there are likely other residues that can be phosphorylated since the S240A mutant could still be phosphorylated albeit at a reduced level (Figure 2.6B). Interestingly, Rabin8 S240 was followed by a stretch of T241, S242 and S243. When all S/T240-243 are mutated to Ala NDR1 no longer phosphorylated Rabin8 (Figure 2.6B).

2.3.5 AAK1 controls dendrite arborization in a similar way to NDR1/2

Next, we investigated the function of AAK1 on dendrite development and synaptic maturation. To test if AAK1 kinase activity depends on S635 in C-terminal AP-2 binding domain, we examined AAK1 autophosphorylation and found it was not affected by S635A mutation (data not shown). We generated a phospho-specific antibody for AAK1 Ser635 and asked if NDR1-CA could phosphorylate AAK1 at this residue in COS-7 cells. We found that NDR1-CA specifically phosphorylated this residue (Figure 2.6C), confirming this signaling in cells. To test AAK1's functional role we expressed AAK1 kinase dead (AAK1-KD) K74A (Conner and Schmid, 2003), the AAK1 non-phosphorylatable mutant S635A (AAK1-SA) or the AAK1 phospho-mimetic mutant S635D (AAK1-SD) together with GFP, or vector with GFP as control, in dissociated hippocampal neurons. Similar to NDR1 loss of function, AAK1-KD and AAK1-SA had increased branching within 50 μm from the soma (Figure 2.7A,B). In contrast, AAK1-SD decreased branching (Figure 2.7A,B) similar to NDR1-CA. Dendrite length was also increased in AAK1-KD and reduced in AAK1-SD mutants (Figure 2.7B) in a similar way to the effect caused by NDR1/2 functional manipulations. AAK1 siRNA, which knocked down AAK1 efficiently

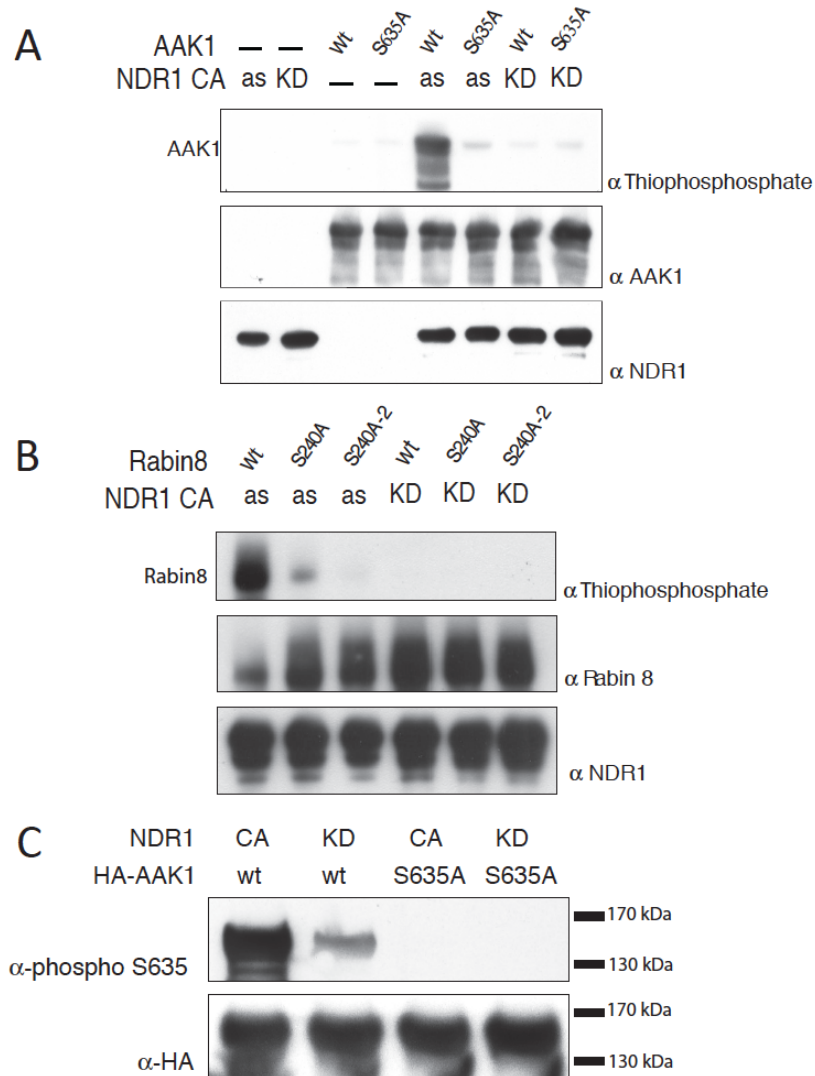


Figure 2.6 A. & B. Validation of AAK1 and Rabin8 phosphorylation sites by direct in vitro kinase assays. A. In vitro kinase assay confirmation of AAK1 S635 as the NDR1 specific phosphorylation site. In vitro kinase assays were performed by incubating the indicated NDR1-as-CA with purified wild type AAK1-HA or S635A AAK1-HA protein. Reaction was done using Benzyl-ATP- γ -S which is used by NDR1-as-CA and not AAK1 to prevent the phosphorylation signal caused by AAK1 autophosphorylation when regular ATP is used. Immunoblot with anti-thiophosphate ester specific antibody reveals S635 on AAK1 as the only NDR1 phosphorylation site on AAK1. B. Similar experiment as in E demonstrating Rabin8 as an NDR1 phosphorylation substrate protein. Rabin8 is phosphorylated by NDR1-as-CA in vitro and this phosphorylation is greatly diminished in Rabin8 S240A mutant indicating this site as the major phosphorylation site. When S/T 240-243 are all mutated to Ala (Rabin8-AAAA) all NDR1-as can no longer phosphorylate Rabin8 indicating that these residues may also be phosphorylated when S240 is mutated to Ala. C. HA tagged AAK1 wild type and AAK1 S635A were expressed in COS-7 cells with NDR1-CA or NDR1-KD. Phospho-specific S635 antibody we generated was used to detect phosphorylated AAK1 at S635. HA immunoblot is shown to detect total amount of AAK1 expressed.

(data not shown), increased dendrite branching and length and this effect was rescued with siRNA resistant AAK1 (Figure 2.7A,B,C). The dendritic spines appeared normal in AAK1-KD and AAK1-SA mutants (data not shown). However, reducing AAK1 had little effect on spine maturation as neurons expressing AAK1-KD or AAK1-SA did not exhibit reduction in mature spines or increase in filopodia (Figure 6E & F). Thus, although overactive NDR1 and constitutively phosphorylated AAK1-SD could lead to elimination of dendritic spines, most likely other NDR1/2 substrate (s) contribute to spine maturation by NDR1/2.

In order to explore if AAK1 is downstream of NDR1/2 in dendrite development, we performed epistasis experiments. Neurons were transfected with GFP expressing empty siRNA plasmid (pGmir) together with empty HA expressing plasmid (prk5) as control. NDR1si and NDR2si (GFP being co-expressed in the siRNA plasmid) + HA caused an increase in proximal dendrite branching (Figure 2.7A,C), total dendrite branching and length similar to previous data (Figure 2.7A,B). The effect of NDR1si NDR2si was rescued with AAK1-SD-HA co-expression (Figure 2.7C). In complementary experiments we transfected NDR1-CAmyc with GFP expressing empty siRNA plasmid and observed robust reduction in proximal dendrite branching (Figure 2.7C). These effects of NDR1-CA-myc were partially rescued with co-expression of AAK1si (instead of empty siRNA plasmid), indicating that AAK1 activity was necessary to limit dendrite branching.

2.3.6 Rabin8 is necessary for spine maturation

Next, we investigated Rabin8's function on dendrite development and spine maturation in hippocampal cultures. We first examined its function by mutating the

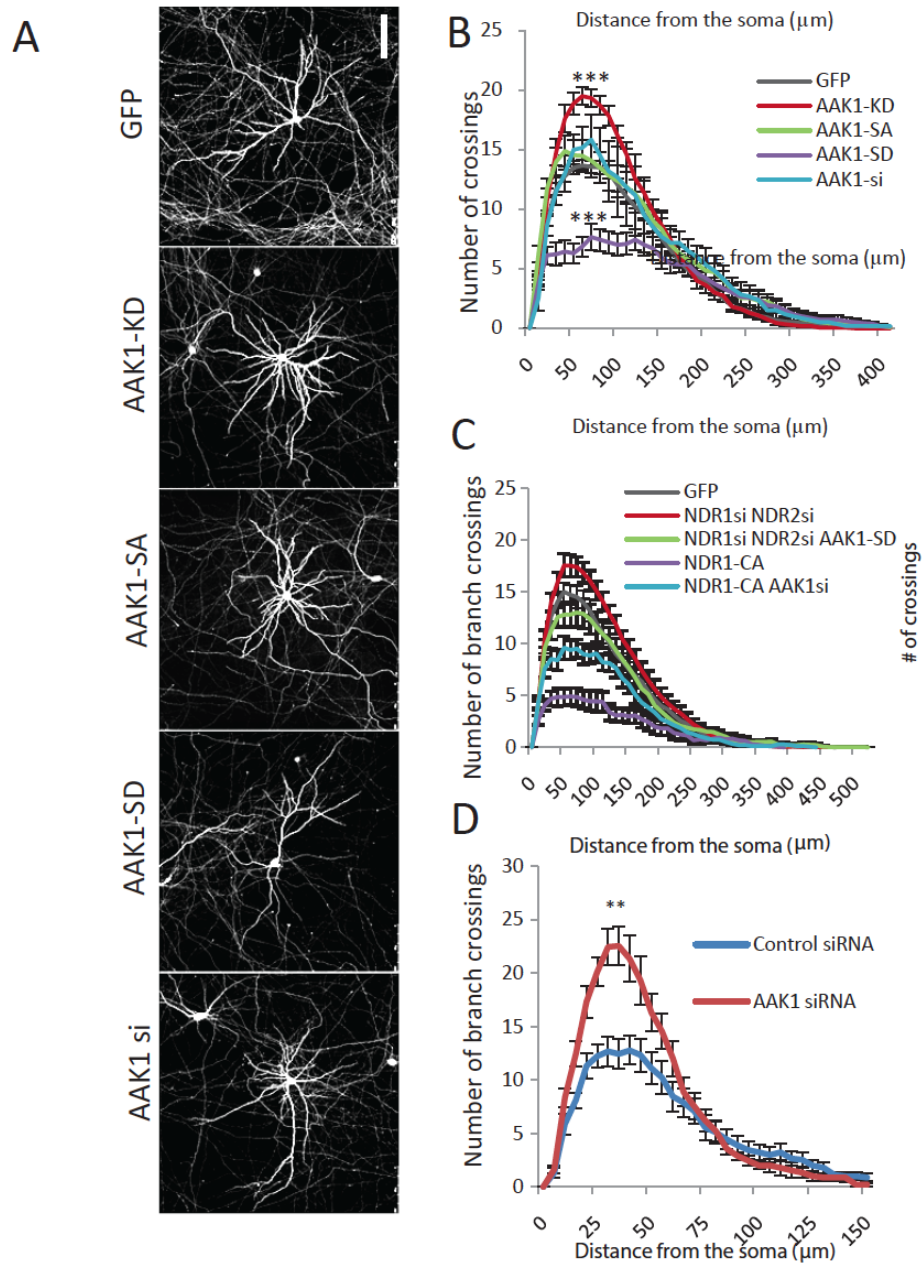


Figure 2.7 AAK1 affects dendrite branching and length in dissociated hippocampal neurons. A. Neurons expressing control vector or AAK1 mutants: AAK1-KD, AAK1-SA and AAK1-SD or AAK1-si together with GFP. Scale bar is 100 μm . B. Dendrite branching statistics are done via sholl analysis at 50 μm distance from the soma for AAK1-KD, AAK1-SA and AAK1-SD or AAK1-si. C. Dendrite branching statistics are done via sholl analysis at 50 μm distance from the soma for GFP, GFP + HA, NDR1si NDR2si +HA, NDR1si NDR2si + AAK1-SD-HA, NDR1-CA-myc + GFP, NDR1-CA-myc + AAK1si. D. Sholl analysis of AAK1 siRNA expressing neurons in comparison to Control siRNA. Dendrite branching is increased at 40 μm (N = 9 for each group, $p < 0.01$).

Rabin8 phosphorylation site and expressing these mutants in dissociated hippocampal neurons. We made Rabin8 phosphomutant where S240 as well as T241, S242 and S243 were mutated to Alanine (Rabin8-AAAA) which cannot be phosphorylated (Figure 5F) or to phosphomimetic Glutamate (Rabin8-EEEE). We found that these Rabin8 mutants and Rabin8 siRNA did not affect dendrite branching (data not shown) indicating that Rabin8 phosphorylation by NDR1 is likely not involved in limiting dendrite branching.

Next, we examined dendritic protrusion morphologies in cultures and found that Rabin8-AAAA expression but not Rabin8-EEEE resulted in increased filopodia and atypical spines and Rabin8 siRNA increased filopodia density (Figure 2.8A,B). These data indicate that Rabin8 phosphorylation by NDR1/2 contributes to spine maturation by reducing filopodia and increasing mushroom spines. Rabin8-AAAA and Rabin8si produce less pronounced defects on spines than NDR1/2 loss of function in cultures. This could be because other NDR1/2 substrates acting in parallel to Rabin8 also contribute to spine morphogenesis or these manipulations do not completely block Rabin8 function (incomplete knockdown or dominant negative effect).

Nevertheless, Rabin8 loss of function produced spine morphological changes along the same direction as NDR1/2 loss of function. Therefore we hypothesize that NDR1/2 and Rabin8 function in dendrites to ensure correct formation of dendritic spines.

2.4 Discussion

In this chapter we used dominant negative, constitutively active, siRNA expression and chemical genetics to inhibit kinase function, to demonstrate the critical role of

NDR1/2 on dendrite arbor morphogenesis and spine maturation of mammalian pyramidal neurons *in vitro* and *in vivo* (Figure 8). Using chemical genetic substrate identification by tandem mass spectrometry, we identified several direct substrates of NDR1 and the NDR1 phosphorylation sites. Among these, we validated AAK1 and Rabin8 as NDR1 targets *in vitro* and we further showed that AAK1 and Rabin8 are critical for limiting dendrite branching and length and promoting spine maturation, respectively.

2.4.1 NDR1/2, dendrite pruning and tumor-suppressors

During development previously formed dendrites are pruned in dentate granule neurons and selective dendrites are eliminated in layer 4 cortical spiny stellate neurons (Espinosa et al., 2009). It will be interesting to test whether controlled activity of NDR1/2 may regulate these and other dendrite pruning phenomena given that NDR1/2 activity is necessary and sufficient to limit branching *in vitro* and *in vivo* as shown for pyramidal neurons in our study. Pro-apoptotic signaling cascades can positively regulate dendrite pruning during *Drosophila* metamorphosis (Kuo et al., 2006) and also act to weaken synapses in mammals (Li et al., 2010). Since NDR1/2 is also a tumor suppressor (Cornils et al., 2010) and NDR1/2 promotes apoptosis in response to apoptotic stimuli in mammalian cells (Vichalkovski et al., 2008), NDR1/2 adds to the growing list of tumor suppressors which also function in neuronal growth and plasticity. In support of this scenario, the NDR1/2 homolog Trc is shown to be downstream of TORC2 (target of rapamycin complex 2) in fly which functions in controlling cell size and is implicated in cancer (Koike-Kumagai et al., 2009).

2.4.2 AAK1 phosphorylation regulates dendrite branching and length

Manipulations that disrupt NDR1/2 or AAK1 function cause similar increases in dendrite branching and length. In contrast, expression of constitutively active NDR1 and AAK1 phosphomimetic at the NDR1 phosphorylation site reduced branch number and length. We find that AAK1-SD rescued the phenotype of increased branching caused by NDR1si. NDR2si and AAK1siRNA partially rescued the severe reduction in dendrite branching caused by NDR1-CA. These findings indicate that AAK1 phosphorylation by NDR1/2 mediates its function in limiting branching and length.

AAK1 is originally identified as an alpha-adaptin binding protein (Conner and Schmid, 2002). It is necessary for efficient endocytosis and receptor recycling in mammalian cells in culture (Henderson and Conner, 2007). AAK1 phosphorylates AP-1 coat component $\mu 1$ with similar efficiency as it phosphorylates AP-2 component $\mu 2$ (Henderson and Conner, 2007), raising the possibility that it can function in multiple adaptor coat complexes. Adaptor coat complexes are central to vesicle formation on Golgi, endosomes and the plasma membrane (McNiven and Thompson, 2006; Traub, 2009). AP-2 is important for clathrin mediated endocytosis at the plasma membrane (McNiven and Thompson, 2006; Traub, 2009) whereas AP-1 coat is involved in post-Golgi and endosomal vesicle formation (McNiven and Thompson, 2006; Robinson, 2004). It is well known that secretory membrane trafficking is critical for dendrite morphogenesis (Horton and Ehlers, 2003; Horton et al., 2005; Ye et al., 2007; Ye et al., 2006). AAK1 and its yeast homolog *prk1p/ark1p* are also necessary for endocytosis (Henderson and Conner, 2007; Sekiya-Kawasaki et al., 2003). Importantly, a potential Cbk1p phosphorylation site was identified in Prk1p. Prk1p's role on endocytosis depends

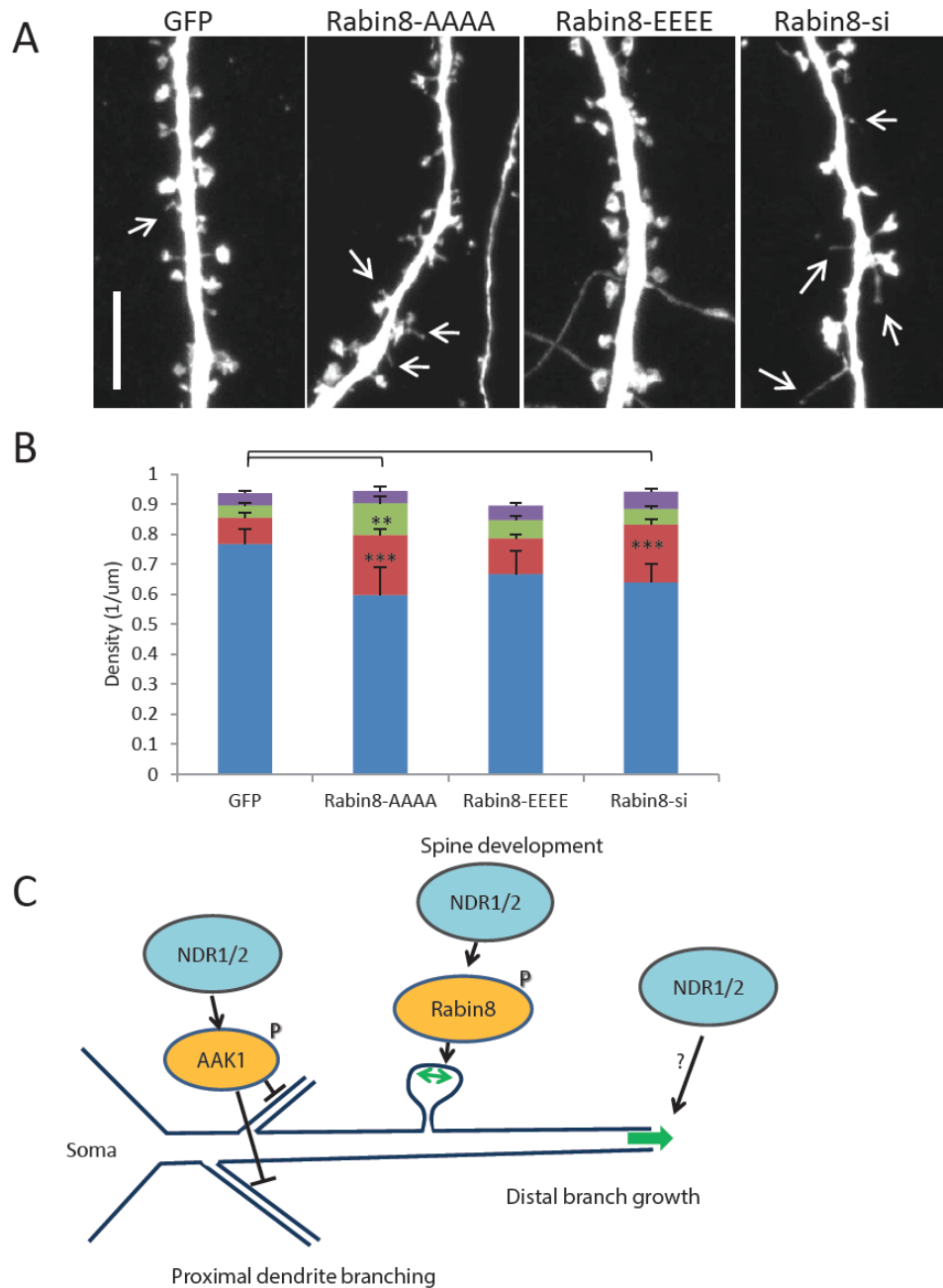


Figure 2.8 Rabin8 affects spine morphogenesis in dissociated hippocampal neurons. A. Dendritic spine morphologies of control, Rabin8 mutants and siRNA expressing neurons. Arrows point to filopodia. Scale bar is 6 μm . B. Quantification of spine morphologies. N = 23, 13, 12 & 17, for GFP, Rabin8-AAAA, Rabin8-EEEE and Rabin8-si, respectively. D. Model representing NDR1/2's function on dendrite development and spine morphogenesis based on data from hippocampal cultures and cortical neurons in vivo. Reduced levels of NDR1/2 activity leads to increased proximal branching and reduced distal growth while inhibiting spine maturation. Increased levels of NDR1 activity leads to reduced proximal dendrite branching with increased distal growth while reducing total dendritic protrusion density.

on its ability to destabilize actin cytoskeleton at endocytic zones (Toshima et al., 2005). A similar mechanism of actin destabilization could underlie the loss of dendritic spines in NDR1-CA or AAK1-SD expressing hippocampal neurons. Thus several line of evidence suggest that AAK1 regulates intracellular vesicle trafficking. How AAK1 function regulates dendrite morphogenesis remains to be investigated.

2.4.3 Rab8 GEF Rabin8 regulates spine morphogenesis

Expression of AAK1-KD or AAK1 siRNA did not affect spine morphology, suggesting additional NDR1/2 substrates may be involved in spine morphogenesis. Rabin8, first identified as a Rab3 interacting protein (Brondyk et al., 1995), is known to act as a guanine exchange factor for Rab8 rather than Rab3 (Hattula et al., 2002). Rab8 is a small GTPase specialized in post-Golgi vesicle budding and transport to the plasma membrane (Stenmark, 2009). In hippocampal cultures we find that Rabin8 is predominantly enriched in the Golgi in soma and proximal dendrites. In yeast, Rabin8 homolog Sec2p was found to be phosphorylated by yeast NDR kinase Cbk1p and was shown to account for a subset of the Cbk1p mutant defects (Kurischko et al., 2008). Importantly, the phosphorylation site is conserved between Sec2p and Rabin8. It thus appears that NDR kinase regulation of vesicle trafficking is an evolutionarily conserved function for controlling polarization and cell morphology. Our data suggest that Rabin8 and its phosphorylation by NDR1/2 is essential for spine maturation, in cultured neurons and *in vivo*. Rabin8 could affect Rab8 function to form and/or deliver post-Golgi vesicles to dendritic membrane so as to allow the synapses to mature and increase in spine head diameter. In support of this hypothesis, Rab8 GTPase dominant negative mutant

expression in cultured hippocampal slices alters AMPA receptor delivery to surface (Brown et al., 2007; Gerges et al., 2004). Expression of phosphomimetic Rabin8-EEEE partially rescued the phenotype due to NDR1/2 loss of function by siRNA, indicating that other NDR1/2 substrates likely contribute to spine morphogenesis.

NDR1/2 regulates dendrite growth

Loss of NDR1/2 affects preferentially the proximal dendritic branching, causing an increase in proximal branching and a decrease in distal branching. At the same time activated NDR1-as causes increased dendrite branching in the distal regions as shown in sholl analysis. Therefore, NDR1/2 may function in promoting distal growth at the expense of proximal branch additions. NDR1/2's role on branch extension and its potential downstream effectors remain to be investigated. Our data showing reduced dendrite length by Rabin-AAAA suggests that Rabin8 may be involved in this process.

2.4.4 Other candidate substrates of NDR1/2

It is interesting to note that some of the potential substrates of NDR1/2 identified in our study could also affect vesicle trafficking. For instance, PI4KB can catalyze formation of phosphatidyl inositol 4 phosphate (PI4P), which is an intermediate in the formation of phosphorylated lipids such as PI3,4 bisphosphate, PI4,5 bisphosphate and PI3,4,5 trisphosphate (De Matteis et al., 2005). These phospholipids are known to affect membrane trafficking in post-Golgi and recycling membrane compartments (De Matteis et al., 2005). Another potential substrate, Rab11fip5, is a member of Rab11 family

interacting proteins (Horgan and McCaffrey, 2009), which could affect membrane trafficking from recycling endosomes on dendrites (Wang et al., 2008).

2.4.5 Chemical genetics for kinase substrate identification

The chemical genetics and covalent capture method for kinase substrate identification is a powerful method for rapid mapping of kinase signaling pathways with the unique advantage of phosphorylation site identification. This method also allows the identification of substrates from complex tissue homogenates where the protein complexes may be better preserved when compared to other methods which involve gel electrophoresis or chips. Prior to this study, no NDR1/2 substrates have been identified in any multicellular organisms and only two substrates have been found for yeast Cbk1p. We were able to identify 5 novel mammalian substrates and validated two of these functionally. Our screen identified the mammalian homolog of one of the yeast substrates Sec2p, confirming its effectiveness and establishing an evolutionarily conserved branch of NDR kinase signaling. Our technique offers an unbiased method for identifying kinase substrates from different tissues, developmental stages and pathologies. This approach would make it possible to determine how NDR1/2 activity and targets are altered in pathologies such as neurodevelopmental, neurodegenerative diseases and cancer.

2.5 Experimental Procedures

Kinase assays and covalent capture for phosphorylation target identification

NDR kinase assays were done as described (Stegert et al., 2005). Covalent capture of thiophosphorylated substrate proteins was performed as described (Hertz et al., 2010)

Chapter 3

**Development of a chemical genetic approach for human
Aurora B kinase identifies novel substrates of the chromosomal
passenger complex**

2.1 Abstract:

To understand how the chromosomal passenger complex (CPC) ensures chromosomal stability, it is crucial to identify its substrates and to find ways to specifically inhibit the enzymatic core of the complex, Aurora B. We therefore developed a chemical genetic approach to selectively inhibit human Aurora B. By mutating the gatekeeper residue L154 in the kinase active site, the ATP binding pocket was enlarged but kinase function was severely disrupted. A unique second-site suppressor mutation was identified that rescued kinase activity in the L154 mutant and allowed the accommodation of bulky N⁶-substituted adenine analogs. Using this analog-sensitive Aurora B kinase we found that retention of the CPC at the centromere depends on Aurora B kinase activity. Furthermore, analog-sensitive Aurora B was able to use bulky ATP γ S analogs and could thiophosphorylate multiple proteins in cell extracts. Utilizing an unbiased approach for kinase substrate mapping we identified several novel substrates of Aurora B, including the nucleosomal-binding protein HMGN2. We confirmed that HMGN2 is bona-fide Aurora B substrate *in vivo* and show that its dynamic association to chromatin is controlled by Aurora B. Additionally, by making a nuclear excluded Aurora B construct, we were able to identify additional putative Aurora B targets that may be important in mitosis.

3.2 Introduction

Faithful chromosome segregation requires that the duplicated sister-chromatids bi-orient on the mitotic spindle, and that anaphase onset does not start before this is accomplished for all chromosomes. The chromosomal passenger complex is essential for this as it specifically destabilizes incorrectly attached spindle microtubules from the kinetochores of the chromosomes and acts on the mitotic checkpoint that inhibits the APC/C until all chromosomes have acquired the correct bipolar attachments (Ruchaud et al., 2007). In addition, this complex is important for cytoplasmic division and may have additional functions outside mitosis, such as DNA damage repair in G2 (Monaco et al., 2005) and the epigenetic silencing of gene expression (Sabbattini et al., 2007). While it is accepted that the CPC is essential for proper cell division, its potential functions outside mitosis are only beginning to be uncovered. To reveal new *in vivo* functions of the CPC and to understand how this complex is capable of fulfilling all these different functions it is important to specifically and completely inhibit the enzymatic core of the complex (Aurora B) without affecting the stability of the other CPC subunits (INCENP, borealin, survivin).

Current approaches to inhibit Aurora B (siRNA and small molecule inhibitors) are important research tools but they do suffer from variations in the level of protein knockdown or kinase inhibition (Weiss et al., 2007). In particular, the presence of two other Aurora kinases (A and C) with a high degree of homology to Aurora B, makes it particularly challenging to identify small molecules that selectively inhibit Aurora B (Lens et al., 2010). Due to the high level of active site homology, finding an inhibitor concentration that completely inhibits the kinase of interest in cells without affecting any

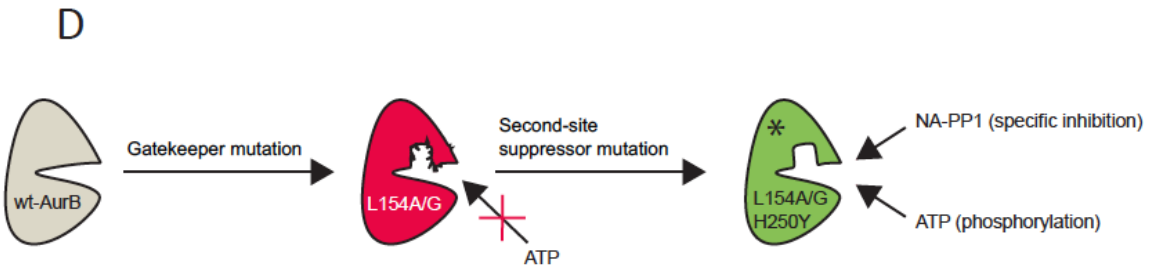
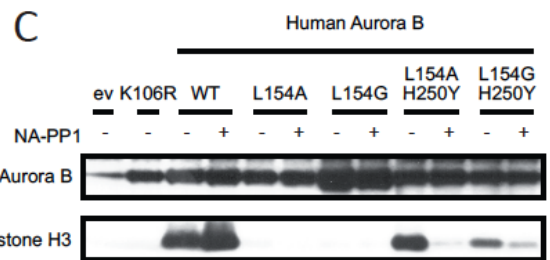
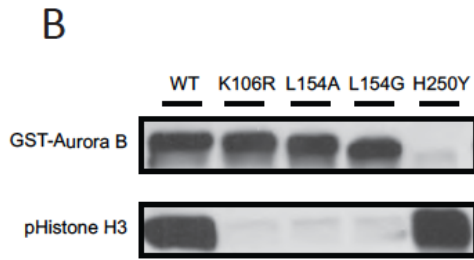
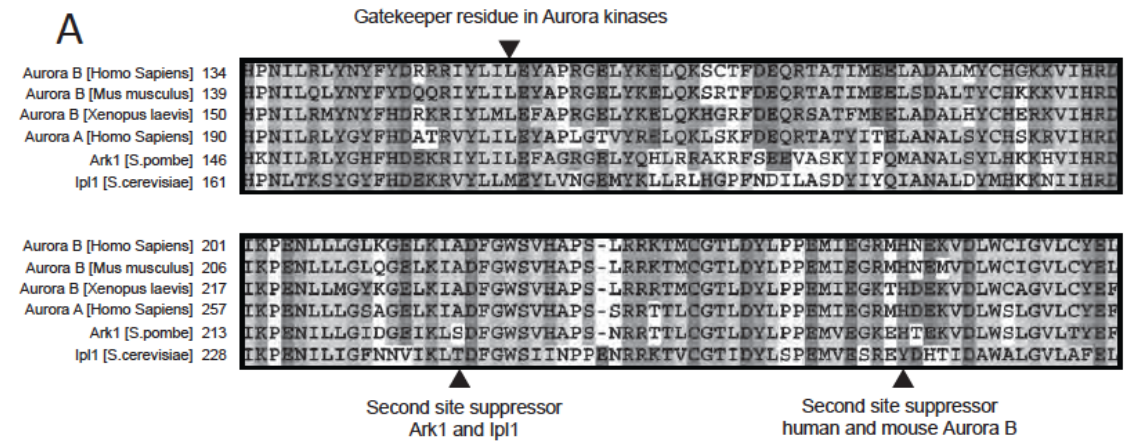


Figure 3.1 The H250Y mutation rescues kinase activity of Aurora B gatekeeper mutants. A. Multiple sequence alignment of the Aurora kinases in different species. The gatekeeper residue and the second site suppressor mutation found in Ark1 and Ipl1 as well as the newly identified second site suppressor mutation for human and mouse Aurora B are indicated. B. In vitro kinase assay with the indicated recombinant GST-tagged Aurora B proteins and histone H3 as substrate. Phosphorylation of histone H3 was detected with an antibody specific for phospho -- serine 10. Note that even a small amount of Aurora BH250Y results in massive phosphorylation of histone H3. C. FLAG-tagged human Aurora B mutants were immunoprecipitated from mitotic U2OS cells. Kinase assays were performed in the presence of ATP and with or without NA--PP1 (2 μ M). Histone H3 was used as substrate. D. The H250Y mutation rescues kinase activity of Aurora B gatekeeper mutants. The double mutants are inhibited by NA--PP1

other kinase is nearly impossible. Hence, using the current approaches to target Aurora B makes it difficult to unequivocally resolve the *in vivo* functions of the CPC and may complicate the assignment of true Aurora B substrates. We have therefore developed a chemical-genetic system that allows specific Aurora B inhibition and direct substrate identification.

Chemical genetics refers to a strategy where a kinase is genetically engineered to render it capable of utilizing non-natural ATP analogs to be preferentially utilized as substrates and additionally to be sensitive to unique inhibition by cell permeable ATP analogs (Bishop et al., 2000b; Shah et al., 1997). This so-called analogue-specific kinase harbors a mutation in the ATP-binding pocket that changes a bulky amino acid (i.e. methionine, leucine, phenylalanine or threonine) into a small amino-acid (glycine or alanine). Mutation of this ‘gate-keeper’ residue enlarges the ATP-binding pocket allowing it to accommodate bulky side-chains of ATP analogs and making it susceptible to cell-permeable derivatives of the Src inhibitor PP1 (PP1 inhibitors) (Bishop et al., 2000a). Approximately 30% of kinases lose their catalytic activity after mutation of the gate-keeper residue, but functionality can be restored by introduction of one or more second-site suppressor mutations (Zhang et al., 2005). Catalytic activity is critical when attempting to map direct kinase substrates in an unbiased manner (Blethrow et al., 2008).

Human Aurora B turned out to be one of the kinases that did not tolerate mutation of the gate-keeper residue (L154) and for which mutation of the predicted second-sites failed to restore functionality. In this chapter, we describe the identification of a unique second-site suppressor mutation that restored activity of the Aurora B gatekeeper mutants and that made the kinase susceptible to inhibition by PP1 analogs. Using these analog-

specific Aurora B mutants we demonstrate that retention of the CPC at the centromere depends on Aurora B kinase activity. We also show that the activated Aurora B is capable of using bulky ATP γ S analogs to thiophosphorylate multiple proteins in complex cell extracts, including a number of known Aurora B substrates. As this approach is not biased with respect to known consensus sites or for particular functional categories of putative substrates, it is particularly useful for identifying novel direct substrates. Indeed, we found a number of potential novel Aurora B phosphorylation sites on previously reported substrates, as well as novel substrates of the kinase including the nucleosomal-binding protein HMGN2. Additionally we have developed a nuclear excluded construct of Aurora B/INCENP that will block phosphorylation of nuclear substrates involved in mitosis, thereby allowing us to identify these targets via our chemical genetic approach.

3.3 Results

3.3.1 Human Aurora B does not tolerate mutation of the Leucine 154 gatekeeper

Generation of an analog-sensitive kinase requires engineering of the ATP-binding pocket by mutation of a bulky amino acid (the so-called ‘gate-keeper’) into a small amino-acid (glycine or alanine), to accommodate bulky side-chains of ATP analogs and making it susceptible to cell-permeable derivatives of the Src inhibitor PP1 (PP1 inhibitors) (Bishop et al., 2000a; Bishop et al., 2000b). The gatekeeper of human Aurora B is leucine-154 (Figure 3.1A) (Blethrow et al., 2004) and this hydrophobic residue was mutated into the smaller alanine or glycine residues to alter the shape of the ATP-binding pocket. Recombinant Aurora B^{wt} readily phosphorylated Ser10 of Histone H3 *in vitro*,

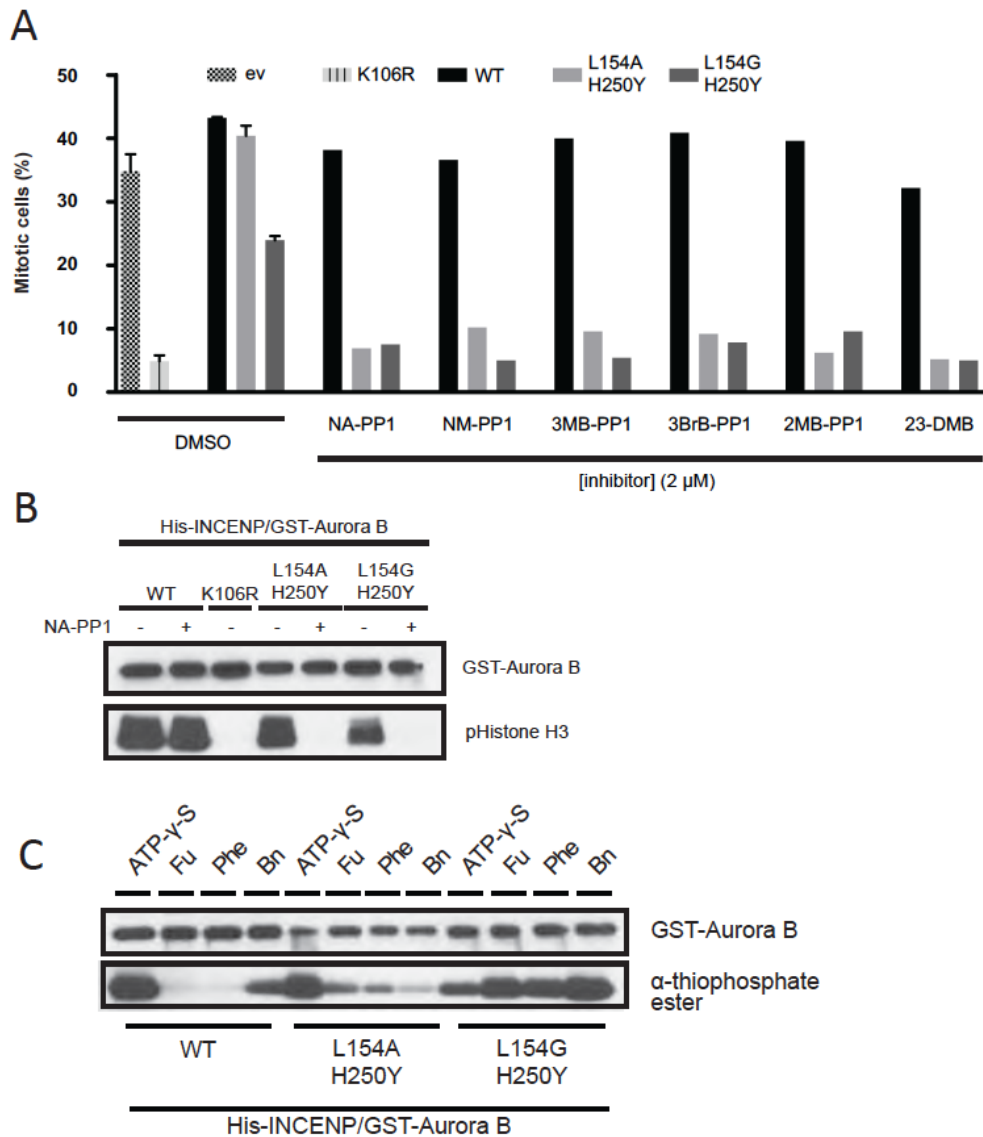


Figure 3.2 The analog-sensitive Aurora B mutants are inhibited by PP1 and can utilize N6 modified ATP analogs. A. U2OS cells expressing the indicated proteins were released from a thymidine-induced G1/S block into medium containing paclitaxel plus or minus the indicated PP1 analogs. Seventeen hours after release, the mitotic index was determined by propidium iodide/MPM2 monoclonal antibody labeling and FACS analysis. B. A, *in vitro* kinase assay with recombinant His-INCENP/GST-tagged Aurora B, co-purified from SF9 cells, in the presence of ATP and with or without NA-PP1 (2 μ M). Histone H3 was used as a substrate. B, *in vitro* kinase assay with recombinant His-INCENP/GST-tagged Aurora B (wild-type or analog-sensitive mutants) in the presence of ATP, N6-furfuryl-ATP γ S (Fu), N6-phenylethyl-ATP γ S (Phe), or N6-benzyl-ATP γ S (Bn). Thiophosphorylated histone H3 was detected with a thiophosphate ester epitope-specific antibody.

but both Aurora B gatekeeper mutants failed to do so, similar to a known kinase-dead Aurora B^{K106R} mutant. In cells, Aurora B resides in a complex with INCENP, borealin and survivin (the chromosomal passenger complex, CPC) and the binding of Aurora B to the COOH-terminal IN-box of INCENP is required for full Aurora B kinase activity (Bishop and Schumacher, 2002; Honda et al., 2003; Sessa et al., 2005). To test if the gate-keeper mutants were active when in complex with the other CPC members, flag-tagged Aurora B^{L154A} and Aurora B^{L154G} mutants were expressed in U2OS cells, immunoprecipitated from mitotic cell extracts, and the protein complexes were subjected to *in vitro* kinase reactions. Also under these conditions only wild-type Aurora B displayed kinase activity while the kinase-dead and gatekeeper mutants were inactive (Figure 3.1B). Thus, mutation of the L154 gatekeeper residue is not tolerated in human Aurora B.

3.3.2 Identification of a unique second-site suppressor mutation for the human Aurora B gatekeeper mutants

Approximately 30% of kinases tested do not tolerate gatekeeper mutations, and we showed that Aurora B falls within this group. For several intolerant kinases second-site suppressor mutations were identified that could rescue kinase activity (Zhang et al., 2005). For the yeast homologues of Aurora B (Ipl1 in *S. cerevisiae* and Ark1 in *S. pombe*) such a second site suppressor mutation was identified (Hauf et al., 2007; Pinsky et al., 2006) and we therefore expected to find the second site suppressor residue for human Aurora B via amino acid sequence alignment. In the *Ipl1-as*, and *Ark1-as* mutants,

respectively T244 and S229, were changed into glycine or alanine (Hauf et al., 2007; Pinsky et al., 2006). Surprisingly, mammalian Aurora B and Aurora A already carry an alanine at that position (Figure 3.1A), indicating that mammalian Aurora's require a different second-site suppressor mutation. Recently four Aurora B mutations were identified in cell lines with acquired resistance for the small molecule Aurora B inhibitor ZM447439 (Girdler et al., 2008). Three of these mutations were located in the catalytic active site, while the fourth, H250Y, was in close proximity of the activation loop and strongly enhanced the Aurora B kinase activity (Girdler et al., 2008) (and Figure 3.1B). Interestingly, multiple sequence alignment showed that Ipl1 had a tyrosine residue at this position (Figure 3.1A).

To test if the H250Y mutation could rescue kinase activity of the Aurora B gatekeeper mutants, we engineered the Aurora B^{L154A/H250Y} and Aurora B^{L154G/H250Y} double mutants by site-directed mutagenesis. FLAG-tagged mutant proteins were expressed in U2OS cells, immunoprecipitated from mitotic cell extracts and kinase activity of the protein complexes against Histone H3 was tested *in vitro*. Strikingly, the Aurora B^{L154A/H250Y} mutant phosphorylated Histone H3 similar to wild-type Aurora B, but unlike Aurora B^{wt}, its activity was inhibited by the bulky PP1 analog NA-PP1 (Figure 3.1C). The Aurora B^{L154G/H250Y} mutant displayed lower kinase activity than the Aurora B^{L154A/H250Y} mutant, but its activity was further inhibited by NA-PP1 (Figure 3.1C). This shows that the H250Y mutation acts as a second site suppressor and rescues the kinase activity of the Aurora B gatekeeper mutants (Figure 3.1D). Of note, both mutants needed an intact CPC (or at least INCENP) to be active, since bacterially expressed recombinant Aurora B mutants were not active (data not shown). Importantly, we found exactly the

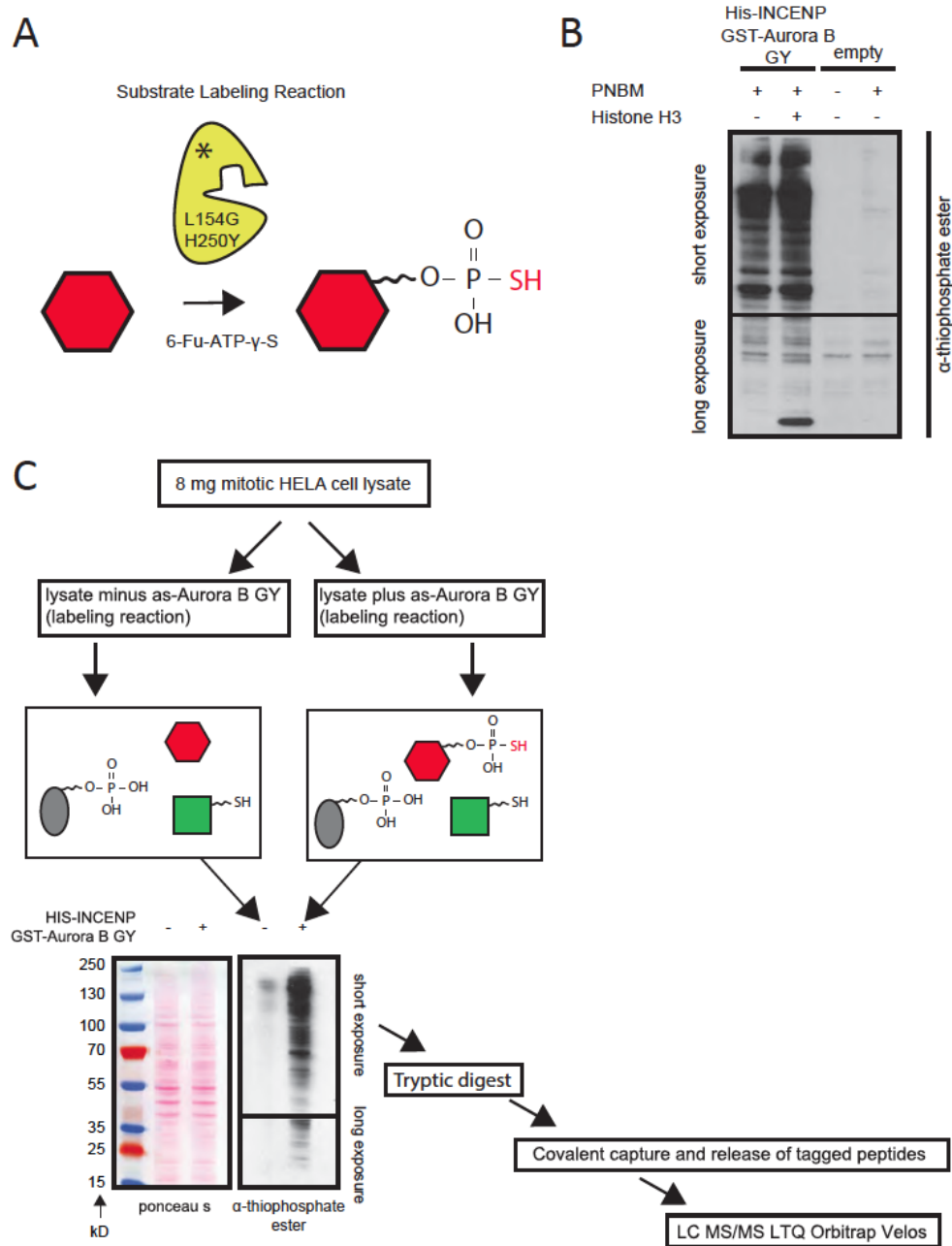


Figure 3.3 Identification of putative Aurora B substrates by covalent capture and release of thiophosphorylated peptides. A, Model for the as-Aurora B specific labeling of substrate (shown in red). B, *in vitro* kinase assay with as-Aurora B (His-INCENP/ GST-Aurora B L154G/H250Y) in the presence of N6-furfuryl-ATP γ S. 50 μ g of a mitotic HeLa cell lysate was used as input, and histone H3 was spiked into this lysate to serve as positive control. For the lower part of the blot (containing proteins with molecular masses of 15–50 kDa), a longer exposure (5 min instead of 15 s for the short exposure) is shown. C, set-up of Aurora B substrate screen using the covalent capture-and-release method.

same results for mouse Aurora B where loss of kinase activity due to mutation of the L159 gatekeeper residue into alanine was rescued by mutation of H255 into tyrosine (Data not shown).

3.3.3 Analog-sensitive Aurora B mutants are inhibited by low concentrations of NA-PP1 in cells

To study the function of Aurora B^{L154A/H250Y} and Aurora B^{BL154G/H250Y} in cells, we analyzed the behavior of Aurora B^{L154A/H250Y} and Aurora B^{BL154G/H250Y} expressing U2OS cells in paclitaxel. Paclitaxel is a microtubule-stabilizing drug that induces a mitotic delay due to the activity of the mitotic checkpoint (Jordan and Wilson, 2004). Inhibition of Aurora B in paclitaxel-treated cells compromises the mitotic checkpoint and cells exit mitosis (Ditchfield et al., 2003; Hauf et al., 2003). The mitotic index of cells treated with paclitaxel was therefore used as a measure of Aurora B kinase function. Aurora B^{wt} - expressing cells were arrested in mitosis after exposure to paclitaxel and addition of 2 μ M NA-PP1 did not affect this mitotic arrest (Figure 3.2A). As expected the mitotic index of Aurora B^{K106R} expressing cells was reduced to <5% (Figure 3.2A), confirming that this kinase-dead mutant is dominant negative and that reduced Aurora B activity overrides the mitotic checkpoint when microtubules are stabilized by paclitaxel (Ditchfield et al., 2003; Lens et al., 2003; Murata-Hori and Wang, 2002). Interestingly, while overexpression of the inactive Aurora B^{L154A} and Aurora B^{L154G} single mutants perturbed the response to paclitaxel Aurora B^{L154A/H250Y} expressing cells reached a mitotic index of approx. 40%, similar to Aurora B^{wt} expressing cells (Figure 3.2A). However, addition of NA-PP1 to the Aurora B^{L154A/H250Y} expressing cells resulted in a dramatic reduction in the mitotic index, indicating that Aurora B^{L154A/H250Y} only acts in a

A

LCMSMS Analysis of enriched phosphopeptides

	Lysate 1	Lysate 2	Lysate 1	Lysate 2	as-Aurora B
Protein (phosphopeptide identified)	-	-	+	+	
Leucine-rich repeat-containing protein 59					
F-actin-capping protein subunit alpha-2					
Putative Aurora B Substrate 1					
Eukayotic initiation factor 4A-I					
Putative Aurora B Substrate 2					
F-actin-capping protein subunit alpha-3					

B

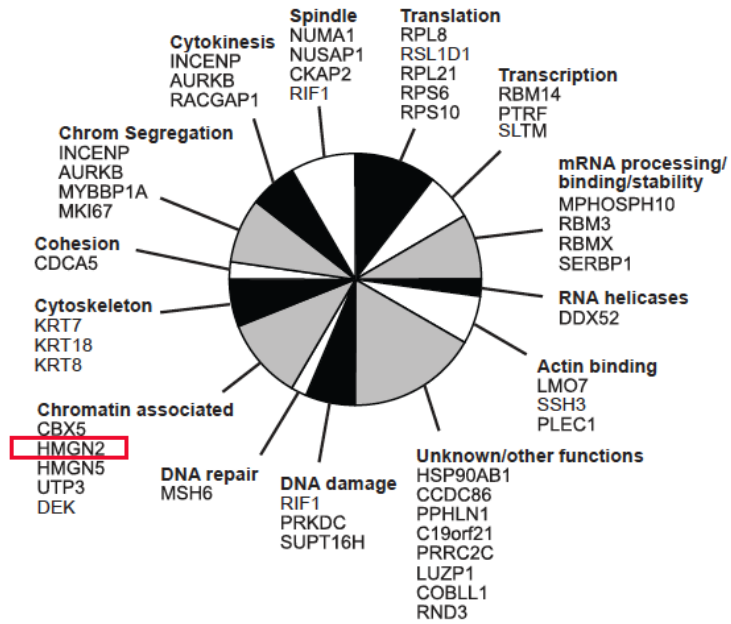


Figure 3.4 Analysis of the resulting peptides identified by mass spectrometry. A. Peptides found by MS analysis only following addition of as-Aurora B, not kinase dead or wt, were characterized as potential substrates. B, potential Aurora B substrates containing the RX(S/T) consensus motif (including ambiguous sites). Substrates were only listed if thiophosphorylated peptides were found in two independent experiments.

dominant-negative fashion when inhibited by NA-PP1 (Figure 3.2A). In line with its reduced activity cells expressing Aurora B^{L154G/H250Y} displayed a reduced mitotic index in paclitaxel (\pm 25%) compared to Aurora B^{wt} and Aurora B^{L154A/H250Y} expressing cells. Addition of NA-PP1 further reduced the mitotic index, showing that Aurora B^{L154G/H250Y} was also sensitive to NA-PP1 (Figure 3.2A). To test which PP1 inhibitor analog was the most potent inhibitor of Aurora B-as kinases, we tested six different PP1 inhibitors (NA-PP1, NM-PP1, 3MB-PP1, 3BrB-PP1, 2MB-PP1 and 23-DMB) against Aurora B^{L154A/H250Y} and Aurora B^{L154G/H250Y} expressing cells and determined the mitotic index after paclitaxel treatment (Figure 3.2A). All of these inhibitors inhibited the Aurora B-as mutants at a concentration of 2 μ M, but titration of NA-PP1, NM-PP1 and 23-DMB showed that both Aurora B-as mutants were most sensitive to NA-PP1 (data not shown).

3.3.4 Analog-sensitive Aurora B mutant can thiophosphorylate multiple proteins in cell extracts

To selectively label and isolate Aurora B substrates from cell extracts one has to use bulky ATP γ S analogs to thiophosphorylate target proteins. However, to achieve this it is crucial to obtain sufficient amounts of active recombinant kinase that can utilize these bulky ATP γ S analogs, We therefore isolated recombinant Aurora B in complex with His-INCENP from insect (Sf9) cells and tested if this recombinant protein complex phosphorylated Histone H3 *in vitro*. Similar to our previous results with the immunoprecipitated proteins, we found that the recombinant INCENP/Aurora B^{wt} and INCENP/Aurora B^{L154A/H250Y} protein complexes readily phosphorylated Histone H3 *in vitro* while phosphorylation by INCENP/Aurora B^{L154G/H250Y} was reduced (Figure 3.2B).

TABLE 3.1
*Overview of the 92 phosphorylated sites found in all 114 peptides
(peptides were found in one or two experiments) corresponding to 58
proteins*

	Number of phosphosites	Site	
		SLIP score of ≥ 6 or singly present in peptide	Ambiguous
Total	92	70	22
RX(S/T) Φ	43	36	7
RX(S/T)X Φ	18	14	4
RX(S/T)XX	7	7	0
Non-RX(S/T)	24	13	11

Again, NA-PP1 only inhibited the recombinant analog-sensitive Aurora B mutants and not Aurora B^{wt}.

Remarkably, though, when we tested three different bulky ATP γ S analogs, we found that INCENP/Aurora B^{L154G/H250Y}, but not INCENP/Aurora B^{L154A/H250Y} and INCENP/Aurora B^{wt} efficiently thiophosphorylated Histone H3 in the presence of all three bulky ATP γ S analogs (Figure 3.2C). Since INCENP/Aurora B^{wt} showed some reactivity with N6-Bn-ATP γ S, and thiophosphorylation of Histone H3 by INCENP/Aurora B^{L154G/H250Y} was more efficient with N6-Fu-ATP γ S than with N6-PhEt-ATP γ S (Figure 3.2C), we choose N6-Fu-ATP γ S to perform a kinase reaction in a whole cell extract prepared from mitotic HeLa cells. As shown in Figure 3.3A,B, INCENP/Aurora B^{L154G/H250Y} could still thiophosphorylate recombinant Histone H3 in the presence of 50 μ g of total cell extract and more importantly, we detected multiple thiophosphorylated proteins in the extract in which recombinant His-INCENP/ Aurora B^{L154G/H250Y} was present that were not present in the negative control indicating these proteins were thiophosphorylated by INCENP/Aurora B^{L154G/H250Y} (Figure 3.3B).

TABLE 3.2
Aurora B substrates unique to this screen

The criteria for inclusion include phosphopeptide(s) found in two independent experiments, RX(S/T) motif, E-score $\leq 10E-4$, SLIP score ≥ 6 , and substrate not found by Kettenbach *et al.* (30).

Name	Full name	Phosphosite	Site found in other phosphoproteome database? (www.phosphosite.org)	Reported function
DEK	DEK	Thr-67	No	Chromatin associated
UTP3	Something about silencing protein 10	Ser-462	No	Chromatin associated
HMGN2	Non-histone chromosomal protein HMG-17	Ser-29	Yes	Chromatin associated
HMGN5	High mobility group nucleosome-binding domain-containing protein 5	Ser-20, Ser-24	Yes	Chromatin associated
KRT8	Keratin, type II cytoskeletal 8	Thr-6, Ser-34	No/Yes	Cytoskeleton
KRT7	Keratin, type II cytoskeletal 7	Ser-27	No	Cytoskeleton
RIF1	Telomere-associated protein RIF1	Ser-2205	Yes	Spindle/DNA damage
PRKDC	DNA-dependent protein kinase catalytic subunit	Ser-511	Yes	DNA damage
RPS10	40 S ribosomal protein S10	Thr-118	No	Translation
RPL21	60 S ribosomal protein L21	Ser-104	Yes	Translation
RPL8	60 S ribosomal protein L8	Ser-130	No	Translation
PTRF	Polymerase I and transcript release factor	Ser-300	Yes	Transcription
SSH3	Protein phosphatase Slingshot homolog 3	Ser-37	Yes	Actin binding
RACGAP1	Rac GTPase-activating protein 1	Thr-249	Yes	Cytokinesis
MPHOSPH10	M phase phosphoprotein 10	Thr-332	No	mRNA processing
HSP90AB1	Heat shock protein HSP 90- β	Ser-452	Yes	Unknown
COBLL1	Cordon-bleu protein-like 1	Ser-955	No	Unknown
PPHLN1	Periplin-1	Ser-110	Yes	Unknown
PRRC2C/BAT2D	BAT2 domain-containing protein 1	Ser-1013	No	Unknown
C19orf21	Uncharacterized protein C19orf21	Ser-348	No	Unknown

3.3.5 Identification of Aurora substrates and site of phosphorylation in cell extracts

Next, we performed two independent kinase reactions with 4 μ g recombinant His-INCENP/Aurora B^{L154G/H250Y} complex and 4 mg of mitotic cell extract, or with 4 mg of mitotic cell extract without addition of the recombinant protein complex (negative control) (Figure 3.3C). Thiophosphorylated peptides were isolated according to the covalent capture-and-release methodology, described by Blethrow *et al.* (Blethrow *et al.*,

2008) and Hertz *et al.* (Hertz et al., 2010a) and peptides were analyzed by mass spectrometry. The phosphopeptides were then compared between the samples, and only peptides that were never identified in the negative control samples but were present with INCENP/Aurora B^{L154G/H250Y} were predicted to be putative Aurora B substrates (Figure 3.4A). In total 114 phosphorylated peptides were identified in the plus His-INCENP/Aurora B^{L154G/H250Y} samples, revealing 92 unique phosphosites in a total of 58 proteins (Table 3.1). When we only considered the phosphosites with a SLIP score threshold of 6, or singly present in the peptide (Baker et al., 2011) (n= 70, Table 3.1), we found in 57 of the 70 phosphosites (81%) an arginine (R) at position -2, in line with the previously predicted Aurora consensus motif [K/R]-X-[S/T][I/L/V](Cheeseman et al., 2002) (where X represents any residue) and in line with a recent peptide-library screen by Alexander *et al.* (Alexander et al., 2011)(Table 3.1). Similar to that work we also found a preference for hydrophobic residues in the +1 (36/57 sites) or +2 position (14/57 sites)(Table 3.1). Moreover, in line with the published finding that a proline (P) at position +1 is not tolerated by Aurora kinases (Alexander et al., 2011), we did not find peptides with an R at -2 and a P at +1. In the 13 non R-X-[S/T] sites we found in 2 cases an arginine (R) or a lysine (K) at -1, and in 3 cases an R at -3, in each case combined with an hydrophobic residue in position +1 or +2, a situation that may also be considered as Aurora-specific (Kettenbach et al., 2011). For 5 out of the 8 remaining non R-X-[S/T] sites, an adjacent R-X-[S/T] motif was not present in the purified peptide, and these could thus represent novel unexpected Aurora sites. Yet, given the fact that one of these sites is a validated Cdk1 site in INCENP (T59) (Goto et al., 2006; Hummer and Mayer, 2009), we deem this possibility unlikely.

Importantly, while T232 of Aurora B was most likely missed due to the nearby cysteine (C235) that can form a thioether linkage with the iodoacetyl-agarose beads and is therefore not liberated by oxidation-promoted hydrolysis (Blethrow et al., 2008), within the R-X-[S/T] group we found back a number of known Aurora B substrates and sites, such as INCENP S893; S894 (Honda et al., 2003; Sessa et al., 2005), Myb-binding protein 1A/MYBBP1A S1303 (Perrera et al., 2010); Vimentin/VIM S73 (Goto et al., 2003). Moreover, we here confirm that the novel site in INCENP (S72) is indeed an Aurora site. A recombinant protein of the N-terminus of INCENP (aa 1-80) was generated and used as substrate in an *in vitro* kinase reaction with the recombinant INCENP/Aurora B^{wt} complex. Indeed, INCENP 1-80 was readily phosphorylated *in vitro*, but its phosphorylation was significantly reduced when S72 was mutated into alanine (Figure 3.5A). Overall, the thiophosphate-labeling approach revealed candidate Aurora B substrates involved in a wide range of cellular functions such as chromosome segregation, cytokinesis, and spindle formation, chromatin remodeling, DNA repair, the DNA damage response, mRNA processing, and transcription and translation (Figure 3.4B). Moreover, we identified at least 20 potential Aurora B substrates that were not found in a recent screen that combined quantitative phosphoproteomics with Aurora kinase inhibition using small molecules (Kettenbach et al., 2011)(Table 3.2).

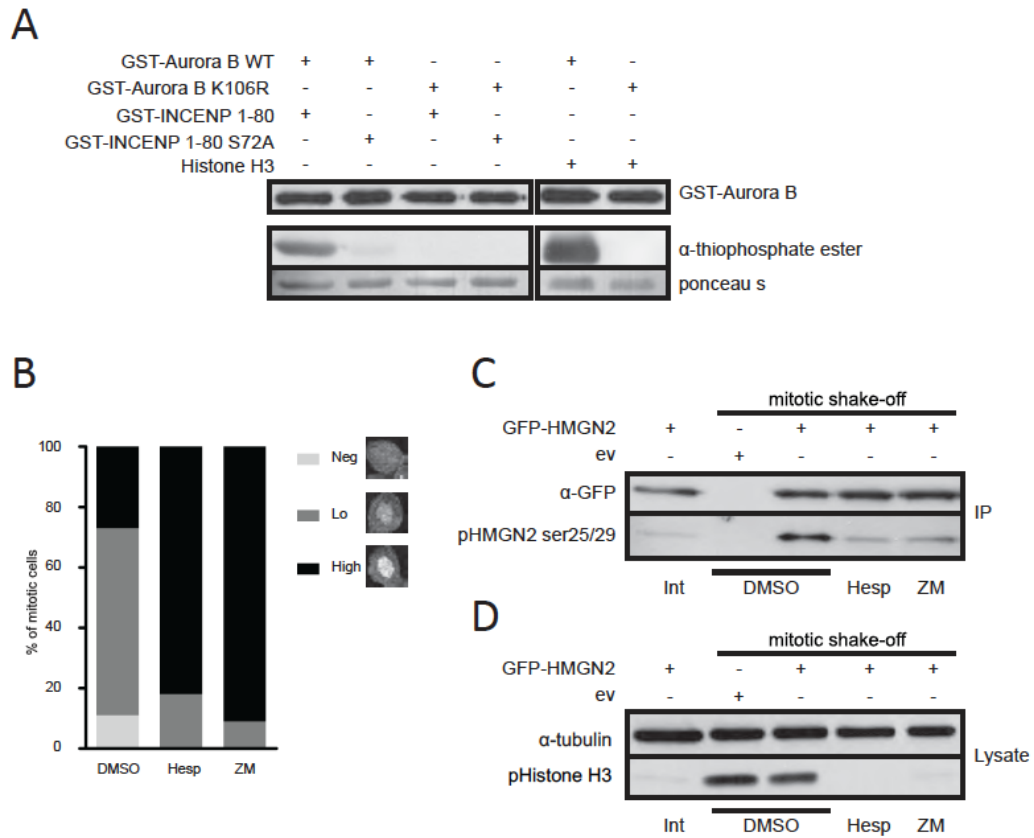


Figure 3.5 Validation of potential novel Aurora B phosphorylation sites and substrate. A, in vitro kinase assay with recombinant His-INCENP/GST-tagged Aurora B (wild-type and kinase-dead), in the presence of ATP γ S. Recombinant GST-INCENP 1–80, GST-INCENP 1–80S72A, or histone H3 was added as substrate. B, U2OS cells were released into nocodazole in the presence or absence of the indicated Aurora B inhibitors. HMGN2, Aurora B, and centromeres (CREST) were visualized with specific antibodies. Images of fields of mitotic cells were captured by a Zeiss LSM microscope and the fraction of mitotic cells with no, low, or high levels of HMGN2 on mitotic chromosomes was quantified. For each condition 100 cells were counted. C, and D. U2OS cells were transfected with either empty GFP vector (ev) or a plasmid encoding GFP-HMGN2. Mitotic cells were collected by mitotic shake-off, and the remaining adherent cells were used as interphase cell input. The overexpressed proteins were immunoprecipitated from the interphase or mitotic cell lysates with an anti-GFP antibody. The precipitated proteins were separated by SDS-PAGE, and Western blots were probed with an antibody specific for phosphorylated Ser-25/Ser-29 in HMGN2 (middle panel) and subsequently re-probed with an anti-GFP antibody (upper panel). Western blots of whole cell extracts were probed with an antibody specific for phosphorylated histone H3 (Ser-10, lower panel).

3.3.6 HMGN2 is a mitotic substrate of Aurora B

To further validate our approach we next asked if the high mobility group nucleosomal binding protein 2 (HMGN2) we identified as a potential Aurora B substrate (Table 3.2, Figure 3.4B) could be validated as a bona fide *in vivo* substrate of the kinase. Since HMGN2 is highly phosphorylated in mitosis (Cherukuri et al., 2008), we tested if Aurora B kinase activity was responsible for its mitotic phosphorylation. Mitotic HeLa cells were treated with two different small molecule inhibitors (Hesperadin and ZM447439) both shown to inhibit Aurora B significantly better than Aurora A (Ditchfield et al., 2003; Hauf et al., 2003), and GFP-tagged HMGN2 was immunoprecipitated from these extracts. The mitotic phosphorylation of S25/S29 in HMGN2 was clearly inhibited by Hesperadin and ZM447439, as was the phosphorylation of Histone H3 at Ser10, a well-known substrate of Aurora B (Figure 3.5C). Interestingly, HMGN2 binds to chromatin in interphase, but the protein dissociates from chromatin when cells enter mitosis (Cherukuri et al., 2008). Both S25 and S29 lie within the nucleosomal binding domain (NBD) of HMGN2 and an HMGN2 S25E;S29E mutant no longer binds to nucleosomes *in vitro* (Ueda et al., 2008). We therefore tested if the mitotic dissociation of HMGN2 was mediated by Aurora B. Indeed when we let cells enter into mitosis in the presence of Hesperadin or ZM447439, we observed a dramatic increase in the number of mitotic cells with enhanced chromosomal localization of HMGN2 (Figure 3.5B). In line with this, HMGN2 appears to re-associate with chromatin in anaphase when Aurora B translocates from the centromeres to the central spindle (data not shown). We have thus identified HMGN2 as a novel mitotic target of Aurora B whose dynamic chromatin association is under control of the kinase.

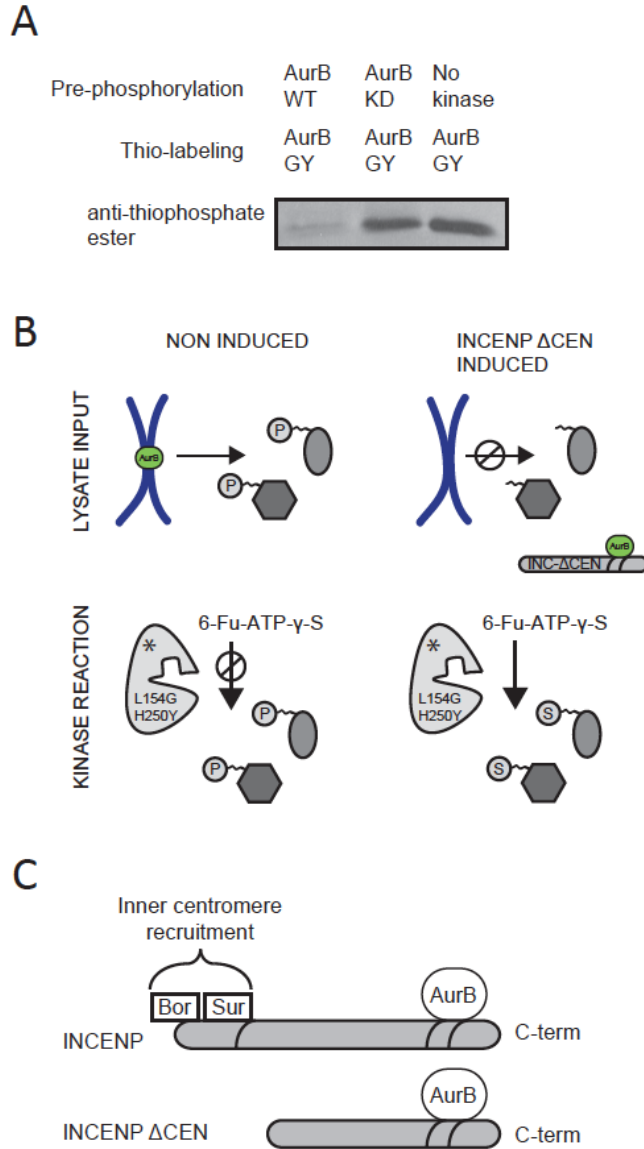


Figure 3.6 Pre-phosphorylation: In vitro kinase assay was performed for 1 hour in the presence of ATP without kinase or either recombinant wild type or kinase dead GST Aurora B proteins followed by thio-labeling for an hour with recombinant GST Aurora B L154G/H250Y and N6-furfuryl-ATP γ S. The decreased labeling after pre-phosphorylation led us to believe that thio-labeling is hampered when substrates are initially phosphorylated. B. When generating mitotic extracts from INCENP Δ CEN expressing cells we expect that substrates normally phosphorylated by Aurora B in mitotic cells will now not be phosphorylated and hence permissive for thio-phosphorylation by Aurora BL154GH250Y. C. Wild type INCENP binds to Borealin and Survivin via its N-terminal CEN-BOX (aa 1-43) whereas Aurora B interacts with the so-called IN-BOX in the C-terminus. Since Borealin and Survivin are known to be essential for CPC inner centromere localization the INCENP Δ CEN mutant (which lacks the CEN-BOX) cannot properly localize. Instead this mutant protein localizes in the cytoplasm and because it can still bind endogenous Aurora B it sequesters the kinase away from its normal sites (i.e. the inner centromeres)

3.3.7 Nuclear excluded Aurora B to identify additional mitotic substrates:

Despite our success in identifying several Aurora B substrates, we were disappointed that we did not identify additional known Aurora B targets. We realized that in this system endogenous Aurora B was present in the nucleus and could therefore phosphorylate its targets before we could label the substrates in the in-vitro labeling reaction. To test this hypothesis, we performed a pre-phosphorylation reaction without kinase or either recombinant wild type or kinase dead GST-tagged Aurora B proteins. Recombinant Histone H3 was used as substrate. We then incubated these reactions with GST-tagged Aurora BL154G/H250Y and N6-furfuryl-ATP γ S in the initial kinase reaction mixture and thio-phosphorylation was performed for 30 min at 30°C. We then detected thiophosphorylated substrates with a thiophosphate ester epitope-specific antibody (Figure 3.6A). In this experiment, which replicates pre-phosphorylation in cells, we can see that thio-labeling is hampered when substrates are initially phosphorylated.

Wild type INCENP binds to Borealin and Survivin via its N-terminal CEN-BOX (aa 1-43) whereas Aurora B interacts with the so-called IN-BOX in the C-terminus (Figure 3.6C). Since Borealin and Survivin are known to be essential for CPC inner centromere localization the INCENP Δ CEN mutant (which lacks the CEN-BOX) cannot properly localize. Instead this mutant protein localizes in the cytoplasm and because it can still bind endogenous Aurora B it sequesters the kinase away from its normal sites (i.e. the inner centromeres). Our hypothesis was that via expression of INCENP Δ CEN we could create a situation in which known and unknown kinetochore and chromosomal substrates of Aurora B are not phosphorylated and thus will be more accessible for thio phosphorylation by Aurora BL154G/H250Y (Figure 3.6B).

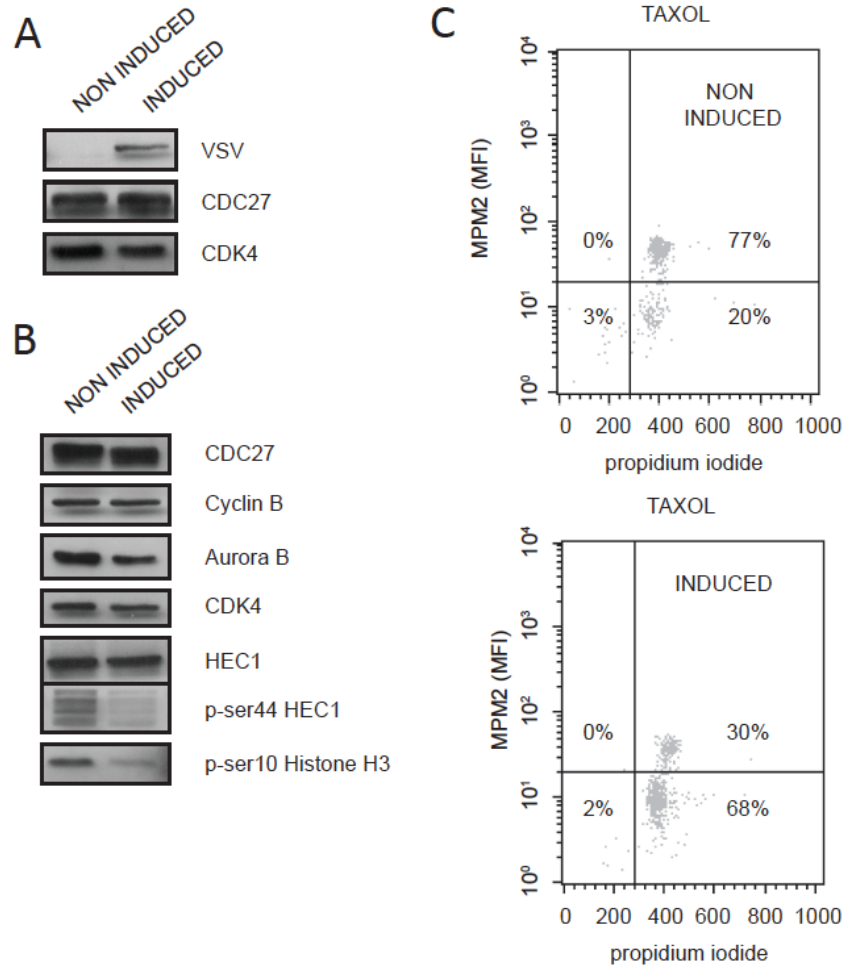


Figure 3.7 A. Stable monoclonal UTR (U2OS cells stably expressing a Tet repressor) expressing VSV-tagged INCENP Δ CEN. Protein expression was induced with 1 μ g/ml doxycyclin and induction of INCENP Δ CEN was tested by western blot using an antibody recognizing the VSV tag. B. Phosphorylation of the known Aurora B substrates, HEC1 (kinetochore), and Histone H3 (chromatin), were determined in mitotic cell extracts using western blot and antibodies specific for HEC1 phosphorylated on Ser44 (DeLuca et al. JCS, 2010), and Histone H3 phosphorylated on Ser10. Equal loading was controlled by detection of CDC27, CDK4 and total HEC1. To prove that only mitotic cells were harvested Cyclin B and Aurora B were also detected. C. The stable monoclonal cell line was released from a thymidine-induced G1/S block into medium containing taxol with or without induction of INCENP Δ CEN. Seventeen hours after release, the mitotic index was determined by propidium iodide/MPM2 monoclonal antibody labeling and FACS analysis. After induction of INCENP Δ CEN cells override the mitotic checkpoint in paclitaxel indicating that Aurora B is not active at the inner centromere.

To obtain proof of principle for this idea we generated a stable U2OS cell lines expressing INCENP Δ CEN under control of a Tet inducible promotor (INCENP Δ CEN-UTR). Stable monoclonal UTR (U2OS cells stably expressing a Tet repressor) expressing VSV-tagged INCENP Δ CEN. Protein expression was induced with 1 ug/ml doxycyclin and induction of INCENP Δ CEN was tested by western blot using an antibody recognizing the VSV tag (Figure 3.7A). Equal loading was controlled by detection of CDC27 and CDK4 using specific antibodies. In this experiment we can see that INCENP Δ CEN is readily expressed in the monoclonal cell line. We next examined the phosphorylation of the known Aurora B substrates, HEC1 (kinetochore), and Histone H3 (chromatin), were determined in mitotic cell extracts using western blot and antibodies specific for HEC1 phosphorylated on Ser44 (DeLuca et al. JCS, 2010), and Histone H3 phosphorylated on Ser10. Equal loading was controlled by detection of CDC27, CDK4 and total HEC1. To prove that only mitotic cells were harvested Cyclin B and Aurora B were also detected. In this experiment we see a reduction in the phosphorylation of both HEC1 and Histone H3 following induction of INCENP Δ CEN (Figure 3.7B).

Aurora B is required to block the progression of mitosis when chromosomes are not properly attached to microtubules, know as the mitotic spindle checkpoint. By blocking Aurora B from entering the nucleus we would expect the spindle checkpoint to be overridden, and upon treatment with a microtubule depolarizing agent such as Taxol, cells would enter mitosis. The stable monoclonal cell line was released from a thymidine-induced G1/S block into medium containing taxol with or without induction of INCENP Δ CEN. Seventeen hours after release, the mitotic index was determined by propidium iodide/MPM2 monoclonal antibody labeling and FACS analysis (Figure

3.7C). After induction of INCENP Δ CEN cells override the mitotic checkpoint in paclitaxel indicating that Aurora B is not active at the inner centromere.

When generating mitotic extracts from INCENP Δ CEN expressing cells we expect that substrates normally phosphorylated by Aurora B in mitotic cells will now not be phosphorylated and hence permissive for thio-phosphorylation by Aurora BL154GH250Y (Figure 3.6B). In addition, since Aurora B is sequestered into the cytosol it may now phosphorylate substrates that are normally not phosphorylated in mitosis. As such it can block these from thiophosphorylation by the analog-sensitive kinase and as a consequence we expect to make the set-up more specific.

In performing this experiment we were able to confirm several known Aurora B substrates that we found previously as well as several well known Aurora B substrates (See Appendix B for the complete list). Overall we found a total of 128 substrate proteins with a total of 86 new sites. Some of the most interesting sites are those that have a known role in mitotic fidelity and are nucleus specific proteins such as Nucleolar RNA helicase 2 and Chromosome transmission fidelity protein 18. In addition we identified a new potential Aurora B phosphorylation site on Histone H4 at S48, previously thought to be a PAK2 phosphorylation site. In conclusion we have identified 86 new potential Aurora B phosphorylation sites, and will begin the work to characterize these sites to analyze their role in Aurora B signaling during mitosis.

4.4 Discussion

We successfully generated an important new research tool for the functional analysis of human Aurora B, a kinase essential for genomic stability. In contrast to a

recent study that identified L138V in Aurora B as a second site-suppressor mutation based on modeling using the published crystal structure of Aurora A bound to ADP (Johnson et al., 2011), the here described H250Y mutation that restored activity of the Aurora B gatekeeper mutants (L154A/G) was found by combining orthologous Aurora sequence alignment and reported information on Aurora B mutations that enhanced kinase activity (Girdler et al., 2006). This could thus be considered as an alternative strategy to find second-site suppressor mutations for kinases intolerant to gatekeeper mutations.

The unique analog-sensitive mutant of Aurora B is functional in cells and inhibited by low concentrations of the PP1 analog NA-PP1, opening up the possibility to stably replace endogenous Aurora B kinase for this mutant and generate cell lines in which Aurora B can be selectively inhibited. Moreover, the Aurora B^{L154G/H250Y} double mutant is capable of using bulky ATP analogs to thiophosphorylate proteins in cell extracts. This resulted in the isolation of multiple unique phosphopeptides of which 71% corresponded to either a R-X-[S/T]-Φ or a R-X-[S/T]-X-Φ motif (where Φ stands for an hydrophobic residue).

In the first approach we identified only highly abundant proteins present in a non-fractionated cell extract as potential Aurora B substrates, but as we expected, we found more Aurora B substrates when using the nuclear excluded Aurora B and expect to find still more when using fractionated cell extracts, enriched for certain subcellular compartments, as input for the kinase reactions (Blethrow et al., 2008). Based on the recent screen by Kettenbach *et al.* (Kettenbach et al., 2011), that combined quantitative phosphoproteomics with Aurora kinase inhibition using small molecules, our candidates

represent only a small portion of the Aurora B substrates. However, the use of chemical inhibitors may affect multiple downstream pathways and non-specific pathways due to off-target kinase inhibition, while our screen will identify only direct Aurora B substrates. Both screens may thus be nicely complementary in finding relevant Aurora B targets. Indeed, we identified at least 20 potential Aurora B substrates that were not uncovered by the Kettenbach screen (Kettenbach et al., 2011) (Table 3.2). Importantly, we found RACGAP1, which is a validated substrate of Aurora B (Goto et al., 2003; Minoshima et al., 2003) and for HMGN2 we demonstrated in this study that it is a novel mitotic target of Aurora B. Moreover, 22 of the 40 recovered R-X-[S/T] Aurora phosphosites were also found in other phosphoproteomic data sets (www.phosphosite.org) (Hornbeck et al., 2004), indicating that the majority of these sites are also phosphorylated *in vivo*.

Advantages of the chemical genetic approach are that only direct targets of the kinase are labeled, and that we can use different functionally relevant subcellular fractions as input, such as purified chromosome fractions and isolated midbodies, to enable more comprehensive coverage of less abundant Aurora substrates. Yet the challenge will be to verify if the identified sites are also *in vivo* phosphorylated and to establish if the sites are indeed specific for Aurora B. Since the recombinant kinase is no longer confined to its normal cellular locations and Aurora B and A tend to phosphorylate overlapping peptide sequences (Alexander et al., 2011), it is expected that both Aurora B and A substrates will be found. Indeed, 5 out of the 17 phospho-sites that overlapped with the screen by Kettenbach *et al.* (Kettenbach et al., 2011), were clustered as Aurora A specific sites in that study, while 8 out of 17 were clustered as Aurora B specific and 4 out of 20 as Aurora ambiguous (the latter meaning that the site is mostly likely

phosphorylated by both Aurora A and B). Thus, combining the advantages of different substrate screens together with functional validation experiments, will built a complete picture of the physiologically relevant Aurora B substrates.

To prove that the *in vitro* thiophosphate-labeling approach could indeed identify novel *in vivo* Aurora B substrates, we selected HMGN2 as a candidate for further validation. HMGN2 belongs to a group of non-histone chromosomal proteins (HMGN1-5) that bind to nucleosomes and modulate the structure and function of chromatin. HMGN2 reduces the compaction of chromatin fibers most likely to facilitate gene expression (Postnikov and Bustin, 2010), and promotes repair of UV-induced DNA lesions (Subramanian et al., 2009). HMGN2 is highly phosphorylated in mitosis and this phosphorylation coincides with the dissociation of the protein from mitotic chromosomes (Cherukuri et al., 2008). We showed that Aurora B kinase is responsible for its mitotic phosphorylation and dissociation from chromosomes. Interestingly, the Aurora B phosphorylation sites (S25 and S29) lie within the RRSARLSA core of the nucleosomal binding domain (NBD) that is conserved between all the members of this protein family (Postnikov and Bustin, 2010), and we therefore predict that all HMGN proteins will be Aurora B targets. Indeed, S20 and S24 of HMGN5 were also identified as potential Aurora sites in our screen (Table 3.1 and Figure 3.4B), and similar to HMGN2 also HMGN5 dissociates from mitotic chromosomes (Rochman et al., 2009). Currently, we do not know why the HMGN proteins have to dissociate from chromatin when cells enter mitosis. Since they reduce chromatin compaction, their mitotic dissociation might contribute to full chromatin condensation in mitosis promoting proper chromosome segregation in anaphase.

In this work, we have generated a powerful new tool to inhibit Aurora B kinase activity and to identify downstream targets of the kinase. The fact that we uncovered candidate substrates involved in a wide-range of cellular functions could indicate that Aurora B may have multiple functions outside mitosis, or that the putative substrates have additional functions during cell division.

Experimental procedures are provided in Appendix C

Chapter 4

A neo-substrate that amplifies catalytic activity of Parkinson's disease related kinase PINK1

4.1 Abstract

Mitochondria have long been implicated in the pathogenesis of Parkinson's disease (PD). Mutations in the mitochondrial kinase PINK1 that reduce kinase activity are associated with mitochondrial defects and result in an autosomal recessive form of early onset PD. Therapeutic approaches for enhancing the activity of PINK1 have not been considered since no allosteric regulatory sites for PINK1 are known. Here we show that an alternative strategy, a neo-substrate approach involving the ATP analog kinetin triphosphate (KTP), can be used to increase the activity of both PD related mutant PINK1^{G309D} and PINK1^{wt}. Moreover, we show that application of the KTP precursor kinetin to cells results in biologically significant increases in PINK1 activity, manifest as higher levels of Parkin recruitment to depolarized mitochondria, reduced mitochondrial motility in axons, and lower levels of apoptosis. Discovery of neo-substrates for kinases could provide a heretofore-unappreciated modality for regulating kinase activity.

4.2 Introduction

Parkinson's disease (PD) is characterized by the loss of dopaminergic (DA) neurons in the substantia nigra, a region in the midbrain that is critical for motor control (Lang and Lozano, 1998). Mitochondrial dysfunction has been closely linked to PD via several mechanisms (Nunnari and Suomalainen, 2012; Rugarli and Langer, 2012), including mutations in the mitochondria-specific kinase PTEN Induced Kinase 1 (PINK1) (Valente et al., 2004) and mitochondria-associated E3 ubiquitin ligase Parkin (Kitada et al., 1998). PINK1 plays an important role in repairing mitochondrial dysfunction by responding to

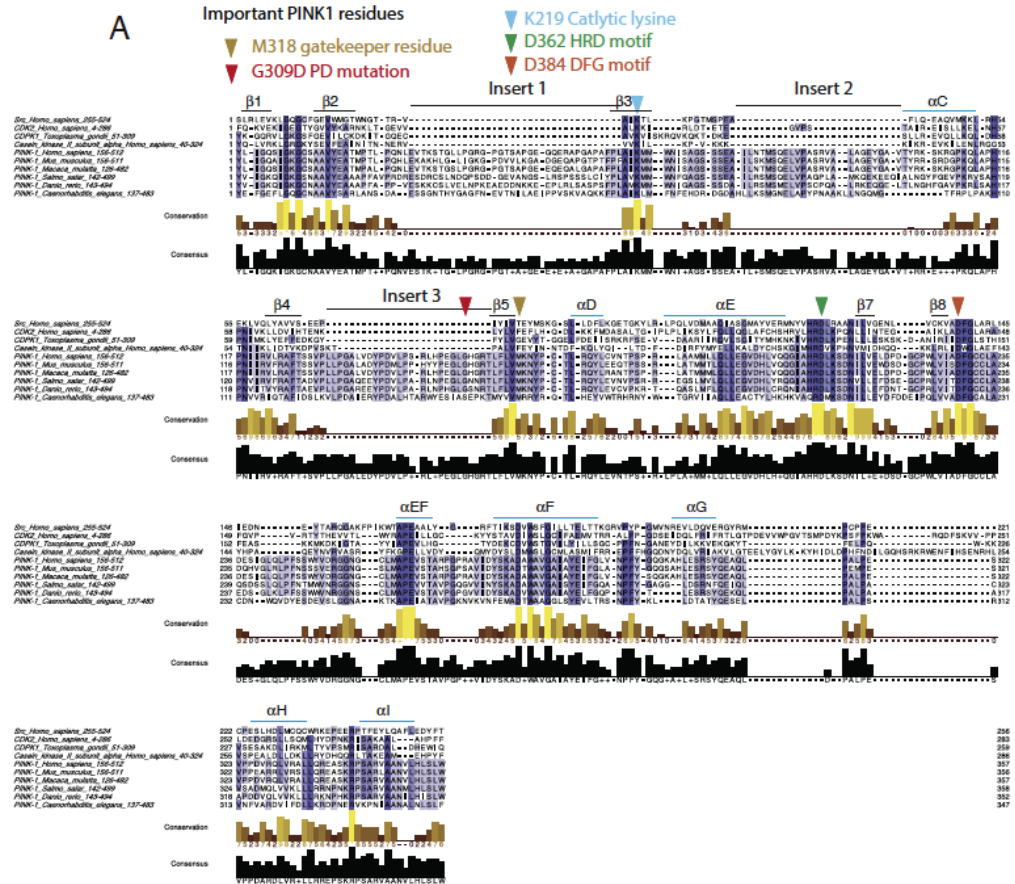


Figure 4.1 Alignment of PINK1 to typical and atypical kinase domains reveals several large inserts in the N-lobe of PINK1. A. T-coffee alignment of multiple PINK1 analogs to homo sapiens Src (secondary structure based on the Src structure shown (Sicheri and Kuriyan, 1997)) and CDK1 reveals a larger residue in the gatekeeper position (gold triangle) of these two kinases that do not accept N⁶ modified “bumped” ATP analogs (Liu et al., 1998b; Merrick et al., 2011). In CDK1, a gatekeeper glycine provides space for “bumped” ATP competitive kinase inhibitors (Lourido et al., 2010). The alignment reveals 3 large inserts in the N-lobe of PINK1, including an insert directly before the predicted gatekeeper residue containing the location of glycine 309 whose mutation leads to a loss of kinase activity. (B) Comparison of kinases in which the activity with ATP and N⁶ modified ATP has been studied. These 17 kinases (14 previously published 3 in preparation) have all been analyzed for the ability to utilize N⁶ modified ATP analogs before and after mutation of the gatekeeper residue.

damage at the level of individual mitochondria. In healthy mitochondria, PINK1 is rapidly degraded by the protease ParL (Meissner et al., 2011); but in the presence of inner membrane depolarization, PINK1 is stabilized on the outer membrane, where it recruits and activates Parkin (Narendra et al., 2010), blocks mitochondrial fusion and trafficking (Clark et al., 2006; Deng et al., 2008; Wang et al., 2011), and ultimately triggers mitochondrial autophagy (Geisler et al., 2010; Narendra et al., 2008; Youle and Narendra, 2011). The PINK1 pathway has also been linked to the induction of mitochondrial biogenesis and the reduction of mitochondria-induced apoptosis in neurons, the latter phenotype due at least in part to the effect of PINK1 on mitochondrial motility, a neuron specific phenotype (Deng et al., 2005; Petit et al., 2005; Pridgeon et al., 2007; Shin et al., 2011; Wang et al., 2011).

Individuals homozygous for PINK1 loss-of-function mutations can develop a form of early onset PD that results from highly selective DA neuronal loss and, in at least one clinical case, shares the Lewy-body pathology of sporadic PD (Gautier et al., 2008; Geisler et al., 2010; Haque et al., 2008; Henchcliffe and Beal, 2008; Petit et al., 2005; Samaranch et al., 2010). Recent work has shown that of 17 clinically relevant PINK1 mutations, those mutants that affect catalytic activity but do not affect cleavage or subcellular localization have the most dramatic effect on neuron viability, further supporting a role for PINK1 activity in the prevention of neurodegeneration (Song et al., 2013). One of the most common of the catalytic mutants, PINK1^{G309D}, shows a ~70% decrease in kinase activity and abrogates the neuroprotective effect of PINK1 (Petit et al., 2005; Pridgeon et al., 2007). However, lower PINK1^{G309D} catalytic activity can be rescued by overexpression of PINK1^{wt}, and increasing PINK1 activity by PINK1^{wt}

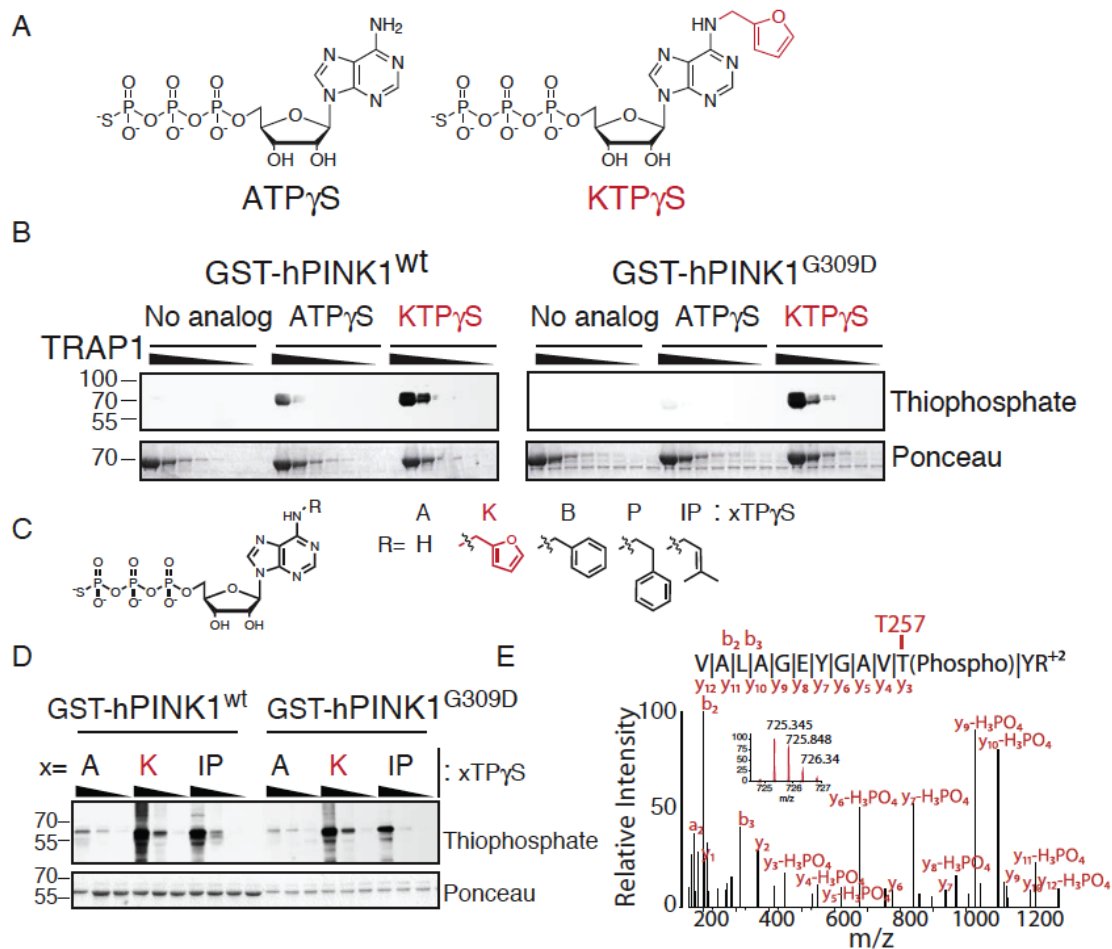


Figure 4.2 Neo-substrate Kinetin Triphosphate (KTP) amplifies PINK1 kinase activity in-vitro. A. Chemical structure of kinase substrate adenosine triphosphate with gamma thiophosphate (ATP γ S) and neo-substrate kinetin triphosphate gamma thiophosphate (KTP γ S). B-D PINK1 kinase assay B, with substrate 60-704TRAP1 (1 mg/ml decreasing by 1/3) and 500 μ M indicated nucleotide C or D, PINK1 alone (4.3 μ M) 100, 200, 400 μ M nucleotide analyzed by immunoblotting for thiophospho labeled TRAP1 and PINK1. E. PINK1 autophosphorylation site identified by specific peptide capture and LCMSMS found only with PINK1^{wt} and KTP γ S indicating this nucleotide is utilized as a bona fide substrate

overexpression has been shown to reduce staurosporine- and oxidative-stress-induced apoptosis in multiple cell lines, suggesting that enhanced PINK1 activity could be an effective therapeutic strategy for PD (Arena et al., 2013; Deng et al., 2005; Kondapalli et al., 2012; Petit et al., 2005; Pridgeon et al., 2007).

Recognizing the therapeutic potential of PINK1/Parkin pathway activation, we began investigating mechanisms for the pharmacological activation of PINK1. Small molecule activation of kinases is typically accomplished by binding allosteric regulatory sites: for example, natural products such as phorbol esters bind to the lipid binding domain of PKCs and recruit the kinase to the membrane (Castagna et al., 1982; Nishizuka, 1984); separately, the AMP activated protein kinase (AMPK) is activated by binding of AMP to an allosteric site (Ferrer et al., 1985; Hardie et al., 2012). However, PINK1 contains no known small molecule binding sites. Another potential strategy might involve manipulation of protein interaction sites or the active site, given that synthetic ligands have been identified which bind to the protein docking sites on the kinase PDK1 (Hindie et al., 2009; Wei et al., 2010), and, separately, that Src activity can be controlled by chemical complementation of an active site catalytic residue, allowing ATP to be accepted only when imidazole was provided to mutant Src (Ferrando et al., 2012; Qiao et al., 2006). However these approaches were not applicable to PINK1 as no structural data for PINK1 is available.

We next turned our attention to sites within PINK1 known to alter its function or stability. Four PINK1 disease associated mutations, including G309D, occur in an unusual insertion in the canonical kinase fold. PINK1, as well as several orthologs, share 3 such large (>15 AA) insertions in the N-terminal kinase domain (Figure 4.1A) that

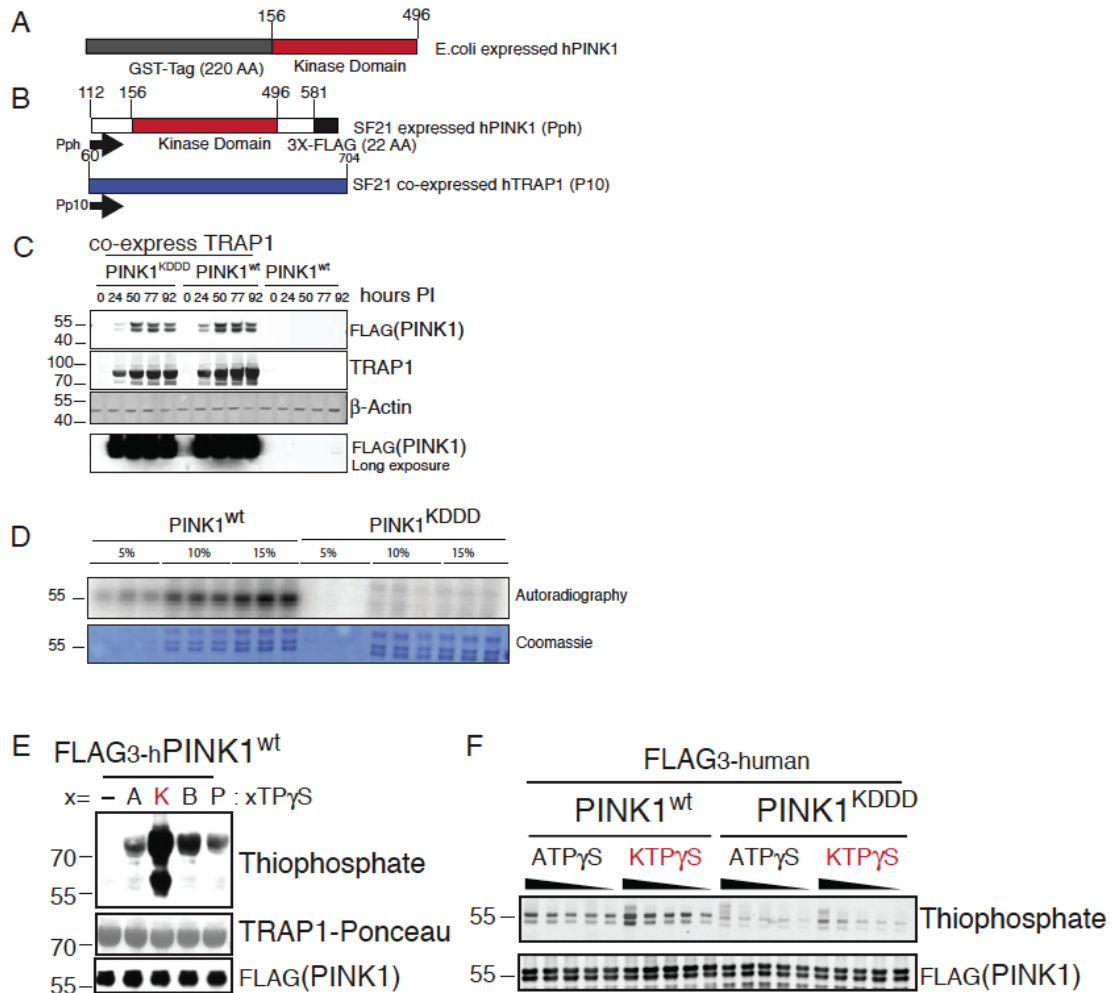


Figure 4.3 Optimized PINK1 expression constructs used to express PINK1 for enzymatic characterization. A GST tagged PINK1 kinase domain (156-496) expressed in bacteria. B. Schematic depicting the expression construct for PINK1 kinase domain (112-581) co-expression with TRAP1 in insect cells. PINK1 is driven by the Pph promoter and TRAP1 is driven by the Pp10 promoter. C SF21 infected insect cells were lysed and analyzed by immunoblotting for FLAG PINK1, TRAP1 and b-actin. TRAP1 expression leads to higher amounts of PINK1 expression. D. Baculovirus produced PINK1KDDD has severely compromised kinase activity with γ 32P ATP, whereas PINK1wt shows robust autophosphorylation activity. F. SF21 produced PINK1 was incubated with 60-704TRAP1 and the indicated nucleotide (structure shown in panel C) and analyzed as in B-D. G. PINK1 kinase assay with indicated nucleotide (250 to 1250 μ M in increments of 250 μ M) analyzed as in B-D reveals much reduced phosphorylation activity with PINK1KDDD lanes 11-20, increased autophosphorylation was seen with neo-substrate KTP γ S over endogenous substrate ATP γ S.

provides the majority of contacts to the adenine ring of ATP. Inserts in the active site of several enzymes have been shown to alter substrate specificity. In one example, the deubiquitinase UCH-L5 can hydrolyze larger ubiquitin chains only when a >14 AA loop is present in the active site (Zhou et al., 2012). In another example, protein engineering of alkyl guanine DNA alkyltransferase through insertion of a loop into the active site allows for recognition of an enlarged O⁶-modified guanine substrate not accepted by the enzyme without the loop insertion (Heinis et al., 2006). In light of these findings, the three insertions in PINK1's adenine binding N-terminal subdomain led us to believe that PINK1 might also exhibit altered substrate specificity.

In considering the possibility that nucleotides other than ATP could be substrates for kinases, we noticed that CK2 can utilize multiple substrates as phospho-donors: GTP as well as ATP, though its activity with GTP is much lower (Niefind et al., 1999). Though it is uncommon for eukaryotic protein kinases to accept alternative substrates in the ATP binding site, kinases engineered with a single mutation to the gatekeeper residue often tolerate ATP analogs with substitutions at the N⁶ position (Liu et al., 1998; Shah et al., 1997). Importantly, no wildtype kinase we had previously studied had shown the ability to accept N⁶ modified ATP analogs (Figure 4.1B).

We discovered that, unlike any kinase we have studied, PINK1 accepts the neo-substrate N⁶ furfuryl ATP (kinetin triphosphate or KTP) with higher catalytic efficiency than its endogenous substrate, ATP. We also found that the metabolic precursor of this neo-substrate (kinetin) can be taken up by cells and converted to the nucleotide triphosphate form, which leads to accelerated Parkin recruitment to depolarized

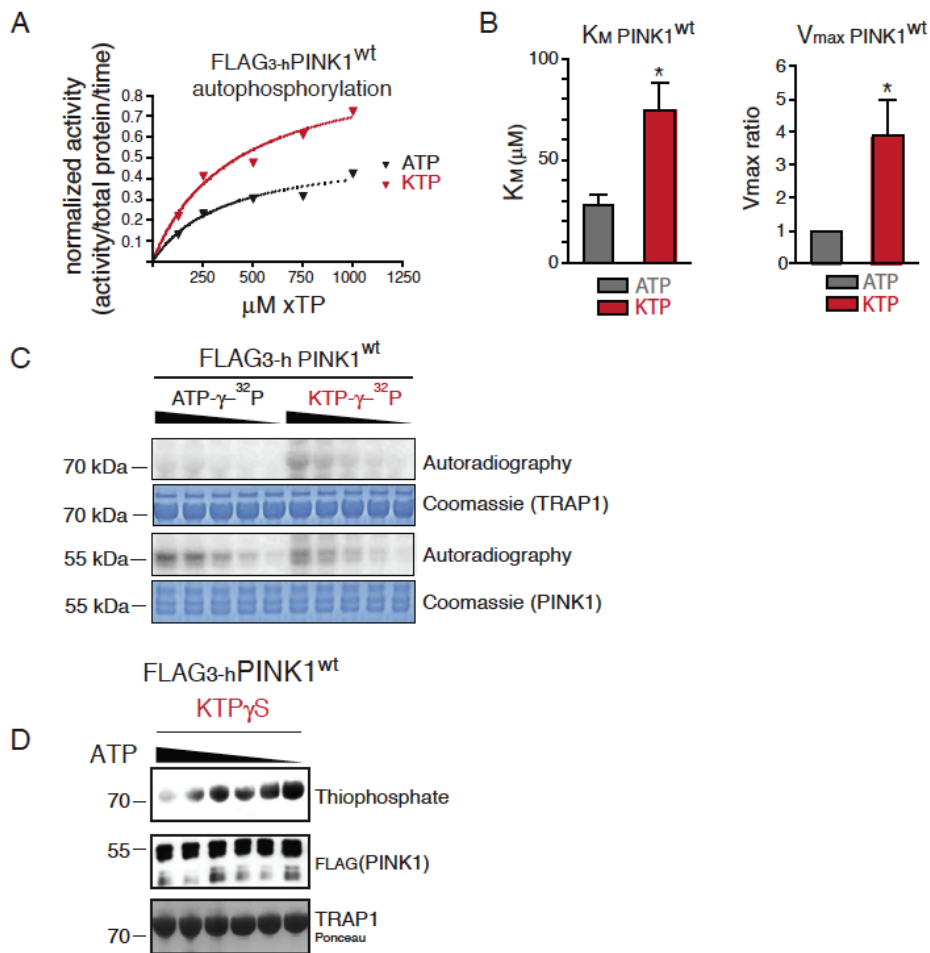


Figure 4.4 A,B PINK1wt was incubated with either ATP γ S or KTP γ S at the indicated concentration. Activity was assessed by western blot for thiophospho PINK1, subtracting t0 background thiophosphate signal and normalizing to total PINK1 signal. Velocity was plotted (a representative experiment shown) and the V_{max} and K_M for each nucleotide was calculated. K_M for ATP γ S and KTP γ S ($27.9 \pm 4.9 \mu\text{M}$; $74.6 \pm 13.2 \mu\text{M}$) (mean + SEM; $p=0.02$; t-test). V_{max} was plotted as the ratio of KTP γ S /ATP γ S (3.9 ± 1.3 fold higher ($p=0.02$; t-test)). C. Kinetin γ 32P ATP was generated using a NDPK-ATP coupled system (Blethrow et al., 2004). PINK1wt was incubated with either radiolabeled ATP or KTP along with substrate TRAP1. PINK1wt phosphorylates TRAP1 with higher activity utilizing KTP- γ 32P than ATP- γ 32P, and autophosphorylates with both nucleotides. D. PINK1wt was incubated with substrate 60-704TRAP1 (74 kDa at 1 mg/ml) and 500 μM nucleotide KTP γ S along with varying amounts of competing non thiophosphorylated ATP (from 2 mM to 62.5 μM in 1:2 dilution series). PINK1 activity was analyzed by western blotting for thiophospho labeled protein. PINK1 utilized KTP γ S, visualized by thiophosphorylation, with up to an 8 fold excess of ATP (lane 1)

mitochondria, diminished mitochondrial motility in axons, and suppression of apoptosis in human derived neural cells, all in a PINK1 dependent manner.

4.3 Results

4.3.1 PINK1 accepts N⁶ modified ATP analog kinetin triphosphate (KTP)

We expressed both PINK1^{wt} and PINK1^{G309D} GST tagged kinase domain (₁₅₆₋₄₉₆PINK1) in *E. coli* (Figure 4.3A,B) and performed kinase assays with a series of neo-substrate analogs. As expected, PINK1^{G309D} displayed reduced activity with ATP; interestingly, however, incubation with N⁶ furfuryl ATP (kinetin triphosphate or KTP) (Figure 4.2A) led to increased levels of transphosphorylation of the mitochondrial chaperone hTRAP1 (residues 60-704) (Figure 4.2B) and autophosphorylation with both PINK1^{G309D} and PINK1^{wt} (Figures 4.2C,D). Using a phosphopeptide capture and release strategy (Blethrow et al., 2008; Hertz et al., 2010b), we were able to identify the T257 autophosphorylation site (Kondapalli et al., 2012) using KTP as the phospho-donor for PINK1 (Figure 4.2E), which showed that this neo-substrate is capable of supporting bona fide PINK1-dependent substrate phosphorylation.

PINK1 is intrinsically highly unstable, and especially so when produced in bacteria (Beilina et al., 2005); therefore, in order to confirm the PINK1-dependency of the observed kinase activity, we took several steps to optimize PINK1 expression. We constructed several FLAG₃ tagged truncation variants of PINK1 and induced expression using baculovirus infected *SF21* insect cells (Figure 4.3B). C-terminally tagged ₁₁₂₋₅₈₁PINK1FLAG₃ expressed the most soluble protein. However, the amount was far below

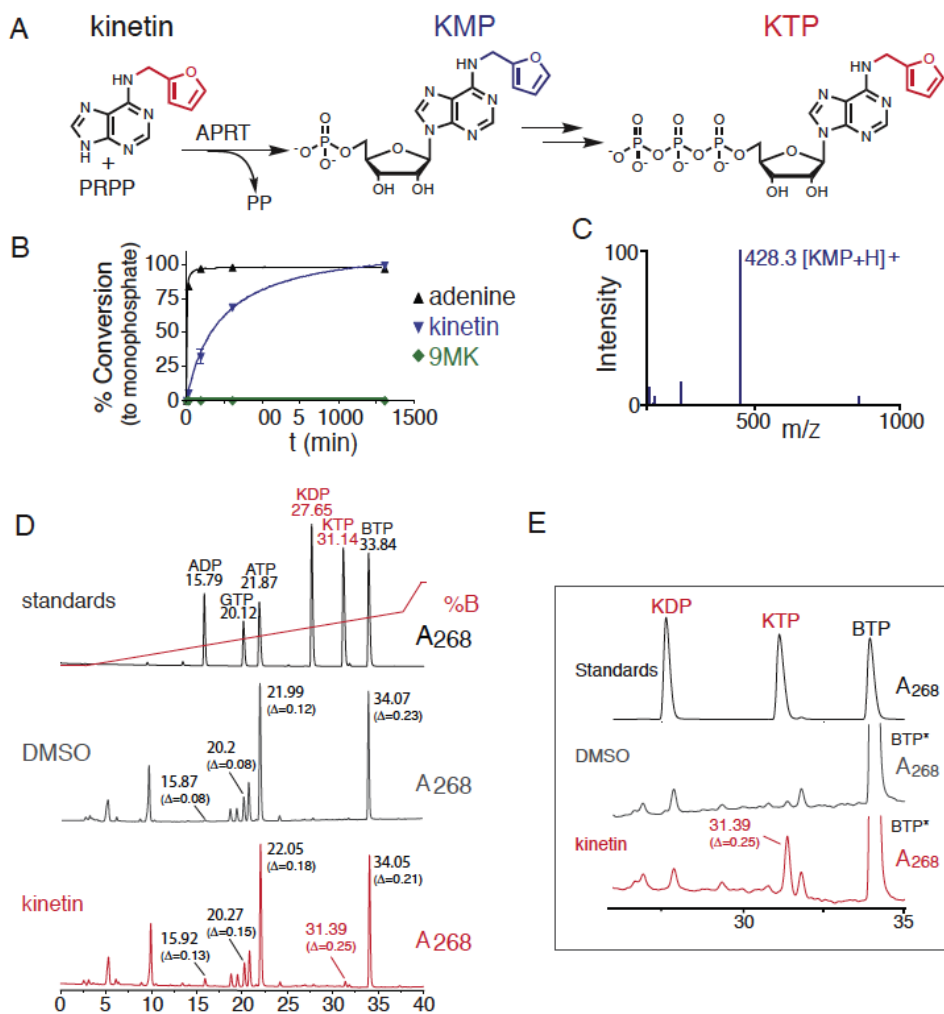


Figure 4.5 Neo-substrate precursor kinetin leads to KTP in human cells. A Schematic of the ribosylation reaction of kinetin to KMP via APRT and PRPP followed by cellular conversion to KTP. B LCMS analysis of production of either AMP (adenine) or KMP (kinetin and 9MK) by LCMS analysis reveals that kinetin can undergo APRT mediated ribosylation to KMP, but N9 methyl-kinetin cannot. C. LCMS analysis of kinetin reaction; major peak represents KMP+H peak at 428.3 m/z. D. HPLC analysis of 20 μ l of either 0.5 mM standards (ADP, GTP, ATP, KDP, KTP, BTP) or cellular lysate of DMSO or kinetin treated HeLa cells with 250 μ M BTP* addition reveals a novel peak present in kinetin treated cells at 31.39 minutes. The retention time of each peak in the cell lysate was offset, that difference is shown here. E. Zoom in of the region from 22.5 to 35 minutes of the HPLC traces shown in D.

what we required for biochemical characterization (Figure 4.3C). Hypothesizing that PINK1 might require interaction with other proteins to fold properly, we co-expressed proteins known to associate with PINK1 such as DJ-1, PARKIN, and TRAP1. Co-expression of full length TRAP1 dramatically increased the stability of PINK1 (Figure 4.3C). This finding enabled us to express larger amounts of properly folded PINK1^{wt}, PINK1^{G309D} and a kinase dead PINK1^{kddd} (residues 112-581 with K219A, D362A, and D384A (Figure 4.1A)). In line with our initial observations, *SF21*-produced-PINK1 activity is also enhanced using KTP but not other nucleotides (Figure 4.3E). We confirmed that PINK1^{kddd} has severely compromised activity (Figure 4.3D,F), and were able to show that PINK1^{wt} could autophosphorylate with a 3.9 ± 1.3 fold higher ($p=0.02$; t -test) V_{max} and a higher K_M ($27.9 \pm 4.9 \mu\text{M}$ vs. $74.6 \pm 13.2 \mu\text{M}$) for the neo-substrate KTP versus ATP (Figures 4.3F and 4.4A,B). As the previous assays utilized ATP with a γ -thiophosphate as a tracer, we wanted to confirm the activity using an orthogonal tracer, γ -³²P ATP to visualize PINK1 activity. Therefore, we generated KTP with a γ -³²P labeled phosphate, and were able to see that using this orthogonally labeled version of KTP PINK1^{wt} transphosphorylation of ₆₀₋₇₀₄TRAP1 is increased relative to γ -³²P ATP (Figure 4.4C).

Since KTP would have to compete with millimolar intracellular ATP concentrations in order to function, we performed a competition assay with γ -thiophosphate labeled KTP versus ATP. We found that the KTP γ S signal persisted even when ATP was present at 4 fold greater concentration than KTP γ S (2 mM vs. 0.5 mM) (Figure 4.4D) suggesting that PINK1 can be activated by KTP in the presence of cellular ATP.

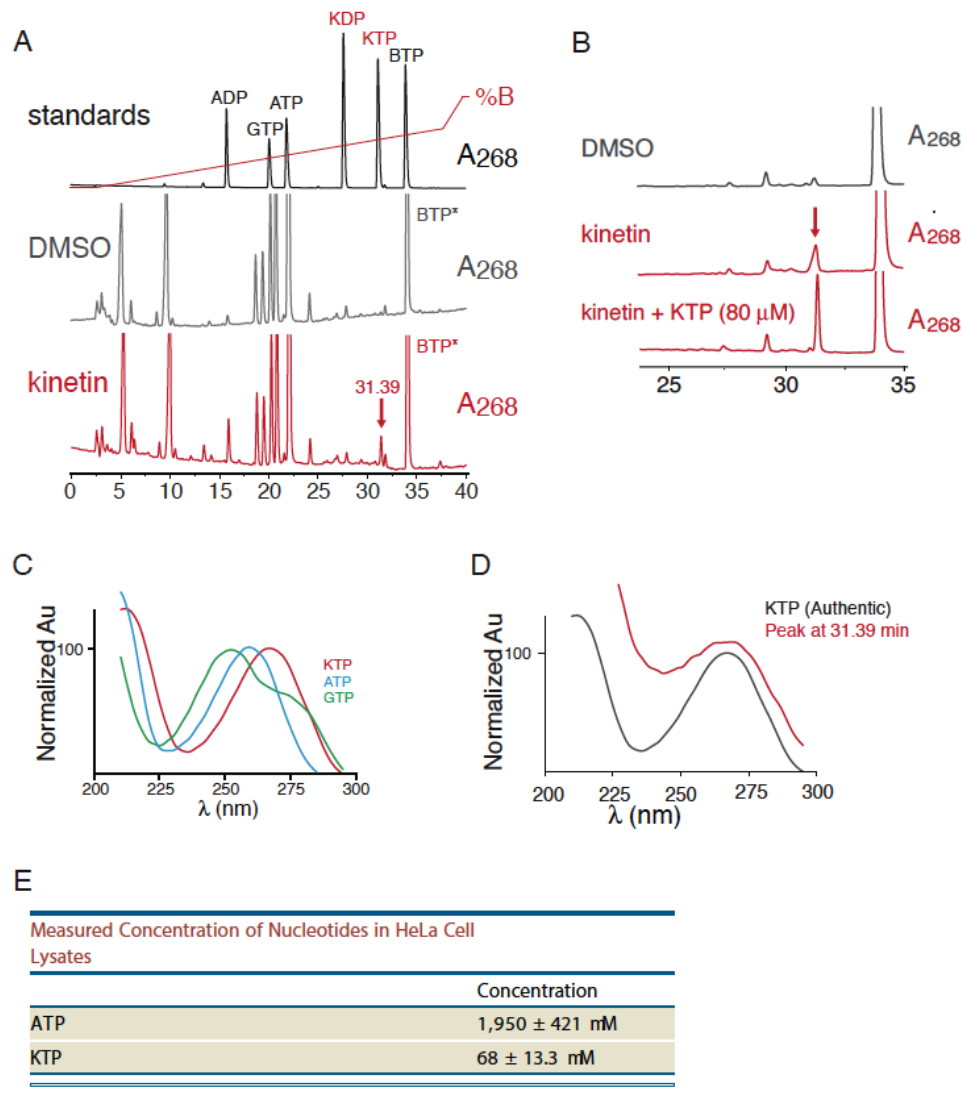


Figure 4.6 Neo-substrate precursor kinetin leads to KTP in human cells A. HPLC analysis of standards (ADP, GTP, ATP, KDP, KTP, BTP) or cellular lysate of DMSO or kinetin treated HeLa cells with 250 μ M BTP* addition reveals a novel peak present in kinetin treated cells at 31.39 minutes. B. Zoom of HPLC analysis of DMSO or kinetin treated cell lysate with BTP addition, or kinetin cell lysate with BTP addition and KTP addition reveals an increase in the peak that co-elutes with KTP (186%) where BTP decreases to 76% of original area suggesting the peak is KTP. C. Absorbance spectrum of the standards GTP, ATP and KTP. D. Absorbance spectrum of peak at 31.39 minutes in kinetin treated cells compared to absorbance spectrum of KTP in standard. E. Measured concentration of nucleotides in HeLa cells.

4.3.2 KTP is produced in human cells upon treatment with KTP precursor kinetin

Our results showing in vitro increases in PINK1 activity using KTP led us to investigate the ability to achieve enhanced activity of PINK1 in cells. One major challenge to activating PINK1 in cells is that ATP analogs like KTP are not membrane permeable; however, previous work has shown that certain cytokinins can be taken up by human cells and converted to the nucleotide triphosphate form (Ishii et al., 2003). Additionally, recent work in cells expressing hypomorphic mutant CDK2 alleles showed that the activity of CDK2 could be increased in cells by providing nucleotide analog precursors that can be converted to the nucleotide triphosphate form and are able to fit into the hypomorphic CDK2 active site (Merrick et al., 2011).

The first step in bioconversion is ribosylation of the cytokinin to a 5'-monophosphate form, which can be mediated by adenine phospho ribosyl transferase (APRT)(Kornberg et al., 1955; Lieberman et al., 1955b) (Figure 4.5A). Following established protocols (Parkin et al., 1984), we incubated either adenine, kinetin or negative control N⁹ methyl-kinetin (9MK) with 5'-phosphoribosyl pyrophosphate (PRPP) and APRT and assayed the reaction by LCMS (Figure 4.5B). Adenine converted rapidly to AMP, achieving near-complete conversion (84%) after 10 minutes of reaction time; kinetin's conversion to KMP (Figure 4.5C) was markedly slower, requiring 150 minutes for half to be converted. The control compound 9MK is not converted to KMP even after 16 hours of incubation (Figure 4.5B) whereas kinetin was completely converted to KMP in this time frame. This experiment demonstrated that the ribosylation of kinetin is biosynthetically possible using the enzymatic route for AMP production.

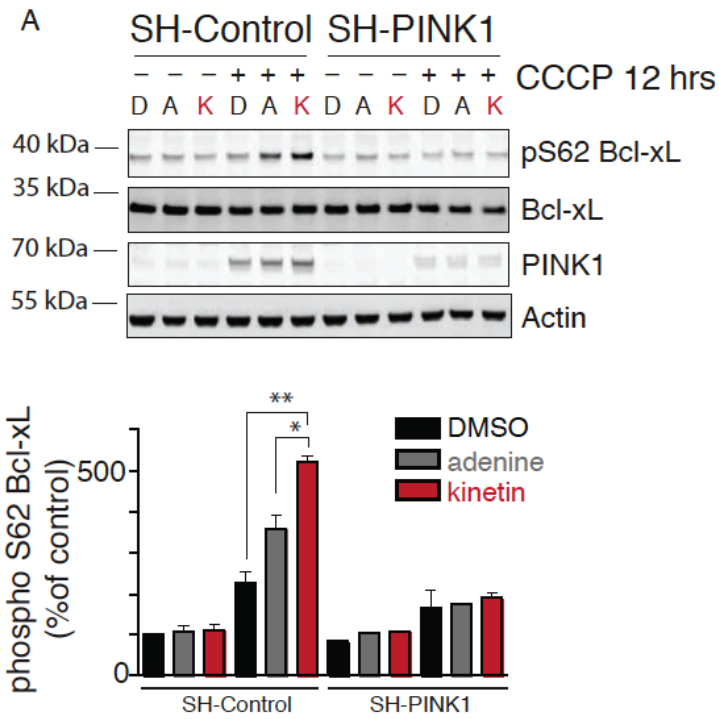


Figure 4.7 A. Immunoblot analysis with the indicated antibodies for phosphorylation on serine 62 of Bcl-xL reveals an increase following kinetin treatment. B. Quantitative analysis of data shown in G where a significant increase in the phosphorylation of Bcl-xL on serine 62 with pre-treatment with kinetin versus DMSO or adenine ($p=0.01$, $p=0.04$; t-test) in SH-Control expressing cells not in SH-PINK1 cells. (P values shown are the result of two-tailed student's t-test, * $P<0.05$ ** $P<0.01$) (all values shown are mean + sem)

Our next step was to ask whether KMP could be converted to the nucleotide triphosphate form (KTP) required for it to serve as a neo-substrate for PINK1. Work by many labs has demonstrated that ribosyl nucleotide analogs can be phosphorylated to nucleotide triphosphate forms by endogenous enzymes (Krishnan et al., 2002; Lieberman et al., 1955a; Ray et al., 2004). To confirm the presence of intracellular KTP following incubation with kinetin, we adapted an ion-pairing HPLC analysis method on a reverse phase C18 column (Figure 4.5D) according to established methods (Vela et al., 2007). After treatment with kinetin or DMSO, cells were lysed and analyzed for the presence of peaks eluting at the retention time of KTP. An internal standard of BTP (denoted by * in Figures 4.5D,E and 4.6A,B) was added following lysis. Analysis of the kinetin-treated cells revealed a peak that co-elutes (offset by a consistent amount (Figure 4.5D)) with synthetic KTP, a result not seen in any of our controls (Figure 4.5D,E and 4.6A). The UV absorbance maximum measured with a diode array detector is the same as KTP (Figure 4.6D)(absorbance peak at 268 nm) and significantly different than that of either ATP or GTP (Figure 4.6C) both of which have significantly different retention times. In a separate HPLC analytical run an aliquot of authentic KTP (to 80 μ M) was added to authenticate the putative KTP peak (Figure 4.6B). The peak grew to 186% of its original area, while the peak of the standard BTP decreased to 76% of its original area, suggesting that these were the same substance. From these data we calculate an ATP concentration of 1950 ± 421 μ M and KTP concentration of 68 ± 13 μ M (3 biological replicates Figure 4.6E), is produced upon incubation with kinetin.

4.3.3 Kinetin increases phosphorylation of PINK1 substrate anti apoptotic Bcl-xL

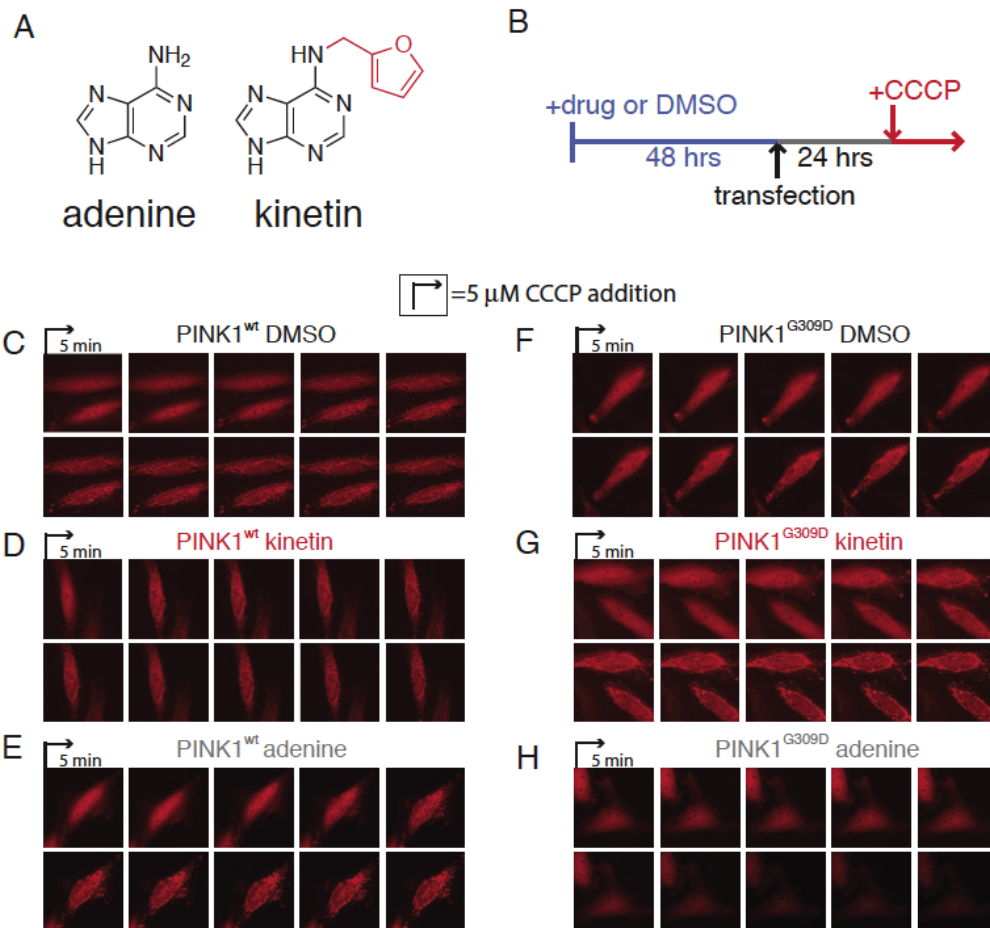


Figure 4.8 Analysis in HeLa cells reveals that PINK1 neo-substrate kinetin accelerates PINK1 dependent Parkin recruitment in cells. A. Chemical structure of adenine or kinase neo-substrate precursor kinetin. B. Schematic depicting HeLa cell drug treatment. (C-H) Sequential images of HeLa cells expressing mCherryParkin, mitoGFP and PINK1wt (C-E) or PINK1G309D (F-H) following CCCP induced depolarization.

Bcl-xL is a member of the Bcl-2 protein family that plays a key regulatory role in mitochondrial-induced apoptosis (Adams and Cory, 1998; Gross et al., 1999). PINK1 phosphorylates Bcl-xL at serine 62 in response to mitochondrial depolarization blocking cleavage to a pro-apoptotic form (Arena et al., 2013). We therefore measured PINK1-dependent phosphorylation of Bcl-xL in human SH-SY5Y cells following CCCP-induced depolarization. We analyzed DMSO, 50 μ M adenine or 50 μ M kinetin treated SH-SY5Y cells at 12 hours post 50 μ M CCCP addition (Figure 4.7A) and observed a significant ($p=0.01$, $p=0.04$; t-test) (Figure 4.7A) increase in phospho Bcl-xL (S62) only in kinetin treated cells compared to DMSO or adenine, where PINK1 expression has not been silenced by shRNA. These results confirm that CCCP mediated depolarization will induce PINK1 dependent phosphorylation on S62, and suggest that kinetin stimulates this activity in a PINK1 dependent manner.

4.3.4 Kinetin accelerates Parkin recruitment to depolarized mitochondria in a PINK1 dependent manner

Parkin recruitment to depolarized mitochondria is PINK1 dependent; (Narendra et al., 2010) therefore, we postulated that enhancement of PINK1 activity might accelerate this process. We treated cells with either kinetin or adenine (Figure 4.8A) and measured Parkin localization following CCCP mediated mitochondria depolarization. HeLa cells, which have low levels of endogenous PINK1 and PARKIN, were transfected with PINK1^{wt} or PINK1^{G309D}, mCherryParkin, and mitochondrial-targeted GFP (mitoGFP). After 48 hours of incubation with 25 μ M adenine, kinetin or equivalent DMSO (Figure 4.8B), we imaged every five minutes following CCCP-mediated depolarization of

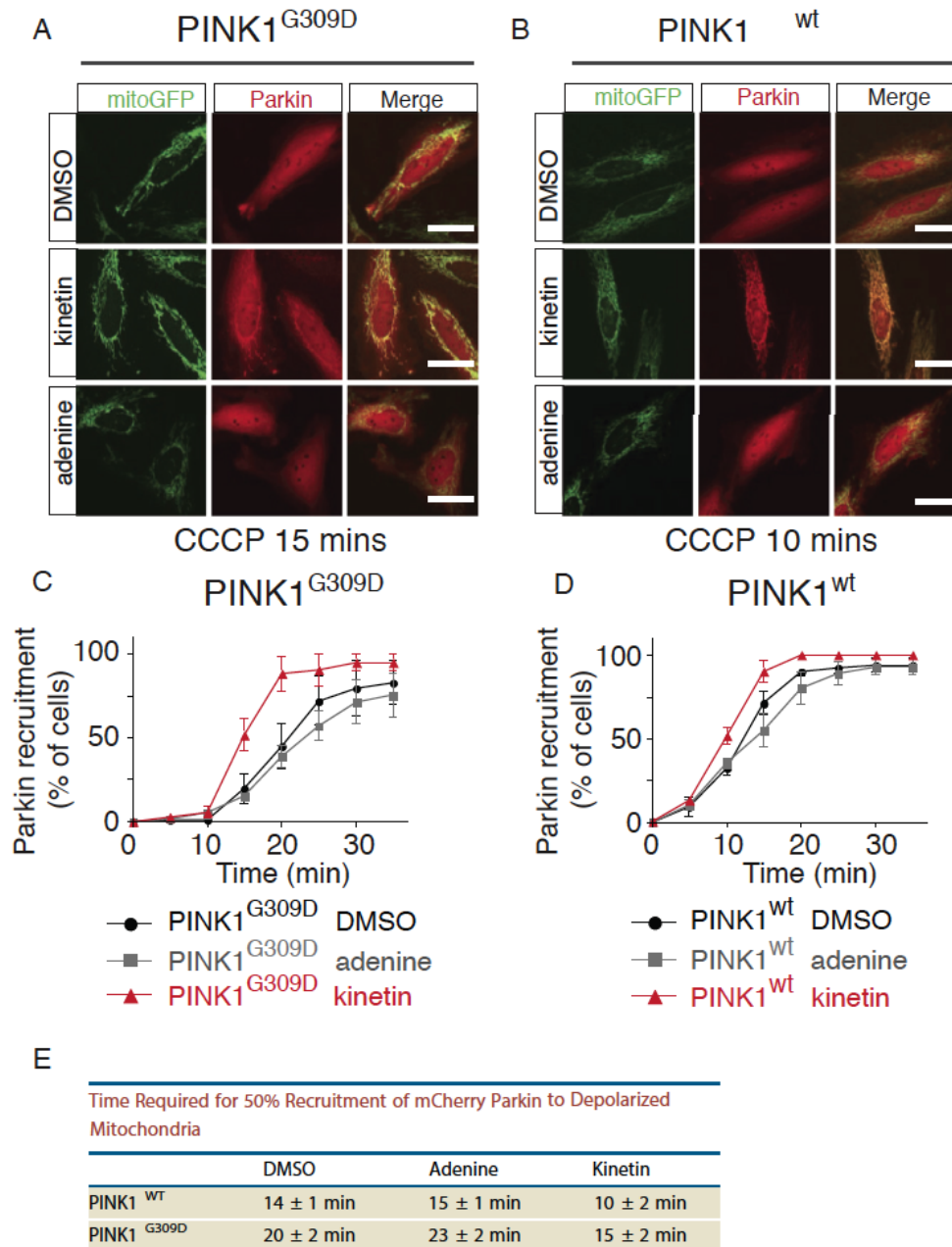


Figure 4.9 A-B HeLa cells treated with indicated drug, co-transfected with mitoGFP, mCherryParkin, and indicated PINK1 construct imaged at either 10 or 15 minutes after 5 μ M CCCP addition. C-D Kinetin treated cells reached R50 significantly faster than with adenine or DMSO (all data shown is mean + sem) by two-way ANOVA analysis kinetin has an effect in both cases when compared to adenine (wt; $F=25.41$ $p<0.0001$, G309D; $F=31.89$, $p<0.0001$) and DMSO (wt; $F=21.94$ $p<0.0001$, G309D; $F=12.79$, $p<0.0011$), no significant difference for DMSO adenine in either case (at least 150 cells/experiment $n=3$ experiments-all values are mean + sem). E. 50% recruitment times.

mitochondria (Figures 4.8C-H and 4.9A,B) and calculated the percentage of GFP labeled mitochondria with mCherryParkin associated (Figures 4.9A-D).

In line with previous reports (Narendra et al., 2010), transfection of PINK1^{G309D} slowed the 50% recruitment (R_{50}) time of mCherryParkin to depolarized mitochondria (23 ± 2 min vs. 15 ± 1 min R_{50}) (Figure 4.9C,E). The addition of kinetin, but not adenine, decreased the R_{50} for Parkin in PINK1^{G309D} cells from 23 ± 2 to 15 ± 2 min, and also decreased the R_{50} for PINK1^{wt} cells from 15 ± 1 to 10 ± 2 min (Figure 4.9C-E). Using an image analysis algorithm (Figure 4.10A,B) that quantified the time dependent change in co-localization, we found that PINK1^{wt} expressing cells achieved a maximum change in co-localization of 0.112 with DMSO or adenine and 0.13 with kinetin treatment (Figure 4.10C). PINK1^{G309D} expressing cells treated with DMSO or adenine achieved delta co-localization of 0.076, but upon addition of kinetin returned to near- PINK1^{wt} levels (0.124) (Figure 4.10D). These results suggested significant rescue of PINK1^{G309D} activity using kinetin. Two-way ANOVA analysis revealed that kinetin has an effect in both cases (wt; $F=24.10$ $p<0.0001$, G309D; $F=54.14$, $p<0.0001$). Additionally, in line with in vitro results in which benzyl triphosphate (BTP) did not activate PINK1 as robustly as KTP (Figure 4.3E), benzyl adenine is in general less active than kinetin in cells, although it also demonstrated some acceleration of Parkin recruitment (Data not shown). However, benzyl adenine has been shown to be cytotoxic in other assays (Ishii et al., 2002), therefore, despite PINK1 activation potential of benzyl adenine we decided to focus on KTP to use as a neo-substrate to amplify PINK1 activity.

To test the PINK1-dependency of our findings, we assayed PINK1 activity by using phospho-specific antibodies raised against the PINK1-specific S65 phosphosite on

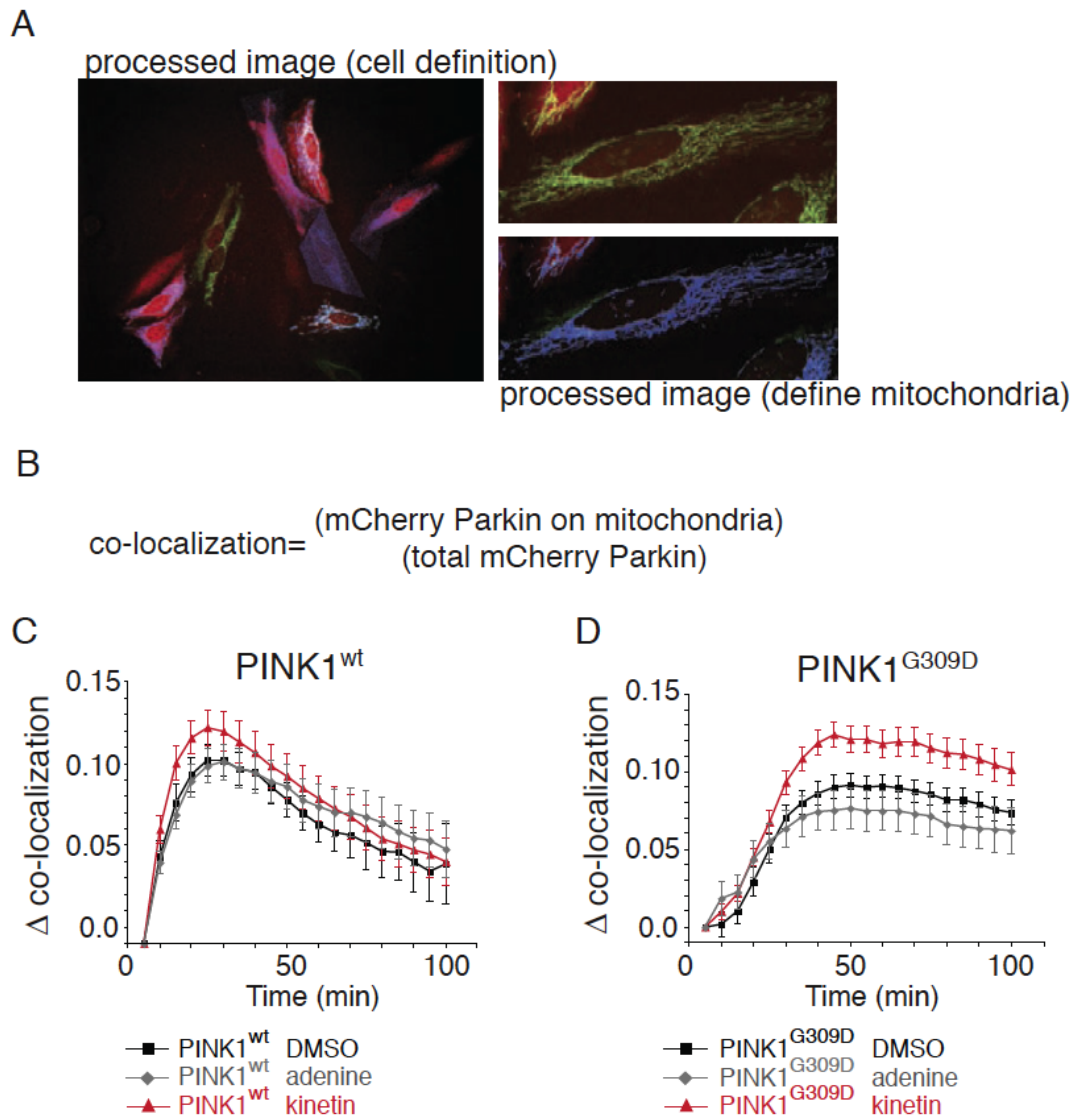


Figure 4.10 Automated quantitation reveals that PINK1 neo-substrate kinetin accelerates PINK1 dependent Parkin recruitment in cells. A. A cell mask was determined for each cell by manually drawing the cell boundary and a mitochondrial mask was determined, depicted in the lower right panel. B equation used to calculate the extent of co-localization. C,D. HeLa cells meeting a threshold of Parkin expression were quantitated using our co-localization algorithm to identify mitochondria (mitoGFP) and calculate the amount of mCherryParkin on mitochondria. Two-way ANOVA analysis revealed that kinetin has an effect in both cases when compared to adenine (wt; $F=43.65$ $p<0.0001$, G309D; $F=84.02$, $p<0.0001$) and DMSO (wt; $F=29.65$ $p<0.0001$, G309D; $F=85.88$, $p<0.0001$) at least 40 cells/experiment $n=3$ experiments.

Parkin (Kondapalli et al., 2012). We observed a small but reproducible increase in the phosphorylation level of Parkin following CCCP treatment in a PINK1-dependent manner (Figure 4.11A,B). In a finding that supported our co-localization results, we also found that the addition of neo-substrate kinetin ($p=0.03$; t -test), but not adenine ($p=0.30$; t -test), to PINK1^{G309D} mutant expressing cells increased the phosphorylation levels of Parkin (Figure 4.11C,D). The addition of an adenosine kinase inhibitor (AKI) blocking the conversion of kinetin to KTP prevented this effect ($p=0.31$; t -test) (Figure 4.11D).

4.3.5 Kinetin blocks mitochondrial motility in axons in a PINK1 dependent manner

Increasing PINK1 activity markedly decreases the mobility of axonal mitochondria and this is thought to be the first step in the sequestration and removal of damaged mitochondria (Wang et al., 2011). To determine if PINK1 activation by kinetin also decreases mitochondrial motility, we examined the mobility of axonal mitochondria in rat hippocampal neurons co-transfected with mitoGFP to identify mitochondria and N-terminal mCherry-tagged Synaptophysin to identify axons (Hua et al., 2011; Nakamura et al., 2011). Cells were pre-treated for 48 hours with 50 μ M kinetin, adenine, 9-methyl-kinetin (9MK shown in Figure 4.12A) or equivalent DMSO, and mitochondrial motility was imaged live. Kymographs were generated (Figure 4.12B-E) using standard techniques. Kinetin markedly inhibited the percentage of moving mitochondria when compared to DMSO ($p=0.0005$; t -test)(Figure 4.12D,F). In contrast, kinetin analog 9-methyl-kinetin (9MK) (Figure 4.12A,E,F), which cannot be converted to a nucleotide triphosphate form, did not affect mitochondrial motility when compared to DMSO

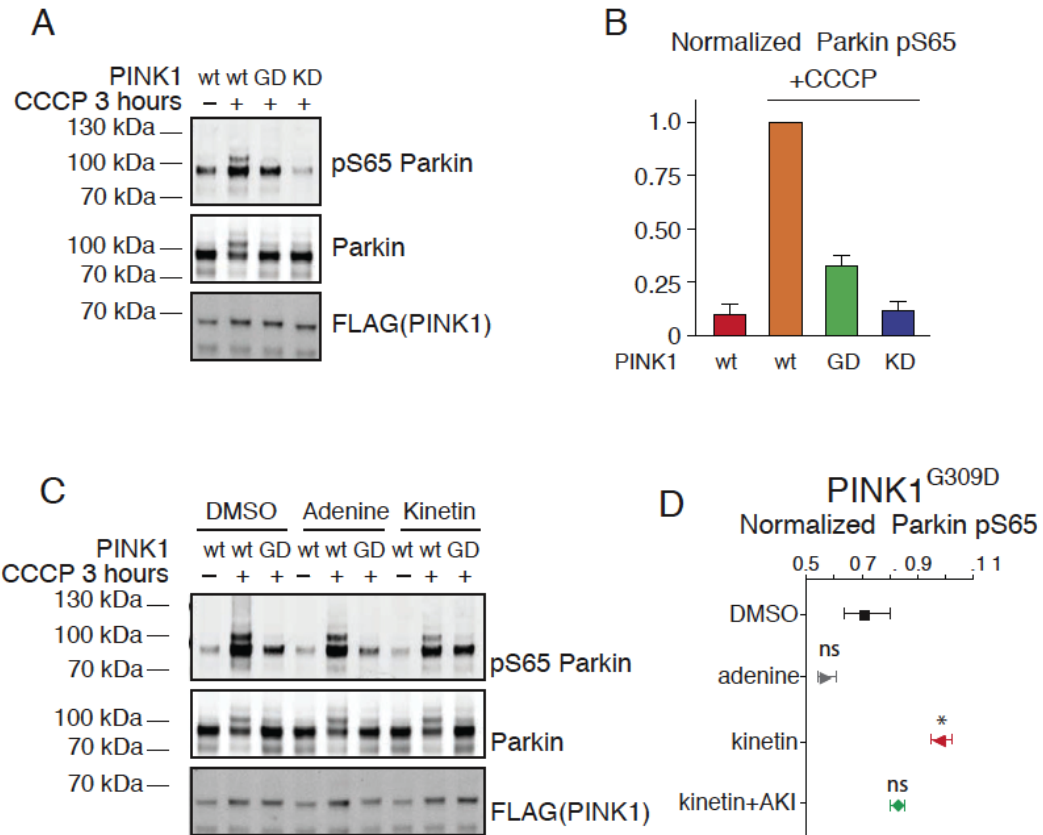


Figure 4.11 Quantitation of PINK1 mediated Parkin phosphorylation at serine 65. A,B HeLa cells were transfected with mCherryParkin and either PINK1wt, PINK1G309D or PINK1KDDD for 24 hours. Following incubation with CCCPCP for three hours cells were lysed, mCherryParkin was immunoprecipitated and analyzed by immunoblotting with Parkin S65 phospho-specific antibodies. C,D. HeLa cells were transfected with mCherryParkin and either PINK1wt or PINK1G309D for 24 hours, then incubated with 50 μ M adenine, kinetin, kinetin plus 10 nM adenosine kinase inhibitor or equivalent DMSO for 48 hours. mCherryParkin was immunoprecipitated and analyzed by immunoblotting with Parkin S65 phospho specific antibodies. Normalized Parkin phosphorylation was calculated by normalizing phospho S65 Parkin signal by total Parkin levels, normalized to phospho Parkin in untreated cells expressing PINK1wt treated with CCCPCP for three hours.

($p=0.86$; *t*-test). Kinetin also produced a small decrease in the velocity of mitochondria that remain in motion ($p=0.03$; *t*-test)(Figure 4.12G).

To confirm that kinetin decreases mitochondrial motility through effects on PINK1, we also performed experiments in hippocampal neurons derived from wild-type (C57BL/6) and PINK1 KO mice (Xiong et al., 2009) after treatment with DMSO, kinetin or 9MK. Consistent with the results in rat neurons, kinetin also significantly decreased mitochondrial motility in control neurons ($p<0.0001$; *t*-test) when compared with either 9MK or DMSO (Figure 4.12H). However, kinetin had no effect on the motility of mitochondria in PINK1 KO neurons (Figure 4.12H) ($p=0.64$; *t*-test), and, unlike rat derived neurons, kinetin had no effect on the velocity of mitochondria that remain in motion (Figure 4.12I). These data suggest that kinetin can block mitochondrial motility in a PINK1 dependent manner and that the metabolism of kinetin to KTP is a necessary precursor for that effect.

4.3.6 Kinetin decreases apoptosis induced by oxidative stress in human derived neuronal cells in a PINK1 dependent manner

Previous studies have shown that PINK1 expression can block apoptosis in response to proteosomal stress induced by the proteasome inhibitor MG132 (Klinkenberg et al., 2010; Wang et al., 2007). Caspase 3/7 activity is an early marker for apoptosis therefore, to assess the ability of kinetin to amplify PINK1 activity to block apoptosis, we measured caspase 3/7 activity using a fluorogenic caspase 3/7 peptide cleavage assay in HeLa cells. We treated HeLa cells transfected with Parkin with DMSO or 25 μ M adenine or kinetin for 48 hours, followed by 1 μ M MG132 for 12 hours. We found that kinetin significantly

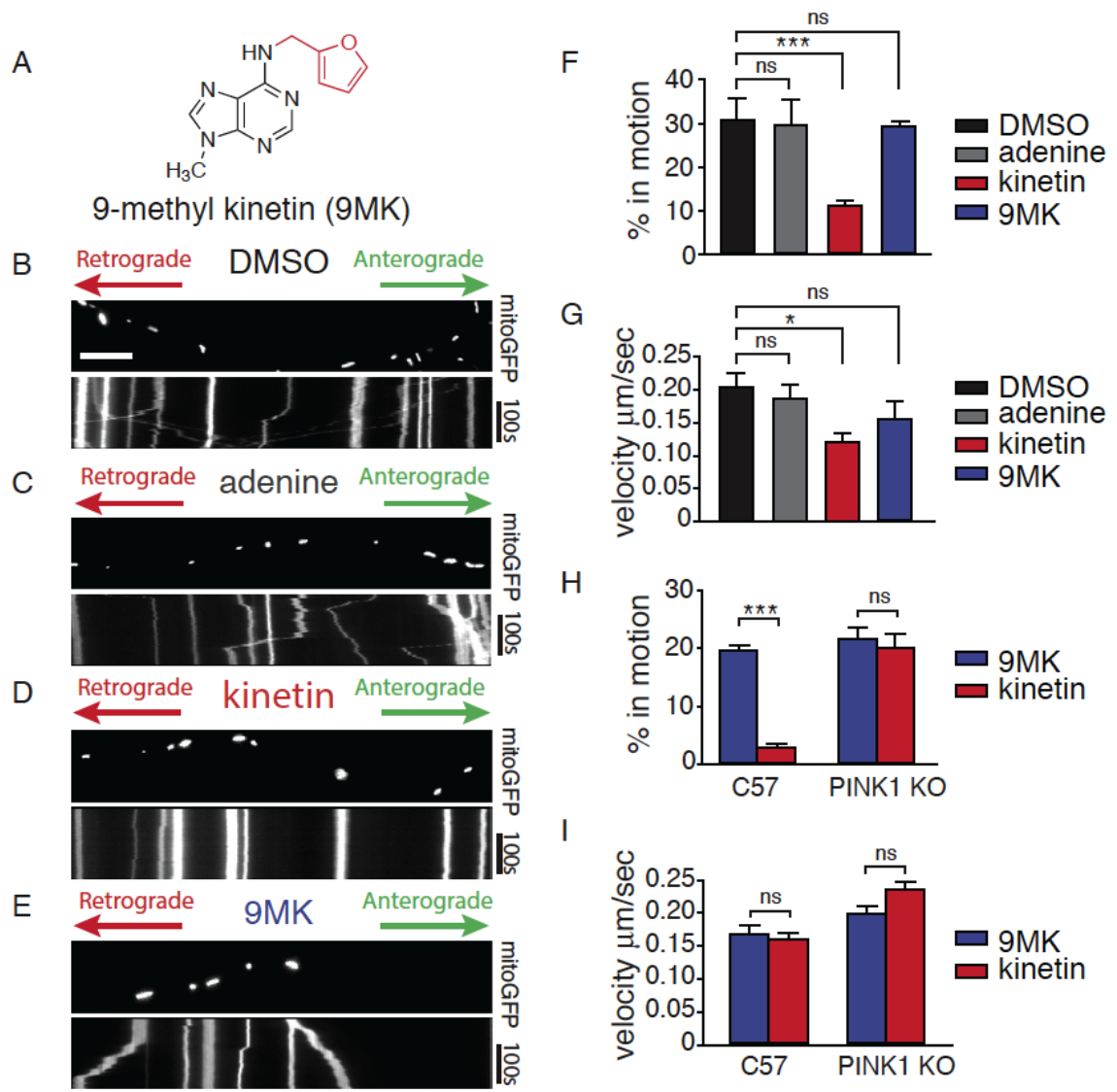


Figure 4.12 Kinetin halts axonal mitochondrial motility in a PINK1 dependent manner. A. Chemical structure of negative control non-metabolizable kinetin analog 9-methyl-kinetin. B-E. Kymograph for analysis of mitochondrial movement in representative PINK1wt expressing rat derived hippocampal axons transfected with mitoGFP. Scale bar represents 10 μm . F. The percentage of time each mitochondrion was in motion was determined and averaged. Kinetin significantly blocks mitochondrial motility whereas 9MK has no effect (DMSO-kinetin, $P=0.0005$; DMSO-9MK, $P=0.86$) G. Kinetin induces a small decrease in velocity (DMSO-kinetin, $P=0.03$; DMSO-9MK, $P=0.24$). H. Kymograph for analysis of mitochondrial movement in C57BL/6 shows a response to kinetin (kinetin 9MK, $P<0.0001$), whereas in PINK1 knockout derived hippocampal axons kinetin has no effect (kinetin 9MK, $P=0.64$). I. Both kinetin and 9MK have no effect on mitochondrial velocity of moving mitochondrion (C57BL/6 kinetin-9MK, $P=0.64$; PINK1 KO, $P=0.074$) (all values are mean + sem, analysis was two tailed students t-test)

($p=0.005$, $p=0.004$;t-test) reduced Caspase 3/7 cleavage versus DMSO or adenine pre-treatment, and that knockdown of PINK1 abrogated this effect (Figure 4.13B,D).

We then tested whether kinetin would be tolerated by cultured DA neurons. Previous work has shown KTP precursor kinetin to be extremely well tolerated in both mouse models and in human clinical testing (Axelrod et al., 2011; Shetty et al., 2011). To confirm these results, we treated DA neurons with 50 μM kinetin or adenine, and measured cell density after 10 days. Kinetin and adenine have no effect on cell density, indicating that neither promotes apoptosis of cultured DA neurons (Figure 4.13A).

We next utilized patient-derived neuroblastoma SH-SY5Y cells, which are also known to exhibit decreased apoptosis upon overexpression of PINK1 (Deng et al., 2005; Klinkenberg et al., 2010). We performed a dose-response assay in which SH-SY5Y cells were treated with increasing concentrations of kinetin, adenine or DMSO for 96 hours, 1 μM MG132 for 16 hours, followed by analysis for Caspase 3/7 cleavage activity. As in HeLa cells kinetin pre-treatment significantly decreased Caspase 3/7 cleavage in SH-SY5Y cells (Figure 14A). Two-way ANOVA analysis revealed that kinetin has an effect when compared to DMSO or adenine (Figure 4.14A) (DMSO; $F=34.95$ $p<0.0001$;adenine; $F=38.37$ $p<0.0001$) only in cells where we did not silence PINK1 expression via stable shRNA expression (DMSO; $F=3.552$ $p=0.084$;adenine; $F=1.7$ $p=0.215$) (Figure 4.14A,B and 4.13C) despite a small visible effect, probably due to incomplete knockdown of PINK1 (Figure 4.13C)). These experiments suggest that the kinetin-induced reduction in Caspase 3/7 cleavage activity is PINK1 dependent.

To assay later stages of apoptosis in SH-SY5Y cells, we utilized an independent FACS based method to measure cellular apoptosis. In addition to proteosomal stress,

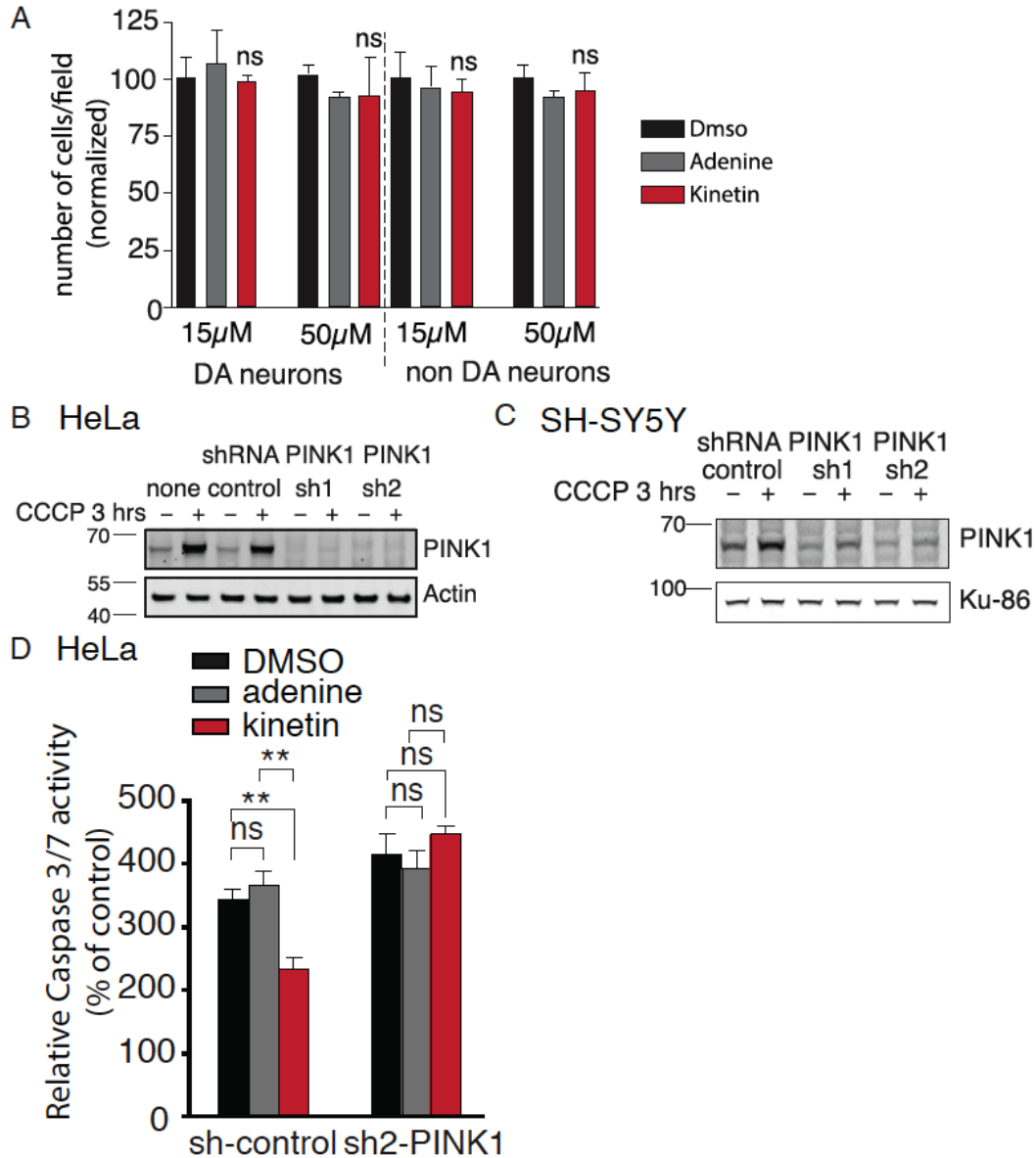


Figure 4.13 Kinetin inhibits oxidative stress induced apoptosis in human cells in a PINK1 dependent manner. A Postnatal dopamine neurons were cultured with 50 µM drug for 10 or 12 days (days 2-14). The mean number of surviving dopamine and non-dopamine neurons per field was quantified. B,C HeLa cells B or SH-SY5Y cells C were infected with a lentivirus (pLKO.1 based vector) expressing either non-mammalian shRNA (sh-control) or one of two (sh1 and sh2) PINK1 directed shRNA constructs. Cells were plated in a six well plates and the indicated lanes depict cells treated with 10 µM CCCP for 3 hours. Following CCCP treatment cells were lysed and analyzed by immunoblotting for PINK1 (cell signaling) and a loading control (all values are mean + sem). D. Caspase 3/7 cleavage activity assay following pre-treatment with DMSO, adenine or kinetin for 48 hours followed by MG132 treatment for 12 hours compared to no MG132 treated cells reveals reduced Caspase 3/7 activity ($p=0.005$, $p=0.004$;t-test) only in sh-control expressing cells not in cells expressing shRNA against PINK1.

PINK1 over-expression is known to block apoptosis induced by H₂O₂ treatment (Deng et al., 2005; Gautier et al., 2008; Petit et al., 2005; Pridgeon et al., 2007). SH-SY5Y cells were treated with 50 μM kinetin, adenine or DMSO for 96 hours, followed by 400 μM H₂O₂ treatment for 24 hours. Using a cytometry-based FACS assay utilizing annexin V and propidium iodide staining, we determined the percentage of apoptotic cells after treatment with DMSO, adenine or kinetin (Figure 4.14C). We observed a significant decrease in the total amount of apoptotic cells following kinetin treatment (Figure 4.14D) (DMSO vs. kinetin p=0.0023; Wilcoxon *T* test), but no significant change with adenine (DMSO vs. adenine, p=0.09; Wilcoxon *T* test). Additionally, we observed a significant drop in apoptosis in shRNA control lentivirus infected cells (DMSO vs. kinetin p=0.008; Wilcoxon *T* test), but no kinetin effect with infection of a lentivirus expressing PINK1-silencing shRNA (Figures 4.14E and 4.13C) (DMSO vs. kinetin, p=0.23; Wilcoxon *T* test). These results demonstrate a PINK1-dependent anti-apoptotic effect, and suggest that kinetin can activate PINK1 to block oxidative stress induced apoptosis of human neural cells.

4.4 Discussion

Our investigation of a neo-substrate approach to modulating PINK1 activity has yielded three significant findings: 1) that the ATP analog kinetin triphosphate (KTP) can be used by both PINK1^{wt} and PINK1^{G309D}; 2) that KTP enhances both PINK1^{wt} and PINK1^{G309D} activity in vitro and in cells, and in the case of the latter version, returns it to near-wt catalytic efficiency; and 3) that KTP precursor kinetin can be applied to neurons to enhance PINK1 activity in several biologically relevant paradigms.

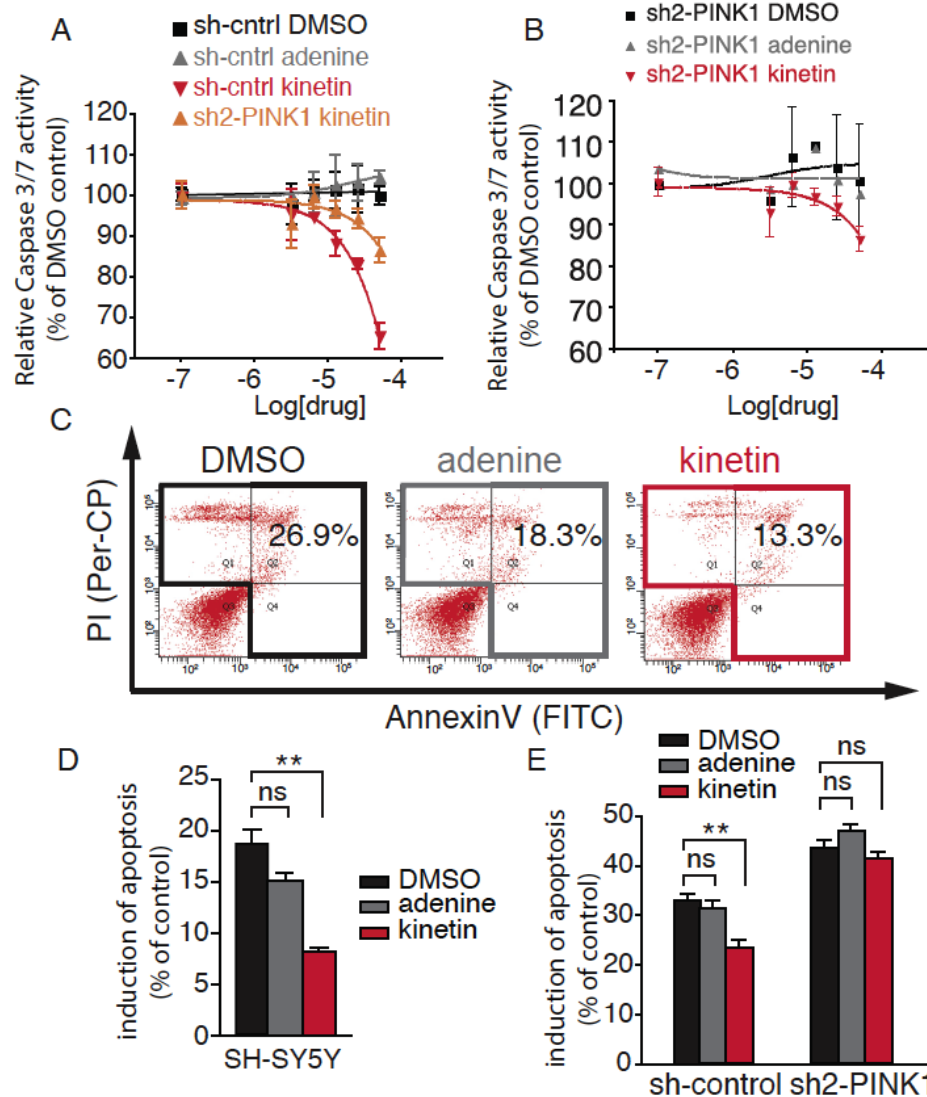


Figure 4.14 Kinetic inhibition of stress induced apoptosis in human cells in a PINK1 dependent manner. A,B, Caspase 3/7 cleavage activity of SH-SY5Y cells pre-treated with indicated concentration of adenine or kinetin for 96 hours followed by MG132 treatment for 12 hours in all conditions. Two-way ANOVA analysis revealed that kinetin has an effect when compared to DMSO or adenine (Figure 5B) (DMSO; $F=34.95$ $p<0.0001$; adenine; $F=38.37$ $p<0.0001$) but no statistically significant effect (DMSO; $F=3.552$ $p=0.084$; adenine; $F=1.7$ $p=0.215$) in cells expressing an shRNA against PINK1 (C) SH-SY5Y cells pre-treated as above, were stained with FITC conjugated Annexin V and propidium iodide and analyzed by FACS. (D) Quantification of (C) shows kinetin treated cells have significantly lower induction of apoptosis (DMSO-kinetin, $P=0.0023$) but adenine had no effect (DMSO-adenine, $P=0.09$). (E) Indicated SH-SY5Y cell lines were treated as in Figure 4.13.D. Kinetin treated cells had significantly lower induction of apoptosis only when PINK1 was present (normalized to DMSO control untreated cells)(sh-control DMSO-kinetin, $P=0.008$) (sh-PINK1 DMSO-kinetin, $P=0.23$)(sh-Control DMSO-adenine, $P=0.48$; sh-PINK1 DMSO-adenine, $P=0.23$) (all values are mean + sem, analysis was Wilcoxon t-test)

The finding that kinetin (or its nucleotide triphosphate form, KTP) can restore PINK1^{G309D} catalytic activity to near-wt levels *in-vitro* and in cells, in light of the fact that mutations in PINK1 produce PD in humans, raises the possibility that kinetin may be used to treat patients who have mutant PINK1. Further, because kinetin has already been shown to be well tolerated in human trials (for familial dysautonomia, an unrelated splicing disorder), and since previous work in mice has shown that kinetin can cross the blood-brain barrier and achieve pharmacologically significant concentrations (Axelrod et al., 2011; Shetty et al., 2011), these results have the potential for near-term clinical relevance.

Although mutations in PINK1 are a rare cause of PD, the development of an effective disease modifying therapy for any neurodegenerative disease would be a tremendous advance, and could provide important therapeutic insights into disease modifying strategies for other types of PD. In fact, the finding that increasing PINK1 activity beyond endogenous levels can protect against a variety of apoptotic stressors (Klinkenberg et al., 2010; Petit et al., 2005; Pridgeon et al., 2007), and that kinetin can also reproduce this protection by enhancing endogenous PINK1 function, raises the possibility that enhancing PINK1 activity may also have therapeutic potential for idiopathic PD.

Current kinase targeted drugs are striking for the single modality of regulating kinase function—inhibition. However, a wide range of kinase dysregulation in disease is caused by a lack of kinase activity: desensitization of insulin receptor kinase in diabetes (Kulkarni et al., 1999); inactivation of the death associated protein kinase (DAPK) in cancer (Kissil et al., 1997); inactivation of the LKB1 tumor suppressor kinase in cancer

(Gao et al., 2011); and decreased PINK1 activity in early-onset Parkinson's Disease. Although many examples of inactive kinases causing disease have been uncovered, there have been no therapeutic approaches for enhancing kinase activity using alternative substrates. Our insights into the potential for manipulating kinase-dependent cellular processes via a specifically targeted neo-substrate may presage the ability to treat other diseases resulting from kinase misregulation with a novel class of neo-substrate kinase activators.

4.5 Experimental Procedures:

4.5.1 Western blot analysis

Western blots analysis was carried out as described (Ultanir et al., 2012) with the indicated antibodies. See Supplementary Information for details.

4.5.2 Expression, purification and enzymatic characterization of PINK1

H. sapiens PINK1 kinase domain (PINK1, residues 156-496 all plasmids obtained from Addgene) with an N-terminal GST tag was expressed using a pGEX vector using standard techniques. *H. sapiens* PINK1 kinase domain with c-terminal extension (PINK1, residues 112-581) with a C-terminal FLAG₃ tag was co-expressed with full length *H.sapiens* TRAP1 in the baculovirus/*Sf21* insect cell system. Following lysis, PINK1₁₁₂₋₅₈₁ kinase was purified using magnetic M2 FLAG affinity resin (Sigma) with the kinase reaction performed on beads after no more than 2 hours following lysis. The reaction was performed using 50 mM Tris-HCl, 150 mM NaCl, 10 mM MgCl₂, 3 mM MnCl₂, 0.5 mM DTT and 1 mg/ml substrate if not otherwise indicated. After reaction at room temperature with rotation, kinase reaction was quenched with 50 mM EDTA and reacted with 1.5 mM p-nitrobenzylmesylate (PNBM) and identified by immunoblot with anti thiophosphate ester antibody (Epitomics) (Allen et al., 2007).

4.5.3 Identification of PINK1 autophosphorylation site by LC/MS/MS

PINK1^{wt} and PINK1^{KDDD} were incubated with KTP γ S in the presence of cell lysate, digested with trypsin, and thiophosphorylated peptides were captured using established methods as described (Ultanir et al., 2012). Captured peptides were analyzed by LC/MS/MS analysis on a Velos Orbitrap (Thermo). PINK1 autophosphorylation site was found only with PINK1^{wt} and KTP γ S which indicates this nucleotide is utilized as a bona fide substrate

4.5.4 Enzymatic production of KMP in vitro

Reaction with APRT, PRPP and either adenine, kinetin or 9MK were carried out as described (Parkin et al., 1984) and as detailed. 0.5 mM adenine, kinetin or 9MK were added to a solution of 100 mM Tris-HCl pH 7.5, 10 mM MgCl₂, 2 mM PRPP (Sigma), and mixed well. Reaction was initiated by addition of 10 U of APRT (Genway Biotech) and the reaction was incubated at 37°C for the indicated time. The reaction was quenched by dilution of the reaction into an equal volume of 0.1% TFA in H₂O with 50 mM EDTA at 4 °C followed by analysis on an Acquity UPLCMS system (Waters). Production of AMP and KMP were quantified by extracted ion spectrum and peak integration.

4.5.5 HPLC analysis for KTP production in cells

HeLa cells were incubated with the indicated drug for 96 hours and nucleotides were extracted and analyzed as described (Ray et al., 2004; Vela et al., 2007) and as detailed. HeLa cells were grown in DMEM supplemented with 10% FBS with either 0.05% DMSO or 25 μ M Kinetin for 96 hours. For each assay six 15-cm plates of confluent

HeLa cells were washed with ice cold PBS, scraped into 5 ml ice cold PBS pelleted and lysed by addition of a volume of 80% Methanol at -80°C equal to the cell pellet for lysis and deproteination. Cells were vigorously resuspended on ice and left for 2 hours at -20°C before vortexing for 10 seconds and centrifugation at top speed. The pellet was then washed with 1 pellet volume of ice cold water and this was added to the lysate along with an appropriate volume of 10 mM BTP to 250 μ M final. 20 μ l was then injected onto a HPLC (Waters) and analyzed by a linear gradient from 100% buffer A (5 mM tetrabutylammonium hydroxide (TBAH) 25 mM KH_2PO_4 5% acetonitrile) to 65% buffer B (5 mM tetrabutylammonium hydroxide (TBAH) 25 mM KH_2PO_4 60% acetonitrile) over 37.5 minutes. Concentration of ATP, KTP and other nucleotides were determined by comparing to a standard dilution curve of each.

4.5.6 Parkin mitochondrial translocation assay

HeLa cells were grown in DMEM supplemented with 10% FBS. Log phase cells were plated in 24 well plates with glass coverslips (Mattek) pretreated with fibronectin. Cells were pretreated with 25 μ M of the indicated compound, followed by transfection with MitoGFP, mCherryParkin, and full length PINK1FLAG₃ in a 1:4:2 ratio using Fugene 6 (Promega). Fields of cells were selected by expression of MitoGFP (6 fields/well-3 wells/condition) and imaged at five-minute intervals following depolarization with 5 μ M CCCP. Quantification was performed according to published protocols (Narendra et al., 2010) and by implementing a Matlab based script (See Supplementary Information for details and for script).

4.5.7 Details on automated quantitation of Parkin mitochondrial translocation

To calculate the fraction of Parkin recruited to mitochondria, a cell mask was determined for each cell by manually drawing the cell boundary and a mitochondrial mask was determined by thresholding the GFP channel using Otsu's method (Otsu, 1979). The fraction of Parkin recruited to mitochondria was then calculated as the total mCherry intensity within the mitochondrial mask divided by the total mCherry intensity within the cell mask. Delta co-localization was calculated by subtracting the fraction of Parkin recruited to mitochondria at $t=0$ from each subsequent timepoint. Cells with poor mCherry expression were excluded by requiring a minimum total mCherry signal within the cell mask.

4.5.8 Mitochondrial motility assay

All experiments were carried out according to IACUC guidelines and UCSF IACUC approved all experiments before execution. Primary hippocampal cultures were prepared from early postnatal (P0-P1) rat or mouse (C57BL6 or Pink1 $-/-$) pups, co-transfected by electroporation (Amaxa) with mitochondrial targeted GFP (mitoGFP) to visualize mitochondria, and mCherry fused to synaptophysin (mCherrySynaptophysin) to visualize axons. Cells were pre-treated for 48 hours with 50 μ M kinetin, adenine, 9-methyl-kinetin or equivalent DMSO at day 9 and imaged live in Tyrode's medium (in mM: 127 NaCl, 10 HEPES-NaOH, pH 7.4, 30 glucose, 2.5 KCl, 2 CaCl₂, 2 MgCl₂) with a 60x water immersion objective on a Nikon Ti-E inverted microscope. Images were captured every 2 s for a total of 200s, and kymographs were generated from each live-imaging movie with

Metamorph software (version 7.7.3.0). Mitochondria were considered moving if they travelled more than 0.67 μm during the 200 s imaging.

4.5.9 PINK1 shRNA production

PINK1 shRNA lentivirus were produced using a pLKO.1 based shRNA (Sigma) by co-transfection of a 6 cm dish of HEK293T cells with pLKO.1 shRNA vector, $\Delta 8.9$ and pMGD2 vectors in a 2:3:1 ratio (3 μg total DNA with 7 μl Fugene 6 in 200 μl of Optimem) and following standard protocols to isolate infective lentivirus particles. HeLa and SH-SY5Y cells were infected with lentivirus followed by selection with puromycin at 10 $\mu\text{g}/\text{ml}$ and 1 $\mu\text{g}/\text{ml}$ respectively.

4.5.10 Dopamine neuron cultures

Midbrain neuronal cultures were prepared from early postnatal (P0-P1) rats as described (Nemani et al., 2010). On day 2, cells were treated with kinetin, adenine, 9-methylkintin or equivalent DMSO (15 μM or 50 μM). On day 14, cells were fixed with 4% paraformaldehyde, and stained against tyrosine hydroxylase (rabbit, Pel-Freez Biologicals) to identify dopamine neurons, and NeuN (mouse, Millipore) to identify total neurons.

4.5.11 Apoptosis assays and phospho S62 Bcl-xL immunoblot analysis

HeLa cells were plated on 96 well assay plates at around 4,000 cells per well and transfected with Parkin in a similar way as in recruitment assays followed by treatment with 25 μM of the indicated drug for 48 hours. Growth medium was then replaced with fresh medium plus 25 μM drug and 1 μM MG132 for 12 hours, followed by addition of one time medium volume Caspase-Glo reagent (Promega), incubated at room temperature in the dark for 1 hour and read on a microplate reader (Molecular Devices) for luminescence.

SH-SY5Y cells (ATCC) were cultured in 1:1 mix of F12K and DMEM supplemented with 20% FBS. The indicated SH-SY5Y cells were plated in 6-well plates at about 500,000 cells/well, pretreated with 50 μM of the indicated drug or DMSO for 96 hours followed by 400 μM H_2O_2 treatment. Subsequently, cells were stained with Annexin V-FITC and PI and analyzed (FACS Diva) on a FACS LSRII Cytometer (Beckman Coulter) Apoptosis was calculated as the difference between H_2O_2 treated samples and the respective control. SH-SY5Y cells pre-treated in the same way followed by 50 μM CCCP treatment for 12 hours were lysed and analyzed for phospho S62 Bcl-xL (Santa Cruz Biotech), total Bcl-xL, PINK1 and β -actin (all Cell Signaling) by immunoblots.

Appendix A. Basic Protocol: Digestion and Covalent Capture of Thiophosphorylated Peptides

A.1.1 Materials

Solutions and Reagents:

50 mM NH_4HCO_3 ,

500 mM EDTA store indefinitely at 22°C

99% pure Urea store indefinitely at 22°C

Siliconized microcentrifuge tubes

1 M *tris* 2-carboxyethyl phosphine (TCEP) in H_2O make fresh.

1 M Dithiothreitol (DTT) store for 6 months at -80°C

Iodoacetyl Agarose Beads (Pierce) store for 6 months at 4°C

200 mM HEPES pH 7.3 store for 4 months at 22°C

Ziptips (10 μL and 100 μL) store for indefinitely at 22°C

Small Disposable Columns (Isolute SPE Accessories Double Fritted Column 120-1021-A and Single Fritted Res 120-1111-A) Biotage store for indefinitely at 22°C

5 M NaCl store for indefinitely at 22°C

5% Formic acid store for 3 months at 22°C

50% Acetonitrile: 50% H_2O store for indefinitely at 22°C

C-18 Sep Pak (Waters) store for indefinitely at 22°C in dessicator

Oasis SPE (Waters)

0.1 % TFA 50 % Acetonitrile H₂O store for indefinitely at 22°C

0.1 % TFA H₂O store for indefinitely at 22°C

Special Equipment:

LTQ Orbitrap, Orbitrap Velos, Orbitrap Elite (Thermo Fisher)

A.1.2 Digestion of labeled protein lysate

In addition to the experimental samples, we recommend the following five control samples:

1. 100 pmol of hyper-thiophosphorylated MBP (see A.2.5)
2. Unlabeled lysate.
3. Unlabeled lysate plus 100 pmol hyper thiophosphorylated MBP.
4. Lysate plus ATP γ S analog minus kinase.
5. An additional covalent capture reaction control (see step 2-1) and the experimental sample: Lysate plus ATP γ S analog plus kinase.

These controls will ensure that all the steps of this protocol are working correctly.

The MBP alone and MBP plus lysate will lead to recovery of only one peptide

(see Expected Results Section for MW). The lysate controls will provide a list of non-specific substrates.

1. To achieve complete digestion it is best to keep the sample volume as low as possible during the digestion.

i. Add Urea to 60% by volume (i.e. for 100 μ l sample volume add 60 mg of urea) to give final urea concentration of 6 M

2. Following addition of Urea, add freshly prepare 1M TCEP to 10 mM final volume.

Incubate the sample at 55°C for 1 hour then cool the sample at room temperature for 10 minutes.

Do not incubate the sample with an alkylating agent such as iodoacetamide. This will react with the thiophosphate group thereby destroying the reactivity of the tag.

3. Dilute the sample by adding 100 mM NH_4HCO_3 such that the final concentration of Urea is 2 M and add additional 1 M TCEP to a final concentration of 10 mM. Then add trypsin in a 1:50-1:10 ratio by weight (1:10 would be 10 μ g trypsin for 100 μ g of lysate protein). Check the pH of the digestion by spotting 0.5 μ L on a pH strip before proceeding as the trypsin is supplied in acetic acid. Add 10% NaOH until the pH is 7.8

As no iodoacetamide is used in this protocol, high concentrations of urea (2 M) and reducing agent (10 mM TCEP) are used to ensure that proteins in the lysate remain unfolded during the digestion. One easy way to optimize the amount of trypsin and the incubation time is to add BSA to the lysate and then to analyze the digested peptides to determine the sequence coverage. Coverage of at least 60-80% of BSA or around 30-35 peptides should be accomplished with <5% missed cleavages.

4. After incubation at 37°C for 6 hrs to overnight, acidify the sample by adding 100% TFA to attain 0.5% TFA

Check the pH of the solution and continue adding TFA until the pH reaches 1-2.

5. Wash a C-18 Sep Pak (or a Oasis HLB) with 10 mL of 0.1% TFA 50% Acetonitrile: H₂O, followed by 10 mL of 0.1% TFA:H₂O. Load the acidified sample to the column and pass it through the column 5 times. Wash the column with 20 mL 0.1% TFA:H₂O. Elute the peptides with 0.8 mL 0.1% TFA in 50% Acetonitrile: H₂O, and then an additional 0.2 mL 100% Acetonitrile . Concentrate to near dryness using a speed vacuum.

Different Solid Phase Extraction columns can lead to differential retention of peptides. We have seen success with both types of column (the more hydrophobic C-18 as well as the more hydrophilic Oasis HLB type column) however each lysate will require optimization. Do not take the sample to dryness, as the peptides may be difficult to resuspend into solution. The peptides should be in

around 50 μ L after evaporation so that the correct reaction volume can be attained.

A.1.3 Covalent Capture of Thiophosphorylated Peptides

6. Prepare the Iodoacetyl agarose beads for each sample by pipeting 100 μ L of the 50% resin slurry into a siliconized 0.5 μ L tube. Spin on a tabletop centrifuge for 30 seconds at 10,000 x g and remove the supernatant. Wash with 200 μ L 200 mM HEPES pH 7.3, spin and remove supernatant. Add 5 μ l 5 mg/mL BSA to the wall of the tube and leave until addition of the peptide mixture.

The beads are supplied in an acidic buffer; washing with 200 mM HEPES pH 7.0 is critical to achieving the correct final pH. The addition of BSA helps by blocking the agarose beads and prevents sample loss by non-specific adsorption.

2-1. In this step set up an additional covalent capture reaction by directly adding several pmols of the thiophosphorylated CREB peptide to the beads in 50% Acetonitrile 50% 20 mM HEPES pH 7.0 with BSA. (10-50 pmol should give a very robust signal)

7. Adjust the pH of the digested labeled peptide mixture by adding 200 mM HEPES pH 7.0 to a final concentration of 50 mM (for example add 37.5 μ L 200 mM HEPES pH 7.0, 10 μ L H₂O and 75 μ L acetonitrile to 50 μ l digested peptides for a final volume of 150 μ l). After adding 200 mM HEPES pH 7.0 check the pH of the peptides again by spotting 0.5 μ L on a pH strip. Add 10% NaOH until pH 7.0. Spin the beads down again, remove

the supernatant and add each sample to one tube of bead mixture followed by room temperature incubation in the dark with gentle rocking for 12-16 hours.

It is critical to make sure the sample is at pH 7.0 before reacting with the Iodoacetyl beads. Adding the additional labeled peptide control at this point will simplify troubleshooting later. To prevent light from generating reactive iodine species within the sample we recommend wrapping the tubes in aluminum foil.

8. Prepare one disposable column for washing and elution of each reaction by washing with 1 mL 50% Acetonitrile: 50% H₂O and 1 mL H₂O.

At this point two methods can be used, a column method or a spin method. The protocol is the same in each case however the column method is detailed below. For the spin method all the washes should be performed by addition of the same volume followed by a short 30 second spin at 10,000 x g.

9. Add the entire reaction to the top of the column and let it drain into a 1.5 mL microcentrifuge tube. Wash the reaction tube with 100 μ L 50% Acetonitrile 50% 20 mM HEPES pH 7.0 being sure to resuspend all the beads, and add the residual beads to the column.

10. Wash the beads by adding 1 mL of each wash liquid to the top of each column. Then push through the wash liquid using a P1000 pipet.

Wash the beads with 1 mL each in the following order:

1. H₂O
2. 5 M NaCl
3. 50% Acetonitrile
4. 5% Formic Acid

If the level of wash liquid drops below the top of the beads the recovery of phosphopeptides is severely reduced. In addition, the order of washing is critical to the success of the washing steps.

11. Prepare a solution of 10 mM DTT and add 1 mL to the column, allowing it to drain half way, and then incubating for 10 minutes with the solution in the column.

The addition of DTT to the beads will react with any available iodoacetyl groups left on the beads and will ensure that no I₂ forms during the oxidation step which can iodinate tyrosine residues (unpublished data).

12. Prepare a fresh solution of 1 mg/mL Oxone pH ~3.5 in water and add 100 µL of this solution to the column being sure to resuspend the beads. After draining the column, add an additional 200 mL and incubate for 10 minutes.

Be sure to resuspend the beads at this point to ensure the complete oxidation of the thiophosphate ester.

13. Immediately desalt and concentrate the phosphopeptides with a 10 μ L C-18 ziptip. Wash the ziptip 3X with 0.1 % TFA 50 % acetonitrile H₂O, then 3X with 0.1 % TFA H₂O. Attach the ziptip to the end of a P200 tip and draw the sample through the tip using the P200 on a setting of 100 μ L passing the sample through the ziptip a total of 4 times. Wash 2X with 20 μ L 0.1 % TFA H₂O and elute by washing 3X with 20 μ L of 0.1 % TFA 50 % Acetonitrile H₂O.

Passing the entire sample through the ziptip multiple times ensures the retention of low abundance peptides. The 10 mL ziptip should fit on the end of a P200 or P1000 tip to simplify the passage of the entire sample across the C-18 column.

14. Concentrate the sample to 10 μ L on a speed vacuum and analyze 5 μ L by tandem mass spectrometry. Typically we use an Orbitrap Velos that includes coupled liquid chromatography on a reverse phase C18 column utilizing a 3–32% acetonitrile gradient in 0.1% formic acid. Analyze the phosphopeptides in positive ion mode. MS spectra are acquired for 1 s. For each MS spectrum the two most intense multiply charged peaks are selected for generation of subsequent collision-induced dissociation MS.

This analysis will provide the identity of both the substrate protein and the phosphorylation site.

15. Analyze the data by centroiding using Analyst QS software or another appropriate software. Search the MS/MS spectra against the entire UniProt database utilizing Protein Prospector or another appropriate software. Typically we select no constant modifications

and allow the following variable modifications: Phospho: Serine, Threonine, Oxidized: Methionine.

Protein Prospector is available free of charge online: <http://prospector.ucsf.edu>

A.2.1 Support Protocols

A.2.1 Materials

Materials for A.2.2, A.2.3

N-6 substituted Adenosine 5'-[γ -thio]triphosphate (exclusively from Biolog) store 10 mM stock in aliquots at -80C for one year and avoid freeze thaw cycles

p-nitrobenzyl mesylate (PNBM) (exclusively from Epitomics: www.epitomics.com) store solid for 1 year at 4°C. A 50 mM stock in DMSO may be stored frozen for one year in one time use aliquots.

Thiophosphate Ester Rabbit Monoclonal Antibody clone 51-8 (1:5,000 in 5% Skim Milk) (exclusively from Epitomics: www.epitomics.com) store for 1 month at 4°C or indefinitely at -20°C

Secondary anti-Rabbit HRP conjugated antibody (Epitomics: www.epitomics.com) store for 1 month at 4°C or indefinitely at -20°C

Materials for A.2.4 (May also require materials above)

Plasmid containing KOI suitable for expression of kinase in mammalian cells

Transfection reagents (e.g., Lipofectamine, FuGene)

Phosphate buffered saline (PBS) store indefinitely at 4°C

Cell scrapers

Protease inhibitor cocktail –EDTA (Roche) store for 1 year at 4°C

Phosphatase inhibitor cocktail (Roche) store for 1 year at 4°C

ATP (Sigma) store solid indefinitely at -20°C

GTP (Sigma) store solid indefinitely at -20°C

2X RIPA Buffer (100 mM Tris-HCl pH 8.0, 150 mM NaCl, 1% NP-40, 0.1% SDS) store indefinitely at 4°C

EDTA (Sigma) store solid indefinitely at 22°C

Protein G Magnetic beads (Invitrogen Dynabeads) store for 1 year at 4°C

Magnetic stand which holds 1.5 mL microcentrifuge tubes

Materials for Appendix A.2.5 (May also require materials from above)

Purified active KOI or Plasmid containing KOI suitable for expression of kinase in *E.coli*

Recombinant GSK3 β

CREB peptide (KRREILSRRPS(p)YR) store for 1 year at -80°C

Dephosphorylated Myelin Basic Protein (2.5 mg/mL) (Millipore)

10 mM stock in water of Adenosine 5'-[γ -thio]triphosphate tetralithium salt (Sigma) store for 1 year at -80°C

Myelin Basic Protein, Histone H1, or other general kinase substrate (Millipore)

10X HEPES buffered saline (HBS) (200 mM HEPES pH 7.4, 1.5 M NaCl) store for 6 months at 22°C

100X MgCl₂ (1 M MgCl₂) store for 6 months at 22°C

Optional: 33X MnCl₂ (100 mM MnCl₂) store for 6 months at 22°C

5X Laemmli sample buffer store for 1 month at 4°C

OMIX 100 µL Ziptip (Varian)

0.1 % TFA 50 % Acetonitrile store for indefinitely at 22°C

0.1 % TFA H₂O store for indefinitely at 22°C

Tris buffered saline 0.5% Triton TX100 (TBST) store for 1 month at 22°C

Speed Vacuum

Equipment necessary for SDS-PAGE and western blotting (gel running apparatus, transfer apparatus, Nitrocellulose or PVDF)

A.2.2 Kinase Reaction with ATP γ S followed by Western Blotting Utilizing Thiophosphate Specific Antibody.

Detection of thiophosphorylated substrate proteins is a critical analysis tool to determine whether this technique will work for a KOI in a particular lysate. An in-vitro kinase reaction with a KOI, substrate and ATP γ S is used here to determine if the kinase will use ATP γ S to thiophosphorylate substrate proteins. If the kinase is able to use ATP γ S to thiophosphorylate substrate proteins the band corresponding to the substrate should be immunoreactive with the thiophosphate ester specific antibody (51-8).

1. On ice prepare a master mix of 1X HBS (or other kinase reaction buffer suitable for the KOI) 1M MgCl₂ (to 10 mM) substrate (or general kinase substrate at 1 mg/mL) and KOI between 50-200 ng per kinase reaction.

Order of addition: H₂O, HBS, MgCl₂ Substrate, KOI. These general conditions will work for most kinases, but check the literature for kinase specific reaction conditions.

2. Label 4 tubes A-D and aliquot 27 µL of master mix into each tube.

Tubes A-C are controls for non-specific alkylation of cysteine residues by the thiol specific alkylating agent PNBM.

3. Add 3 µL 10 mM ATP_γS (final concentration of 1 mM) in two of the samples (samples C and D)

Flick the tubes to mix, and then briefly centrifuge to collect the kinase reaction in the bottom of the tube.

4. Let the reaction proceed for 30 minutes at room temperature (or suitable temp for KOI)

5. Add 1.5 µL of 50 mM PNBM to samples B and D to afford a final concentration of 2.5 mM. The alkylating reaction should proceed for one hour at room temperature. If desired the kinase reaction may be quenched by adding EDTA to 20 mM.

The 50 mM PNBM should be prepared immediately before adding to the samples by dissolving PNBM in DMSO (50 mM is equal to 12 mg/mL).

6. Add 5X Laemmli sample buffer to the samples. Run the samples on a SDS-PAGE gel. Transfer to nitrocellulose or PDVF membrane. Block the membrane for 1 hr with 5% Skim milk (in TBST).

7. Incubate the blot overnight at 4°C with 1:5,000 Thiophosphate Ester Rabbit Monoclonal Antibody, clone 51-8 (in 5% skim milk TBST).

Incubating the blot with the antibody for 1-3 hours at room temperature can also lead to detection of modified proteins with lower sensitivity.

8. After washing 4 times with TBST, incubate blot for 1 hr with anti Rabbit HRP secondary, wash 4 times and then add ECL reagent to visualize PNBM alkylated/thiophosphorylated proteins.

A.2.3 Identification of optimal N⁶ substituted ATP γ S analog

Each analog specific kinase will have a slightly different substrate specificity. To determine the preferred N⁶ substituted ATP γ S each kinase must be tested with several ATP analogs. Following this protocol to perform a kinase assay with several N⁶ substituted ATP γ S analogs will provide the optimal ATP analog for further studies to identify substrates.

1. Follow A.2.2, utilizing several N⁶ substituted ATP γ S analogs in place of ATP γ S to identify which analog is used optimally by the AS KOI.

The optimal analog is the one that results in the most substrate labeling as detected by Thiophosphate Ester Rabbit Monoclonal Antibody, clone 51-8. Wild-type KOI should not be able to utilize this N⁶ substituted ATP γ S analog.

A.2.4 Thiophosphorylation of a candidate kinase substrate in cell lysate

The following method is used to determine if a candidate protein is a substrate of a KOI in a complex protein mixture. First the AS KOI is transiently expressed in cells and activated, then cell lysate is prepared and N⁶ substituted ATP γ S is added to initiate the substrate labeling reaction. Thiophosphorylated proteins are alkylated and the candidate substrate is immunoprecipitated using an antibody against that protein. If a band is detected by IB with Thiophosphate Ester Rabbit Monoclonal Antibody then the candidate is a substrate of the KOI.

1. Grow appropriate mammalian cells on 10-cm dishes.
2. Transfect with plasmid encoding WT or AS KOI using transfection reagent of choice, following manufacturer's protocol.
3. Allow cells to grow for 24-48 hours.
4. If appropriate, stimulate cells to activate KOI.

For example, mitogen activated protein kinase ERK may be activated by epidermal growth factor.

5. Remove media and rinse once with 5 mL cold PBS.
6. Using a cell scraper, lyse and scrape cells on ice in 500 μ L 1X RIPA buffer + 1X protease inhibitor + 1X phosphatase inhibitor.
7. Centrifuge at 10,000 x g for 10 min at 4°C to remove cell debris. Keep supernatant.
8. Add 100 μ M N⁶ substituted ATP γ S, 100 μ M ATP, and 3 mM GTP to each sample (order does not matter).

Recommended concentration ranges for optimizing labeling conditions:

-N⁶ substituted ATP γ S: 50-500 μ M

-ATP: 50-200 μ M

-GTP: 1-3 mM

9. Allow for thiophosphorylation of kinase substrates to occur for 20 minutes at room temperature.
10. Quench reaction with 500 μ L 1X RIPA buffer + 40 mM EDTA (*final [EDTA] = 20 mM*) + 5 mM PNBM (*final [PNBM] = 2.5 mM*), then alkylate with PNBM for 1 hour at room temperature on a rotator.

Follow A.2.2 for preparation of PNBM stock solution.

11. Immunoprecipitate candidate substrate using antibody according to manufacturer's recommendation. Incubate overnight at 4°C.

Save 20 mL input for western blotting to check immunoprecipitation efficiency.

12. Add 40 μ L of 50% slurry of appropriate (protein A or G) magnetic beads to each sample. Incubate 3-4 hours at 4°C on a rotator.

Before use, wash beads once with 1 mL 1X RIPA buffer. Then resuspend in original slurry volume and add to each sample.

13. Using a magnet to collect the beads, wash 5 times w/ 1 mL 1X RIPA + protease inhibitor + phosphatase inhibitor.

Note: Before first wash, save 20 μ l supernatant for western blotting to check immunoprecipitation efficiency.

14. Resuspend beads in 20 μ L 1X RIPA + protease inhibitor + phosphatase inhibitor +1X Laemmli sample buffer.

15. Heat samples at 95°C for 2.5 minutes.

16. Load the samples onto an SDS-PAGE gel and proceed with IB as described in steps 6-8 of A.2.2, blotting with Thiophosphate Ester Rabbit Monoclonal Antibody.

A.2.5 Making a thiophosphorylated positive control peptide and protein

The two control samples, a thiophosphorylated peptide and protein, can be prepared from readily purchasable materials. A kinase reaction is used to make the thiophosphorylated substrates. Mass spectrometric analysis using a MALDI can be used to confirm whether the CREB peptide has been thiophosphorylated. After labeling, the thiophosphorylated myelin basic protein (MBP) can be run on a denaturing polyacrylimide gel followed by an immunoblot using 51-8 (Appendix A.2.4). After this experiment the peptide can be

used to evaluate whether the covalent capture reaction is working properly. Labeled MBP can be added to a lysate as a control for the digestion and covalent capture reactions.

1. On ice prepare two kinase reactions that each contain:

6 μ L 10X HBS

0.6 μ L 1M $MgCl_2$ (to 10 mM)

6 μ L 10 mM ATP γ S (to 1 mM final)

and either 25 μ L 2.5 mg/mL MBP (5 nmol total) or 18 μ L 0.5 mg/ml CREB peptide (5 nmol) and water to a final volume of 60 μ L.

Order of addition: H_2O , HBS, $MgCl_2$ Substrate, KOI.

2. Add 500 ng of recombinant GSK3 β and incubate the reaction at room temperature for 4 hours

3a. Aliquot the reaction containing MBP into 0.5 mL Eppendorf tubes (5 μ L/ tube), snap freeze them in liquid N_2 and store them at $-80^\circ C$ until needed

3b. Use a large capacity ziptip (OMIX 100 μ L) to desalt the CREB thiophosphorylation reaction, eluting into 200 μ L 0.1% TFA 50% Acetonitrile. Concentrate the sample using a speed vacuum to 60 μ L. Aliquot into 0.5 mL Eppendorf tubes (5 μ L / tube) and snap freeze them in liquid N_2 . Store them at $-80^\circ C$ for 3 months or until needed

Utilize the ziptip according to product literature: wash 2X with 0.1% TFA 50% Acetonitrile, 2X with 0.1% TFA H_2O . Pass the sample through the tip 5X being

sure not to introduce any air into the tip. Wash 2X with 0.1% TFA H₂O and then elute 2X with 0.1% TFA 50% Acetonitrile.

A.2.6 Anticipated Results.

The application of this technique to appropriately labeled lysates should result in the identification of phosphopeptides. After subtraction of any phosphopeptides found in the control lysates, these peptides should predominantly be the substrates of the AS kinase that was used in the labeling reaction. The location of the phosphorylation mark on the substrate proteins will also allow the investigator to produce non-phosphorylatable substrates and thus to analyze the biological significance of the phosphorylation mark immediately following confirmation of the kinase-substrate relationship.

Thiophosphorylation of CREB (KRREILSRRPS(p)YR) (1795.84 MH⁺) by GSK3B should lead to a predominant peak at 1891.986 (MH⁺). After covalent capture with iodoacetyl agarose beads followed by specific hydrolysis the only product ion present should be a double phosphorylated CREB peak at 1875.986 (MH⁺). The hyper-thiophosphorylation of Myelin Basic Protein followed by digestion with trypsin and analysis by LC MS/MS will lead to the detection of a thiophosphorylated peptide 1800.8939 (MH⁺) NIVT(Thiophospho)PRTPPPSQGKGR or 1587.7951 NIVT(Thiophospho)PRTPPPSQGK or 796.4044 (MH⁺) NIVT(Thiophospho)PR. After covalent capture with iodoacetyl agarose beads followed by specific hydrolysis the only multiply charged ions present will be the same peptide a phospho group instead of a thiophospho modification, a loss of 16 Daltons. 1784.8939 (MH⁺) NIVT(phospho)PRTPPPSQGKGR, 1587.8001 (MH⁺), NIVT(phospho)PRTPPPSQGK,

or 780.403 (MH+) NIVT(phospho)PR. In addition, incubating the labeled MBP with the lysate to be used for substrate ID and then performing the covalent capture reaction should yield these same peptides, but no background should be seen, as there should be no source of thiophosphate in the lysate for background labeling to occur.

A.2.7 Troubleshooting guide.

Table 1 Troubleshooting Guide for Kinase-Substrate Mapping

Problem	Cause	Solution
No thiophosphorylation of substrate seen during in-vitro ATP γ S kinase reaction	Inactive kinase or kinase does not utilize ATP γ S	Generate sufficient quantities of pure kinase. Check activity with ATP γ ³⁵ S kinase assay.
	Inactive kinase	Generate a constitutively active kinase
Singly charged polymer or detergent ions seen during mass spectrometric analysis	Concentration of detergents is too high in the lysis buffer	Typically the lysis buffer should only contain low amounts of a nonionic, nondenaturing detergent like 0.1% NP-40
No phospho-CREB detected after test covalent capture reaction	pH is too low or high in covalent capture buffer	Check the pH of the flow-through after the covalent capture reaction. Ensure the pH of the agarose beads is correctly adjusted by washing the agarose beads carefully with 200 mM HEPES, pH 7.0.
	Insufficient reaction time for the covalent capture reaction	Incubate the thiophosphopeptides overnight (11-16 hr, especially if using a complex lysate)
	Insufficient incubation with 10 mM DTT	Incubate with 10 mM DTT for at least 120 min following the 5% formic acid wash step
	Nonspecific adsorption of peptides to microcentrifuge tubes	Using siliconized tubes and BSA will reduce nonspecific adsorption
	Thiophospho CREB levels are too low	Increase thiophospho CREB to see a signal, and then adjust other parameters to diagnose where the sample loss is occurring
No thiophospho peptide is detected after digesting the labeled MBP	Levels of TCEP are too low during digestion	Make a fresh solution of 1 M TCEP before the digestion and add to 10 mM in both the reduction and the digestion steps
	Levels of urea are too low during digestion	Do not dilute to 1 M urea, only dilute to 2 M as the additional denaturant will assist in unfolding proteins during the digestion
	Digestion not allowed to proceed long enough	Incubate digestion for a longer time (11-16 hr)
	Insufficient trypsin added	Add trypsin to 1:10 w/w
Phosphopeptides detected in no AS kinase control	Background kinases are utilizing the ATP analogs	Follow all optimization steps to determine the correct amount of ATP, GTP, and N ⁶ -modified ATP to use during the labeling
	Background kinases are utilizing the ATP analogs	Identify which background kinases are utilizing the ATP analogs and include inhibitors for these kinases during the labeling reaction
No phosphopeptides detected in the plus AS kinase reaction	Kinase activity is low	Increase the amount of AS kinase in the labeling reaction
	Stoichiometry of labeling is low	Increase the effective concentration of substrates by fractionating the lysate or by isolating specific subcellular compartments prior to labeling
	N ⁶ ATP analog concentration is too low	Increase the amount of ATP analog in both the negative control and the sample with AS kinase

Appendix B. Aurora B Substrates Identified using nuclear excluded Aurora

gene	uniprot	residue	site	protein
ACTG1	P63261	S	14	Actin, cytoplasmic 2
AKAP2	Q9Y2D5	S	839	A-kinase anchor protein 2
ALDH2	P05091	S	354	Aldehyde dehydrogenase, mitochondrial
ASPM	Q81ZT6	S	170	Abnormal spindle-like microcephaly-associated protein
ATP5I	P56385	S	17	ATP synthase subunit e, mitochondrial
ATP5J	P18859	T S	56 57	ATP synthase-coupling factor 6, mitochondrial
AURKB	Q96GD4	T	16	Aurora kinase B
AURKB	Q96GD4	T S	16 19	Aurora kinase B
AURKB	Q96GD4	S	22	Aurora kinase B
AURKB	Q96GD4	S	37	Aurora kinase B
AURKB	Q96GD4	S&T Y&Y	7&16 8	Aurora kinase B
BANF1	O75531	T&T T&S	2&3 28	Barrier-to-autointegration factor
BRPF3	Q9ULD4	T	407	Bromodomain and PHD finger-containing protein 3
C19orf21	Q81VT2	S	348	Uncharacterized protein C19orf21
CBX5	P45973	S S	92 95	Chromobox protein homolog 5
CCDC86	Q9H6F5	S	255	Coiled-coil domain-containing protein 86
CDK17	Q00537	S S	180 18	Cyclin-dependent kinase 17
CGN	Q9P2M7	S	43	Cingulin
CHCHD6	Q9BRQ6	S	13	CHCHD6
CHTF18	Q8WVB6	T	339	Chromosome transmission fidelity protein 18 homolog
CKAP2	Q8WWK9	T	39	Cytoskeleton-associated protein 2
COQ10A	Q96MF6	T	227	Coenzyme Q-binding protein COQ10 homolog A
CXorf67	Q86X51	S	229	Uncharacterized protein CXorf67
DDA1	Q9BW61	S S	28 33	DET1- and DDB1-associated protein 1
DDX21	Q9NR30	S	109	Nucleolar RNA helicase 2
DDX21	Q9NR30	T	111	Nucleolar RNA helicase 2
DDX3X	O00571	S&S S&S	588&5	ATP-dependent RNA helicase DDX3X
DDX3X	O00571	S S	588 59	ATP-dependent RNA helicase DDX3X
DDX3X	O00571	S S S S	588 59	ATP-dependent RNA helicase DDX3X
DDX3X	O00571	S S S	588 59	ATP-dependent RNA helicase DDX3X
DDX3X	O00571	S	594	ATP-dependent RNA helicase DDX3X
DDX3X	O00571	S	605	ATP-dependent RNA helicase DDX3X
DDX3X	O00571	S S	605 60	ATP-dependent RNA helicase DDX3X
DDX3X	O00571	S	82	ATP-dependent RNA helicase DDX3X
DDX54	Q8TDD1	S T	571 57	ATP-dependent RNA helicase DDX54
DNAJC13	O75165	T	1282	DnaJ homolog subfamily C member 13
E4F1	Q66K89	S	256	Transcription factor E4F1
E4F1	Q66K89	S	260	Transcription factor E4F1
EPB41L3	Q9Y2J2	S	420	Band 4.1-like protein 3
EPB41L4B	Q9H329	S T	347 35	Band 4.1-like protein 4B
ERC1	Q8IUD2	S	389	ELKS/Rab6-interacting/CAST family member 1
FAM171A	A8MVW0	S	25	Protein FAM171A2
FBL	P22087	S	124	rRNA 2'-O-methyltransferase fibrillarin
FLNB	O75369	T T	994 99	Filamin-B
FLNC	Q14315	S S	2623 2	Filamin-C
GNL2	Q13823	S	625	Nucleolar GTP-binding protein 2
GRIN2B	Q13224	S	917	Glutamate [NMDA] receptor subunit epsilon-2
HIST1H4A	P62805	S	48	Histone H4
HMGA1	P17096	T S	39 44	High mobility group protein HMG-I/HMG-Y
HMGA1	P17096	T	53	High mobility group protein HMG-I/HMG-Y
HMGN2	P05204	S	25	Non-histone chromosomal protein HMG-17
HMGN2	P05204	S S	25 29	Non-histone chromosomal protein HMG-17
HMGN2	P05204	S	29	Non-histone chromosomal protein HMG-17
HMGN3	Q15651	S	27	HMGN3
HMGN3	Q15651	S S	27 31	HMGN3
HMGN3	Q15651	S	31	HMGN3
HMGN4	O00479	S S	25 29	HMGN4
HMGN5	P82970	S	20	HMGN5
HMGN5	P82970	S	24	HMGN5
HNRNPA1	P09651	S S	337 33	Heterogeneous nuclear ribonucleoprotein A1
HNRNPA1	P09651	S S Y	337 33	Heterogeneous nuclear ribonucleoprotein A1

gene	uniprot	residue	site	protein
HNRNPA1	P09651	S	338	Heterogeneous nuclear ribonucleoprotein A1
HNRNPA1	P09651	S Y	338 34	Heterogeneous nuclear ribonucleoprotein A1
HNRNPU	Q00839	S	26	Heterogeneous nuclear ribonucleoprotein U
HSP90AB1	P08238	S	452	Heat shock protein HSP 90-beta
HSPB1	P04792	S	82	Heat shock protein beta-1
INCENP	Q9NQS7	S&S S&	103&1	Inner centromere protein
INCENP	Q9NQS7	T	184	Inner centromere protein
INCENP	Q9NQS7	S	197	Inner centromere protein
INCENP	Q9NQS7	S&T&S S	197&2	Inner centromere protein
INCENP	Q9NQS7	S&T&S S	197&2	Inner centromere protein
INCENP	Q9NQS7	T&S T&	213&2	Inner centromere protein
INCENP	Q9NQS7	T S	250 25	Inner centromere protein
INCENP	Q9NQS7	S	255	Inner centromere protein
INCENP	Q9NQS7	S&T S&	291&2	Inner centromere protein
INCENP	Q9NQS7	T S T S	294 29	Inner centromere protein
INCENP	Q9NQS7	T S T S	294 29	Inner centromere protein
INCENP	Q9NQS7	S	350	Inner centromere protein
INCENP	Q9NQS7	S	446	Inner centromere protein
INCENP	Q9NQS7	T	494	Inner centromere protein
INCENP	Q9NQS7	T T	494 49	Inner centromere protein
INCENP	Q9NQS7	S	514	Inner centromere protein
INCENP	Q9NQS7	S	518	Inner centromere protein
INCENP	Q9NQS7	T	59	Inner centromere protein
INCENP	Q9NQS7	S	72	Inner centromere protein
INCENP	Q9NQS7	Y	73	Inner centromere protein
INCENP	Q9NQS7	T S	892 89	Inner centromere protein
INCENP	Q9NQS7	T S S	892 89	Inner centromere protein
INCENP	Q9NQS7	S	893	Inner centromere protein
INCENP	Q9NQS7	S	894	Inner centromere protein
INCENP	Q9NQS7	S	899	Inner centromere protein
INCENP	Q9NQS7	S	909	Inner centromere protein
INCENP	Q9NQS7	S	910	Inner centromere protein
IRAK3	Q9Y616	T S S S	331 33	Interleukin-1 receptor-associated kinase 3
KIAA1522	Q9P206	S	161	Uncharacterized protein KIAA1522
KIF4A	O95239	T	799	Chromosome-associated kinesin KIF4A
KRT18	P05783	S S S	42 44	Keratin, type I cytoskeletal 18
KRT18	P05783	S T	7 8	Keratin, type I cytoskeletal 18
KRT75	O95678	S S	2 5	Keratin, type II cytoskeletal 75
KRT75	O95678	S S	30 33	Keratin, type II cytoskeletal 75
KRT75	O95678	S	5	Keratin, type II cytoskeletal 75
KRT75	O95678	S	51	Keratin, type II cytoskeletal 75
KRT75	O95678	S S	51 52	Keratin, type II cytoskeletal 75
KRT75	O95678	S S S S	51 52	Keratin, type II cytoskeletal 75
KRT8	P05787	S T S S	24 26	Keratin, type II cytoskeletal 8
KRT8	P05787	T S S S	26 31	Keratin, type II cytoskeletal 8
KRT8	P05787	S S	31 34	Keratin, type II cytoskeletal 8
KRT8	P05787	S S S S	31 34	Keratin, type II cytoskeletal 8
KRT8	P05787	S	34	Keratin, type II cytoskeletal 8
KRT8	P05787	S S S S	34 35	Keratin, type II cytoskeletal 8
KRT8	P05787	T	6	Keratin, type II cytoskeletal 8
LARP4	Q71RC2	S	461	La-related protein 4
LINC0034	Q9H761	S	58	Putative uncharacterized protein encoded by LINC00341
LMNA	P02545	T	10	Prelamin-A/C
LMNA	P02545	T S	10 12	Prelamin-A/C
LMNA	P02545	S	22	Prelamin-A/C
LMO7	Q8WWI1	S T	116 11	LIM domain only protein 7
LMO7	Q8WWI1	S	300	LIM domain only protein 7
LMO7	Q8WWI1	S	751	LIM domain only protein 7
LRRC16A	Q5VZK9	S S	1067 1	Leucine-rich repeat-containing protein 16A
LSM14B	Q9BX40	S	349	Protein LSM14 homolog B
LY6H	O94772	S	54	Lymphocyte antigen 6H

gene	uniprot	residue	site	protein
LYRM1	O43325	T S	26 27	LYR motif-containing protein 1
MARCKSL	P49006	S S	101 10	MARCKS-related protein
MIB2	Q96AX9	T	109	E3 ubiquitin-protein ligase MIB2
MKI67	P46013	S	374	Antigen KI-67
MKI67	P46013	S	538	Antigen KI-67
MPHOSPH	O00566	T	332	U3 small nucleolar ribonucleoprotein protein MPP10
MPHOSPH	O00566	T	459	U3 small nucleolar ribonucleoprotein protein MPP10
MRPL15	Q9P015	S	23	39S ribosomal protein L15, mitochondrial
MSH6	P52701	S	14	DNA mismatch repair protein Msh6
MSH6	P52701	S	2	DNA mismatch repair protein Msh6
MSH6	P52701	S S T	2 5 6	DNA mismatch repair protein Msh6
MSH6	P52701	S S T Y	2 5 6	DNA mismatch repair protein Msh6
MSH6	P52701	S	5	DNA mismatch repair protein Msh6
MSH6	P52701	S T	5 6	DNA mismatch repair protein Msh6
MYBBP1A	Q9BQG0	S	1303	Myb-binding protein 1A
MYBBP1A	Q9BQG0	S	1308	Myb-binding protein 1A
MYBBP1A	Q9BQG0	S S	1308 1	Myb-binding protein 1A
NCL	P19338	S S	458 46	Nucleolin
NDC80	O14777	S	302	Kinetochores protein NDC80 homolog
NOC2L	Q9Y3T9	S	49	Nucleolar complex protein 2 homolog
NOC2L	Q9Y3T9	S	56	Nucleolar complex protein 2 homolog
NOC2L	Q9Y3T9	S	67	Nucleolar complex protein 2 homolog
NUCKS1	Q9H1E3	T	179	Nuclear ubi casein and cyclin-dependent kinase substrate
NUMA1	Q14980	T T	1811 1	Nuclear mitotic apparatus protein 1
NUMA1	Q14980	S	1969	Nuclear mitotic apparatus protein 1
NUMA1	Q14980	S	2047	Nuclear mitotic apparatus protein 1
NUMA1	Q14980	S S	2047 2	Nuclear mitotic apparatus protein 1
NUMA1	Q14980	S T	2051 2	Nuclear mitotic apparatus protein 1
NUMA1	Q14980	T	2055	Nuclear mitotic apparatus protein 1
NUSAP1	Q9BXS6	S	240	Nucleolar and spindle-associated protein 1
OAT	P04181	T	148	Ornithine aminotransferase, mitochondrial
PDLIM7	Q9NR12	T	105	PDZ and LIM domain protein 7
PLEC	Q15149	T	2886	Plectin
PLEC	Q15149	Y T	4571 4	Plectin
PPHLN1	Q8NEY8	S	110	Periphilin-1
PPP1R12	O14974	S T	695 69	Protein phosphatase 1 regulatory subunit 12A
PPP1R16	Q96T49	S	350	Protein phosphatase 1 regulatory inhibitor subunit 16B
PPP1R16	Q96T49	S	352	Protein phosphatase 1 regulatory inhibitor subunit 16B
PPP1R18	Q6NYC8	S	468	Phostensin
PRPF3	O43395	S T	356 36	U4/U6 small nuclear ribonucleoprotein Prp3
PRPF3	O43395	T	362	U4/U6 small nuclear ribonucleoprotein Prp3
PRRC2C	Q9Y520	S	1013	Protein PRRC2C
PTRF	Q6NZI2	S	300	Polymerase I and transcript release factor
RBM14	Q96PK6	S	618	RNA-binding protein 14
RBM14	Q96PK6	S	649	RNA-binding protein 14
RBM3	P98179	Y S Y	146 14	Putative RNA-binding protein 3
RBM3	P98179	S	147	Putative RNA-binding protein 3
RBM3	P98179	Y	151	Putative RNA-binding protein 3
RDBP	P18615	S	131	Negative elongation factor E
RNF146	Q9NTX7	S	11	E3 ubiquitin-protein ligase RNF146
RNF146	Q9NTX7	T	17	E3 ubiquitin-protein ligase RNF146
RPL13	P26373	S	52	60S ribosomal protein L13
RPL15	P61313	T	197	60S ribosomal protein L15
RPL17	P18621	S	5	60S ribosomal protein L17
RPL21	P46778	S S	101 10	60S ribosomal protein L21
RPL21	P46778	S	104	60S ribosomal protein L21
RPL27A	P46776	S	16	60S ribosomal protein L27a
RPL28	P46779	S	115	60S ribosomal protein L28
RPL28	P46779	S	68	60S ribosomal protein L28
RPL28	P46779	T	89	60S ribosomal protein L28
RPL30	P62888	S	10	60S ribosomal protein L30

gene	uniprot	residue	site	protein
RPL30	P62888	T S	7 10	60S ribosomal protein L30
RPL34	P49207	S	12	60S ribosomal protein L34
RPL34	P49207	S Y	12 13	60S ribosomal protein L34
RPL34	P49207	S T	12 15	60S ribosomal protein L34
RPL34	P49207	S	23	60S ribosomal protein L34
RPL34	P49207	T	6	60S ribosomal protein L34
RPL36A	P83881	S	46	60S ribosomal protein L36a
RPL39	P62891	T	47	60S ribosomal protein L39
RPL4	P36578	T	339	60S ribosomal protein L4
RPL8	P62917	S	130	60S ribosomal protein L8
RPL8	P62917	S Y	130 131	60S ribosomal protein L8
RPS10	P46783	T	118	40S ribosomal protein S10
RPS13	P62277	S	12	40S ribosomal protein S13
RPS15	P62841	T S	136 137	40S ribosomal protein S15
RPS2	P15880	S	281	40S ribosomal protein S2
RPS3A	P61247	T	153	40S ribosomal protein S3a
RPS4X	P62701	T	247	40S ribosomal protein S4, X isoform
RPS4Y1	P22090	T	247	40S ribosomal protein S4, Y isoform 1
RPS6	P62753	S	235	40S ribosomal protein S6
RPS6	P62753	S S	235 236	40S ribosomal protein S6
RPS6	P62753	S	236	40S ribosomal protein S6
RSL1D1	O76021	T S	312 313	Ribosomal L1 domain-containing protein 1
RSL1D1	O76021	T S S	312 313	Ribosomal L1 domain-containing protein 1
SAFB	Q15424	S	808	Scaffold attachment factor B1
SCAF11	Q99590	T S	947 948	Protein SCAF11
SERBP1	Q8NC51	S	197	Plasminogen activator inhibitor 1 RNA-binding protein
SERBP1	Q8NC51	S S S S	197 198	Plasminogen activator inhibitor 1 RNA-binding protein
SERBP1	Q8NC51	S S S	199 200	Plasminogen activator inhibitor 1 RNA-binding protein
SGOL2	Q562F6	S T	534 535	Shugoshin-like 2
SMTN	P53814	S T S	790 791	Smoothelin
SNTB1	Q13884	T	315	Beta-1-syntrophin
SNW1	Q13573	S T	29 32	SNW domain-containing protein 1
SNW1	Q13573	T S	32 33	SNW domain-containing protein 1
SPIN1	Q9Y657	S S	38 39	Spindlin-1
SPTBN1	Q01082	S	2358	Spectrin beta chain, brain 1
SRRM1	Q8IYB3	S	463	Serine/arginine repetitive matrix protein 1
SRRM1	Q8IYB3	S	465	Serine/arginine repetitive matrix protein 1
SRSF5	Q13243	S	86	Serine/arginine-rich splicing factor 5
SSH3	Q8TE77	S	37	Protein phosphatase Slingshot homolog 3
STAU1	O95793	T	384	Double-stranded RNA-binding protein Staufen homolog 1
STK10	O94804	S T	13 14	Serine/threonine-protein kinase 10
STMN1	P16949	S	16	Stathmin
STMN1	P16949	S	25	Stathmin
SUPT16H	Q9Y5B9	T	494	FACT complex subunit SPT16
SVOP	Q8N4V2	S	297	Synaptic vesicle 2-related protein
TBCD	Q9BTW9	S	731	Tubulin-specific chaperone D
TBCD	Q9BTW9	S	738	Tubulin-specific chaperone D
TBCD	Q9BTW9	Y	740	Tubulin-specific chaperone D
TBCD	Q9BTW9	Y	741	Tubulin-specific chaperone D
TCEB3CL	A6NLF2	T T	431 432	Transcription factor SIII subunit A3-like-2
TINF2	Q9BSI4	S	246	TERF1-interacting nuclear factor 2
TNR	Q92752	T T	548 549	Tenascin-R
TNR	Q92752	S	557	Tenascin-R
TUBB	P07437	T S S	274 275	Tubulin beta chain
UIMC1	Q96RL1	S	677	BRCA1-A complex subunit RAP80
UTP3	Q9NQZ2	S	462	Something about silencing protein 10
VIM	P08670	T S	37 39	Vimentin
VIM	P08670	S	39	Vimentin
VIM	P08670	S	47	Vimentin
VIM	P08670	S T S	47 48	Vimentin
VIM	P08670	Y&T Y&S	53&63	Vimentin

gene	uniprot	residue	site	protein
VIM	P08670	T S S	63 65	Vimentin
VIM	P08670	S	72	Vimentin
VIM	P08670	S S	72 73	Vimentin
VIM	P08670	S	73	Vimentin
ZC3HAV1	Q7Z2W4	T	375	Zinc finger CCCH-type antiviral protein 1
ZC3HAV1	Q7Z2W4	S	378	Zinc finger CCCH-type antiviral protein 1
ZFC3H1	O60293	S T S	352 35	Zinc finger C3H1 domain-containing protein
ZYX	Q15942	S S	169 17	Zyxin
ZYX	Q15942	S S Y	169 17	Zyxin

Appendix C. Aurora B experimental procedures.

C.1.1 Purification of recombinant proteins

The Aurora B/pGEX-4T-1 vectors were introduced into BL21 bacteria and the transformants were plated on LB-agar plates containing ampicillin (Sigma) and chloramphenicol (Sigma). Protein expression was induced for four hours at 30°C by addition of 1mM IPTG (Isopropyl b-D- thiogalactopyranoside, Sigma). After induction, bacteria pellets were lysed in lysis buffer containing 10 mM EGTA, 10 mM EDTA, 0.1% Tween-20, 250 mM NaCl, 5 mM DTT, 0.325 mg/ml lysosome and protease inhibitors (CompleteTM, Roche). Cells were sonicated and centrifuged at 18,000 rpm for 30 min. at 4°C. Supernatants were coupled to Glutathione-Sepharose 4B beads (Amersham Biosciences) and proteins were eluted in buffer containing 50 mM Tris (pH 8.0), 20 mM reduced glutathione (GSH) and 75 mM KCl. The GST-Aurora B/His-INCENP complexes were purified from baculovirus infected SF9 cells. Protein expression was induced for four days at 27°C. SF9 were pelleted and lysed in buffer containing: 50 mM Tris (pH 8.0), 400 mM NaCl, 1.0% NP-40, 0.5% sodium desoxycholate, 20 mM glycerol-2-phosphate, 0.3 mM NaVO₃, 1µg/ml Leupeptin , 1µg/ml Pepstatin, 1µg/ml Aprotitin and 1 mM PMSF. Cells were sonicated and centrifuged at 13,000 rpm for 20 min at 4°C. Supernatants were coupled to Ni-NTA agarose beads (Qiagen) and washed twice in buffer containing 100 mM Na₂HPO₄, 100 mM NaH₂PO₄ , 300 mM NaCl, 10% Glycerol and 20mM imidazole. Protein complexes were eluted in buffer containing 250 mM imidazole.

C.1.2 Immunoprecipitation and in vitro kinase reactions

U2OS cells were transiently transfected with FLAG- or GFP- tagged cDNA constructs. Cells were treated with nocodazole (250 $\mu\text{g/ml}$) for 18 hrs and mitotic cells were collected by shake-off. Mitotic cells were lysed as described previously (12) and cleared lysates were added to Prot A/G beads coupled to anti-GFP or anti-FLAG (M2, Sigma). Immunoprecipitated or recombinant kinases were included into a 25 μl reaction containing kinase buffer (10 mM MgCl_2 , 25 mM Hepes (pH 7.5), 25 mM β -Glycerophosphate, 0.5 mM DTT and 0.5 mM Vanadate) and 0.2 mg/ml Histone H3, 100 μM ATP with or without 2 μM NA-PP1 (Calbiochem). For thiophosphorylation assays different concentrations of $\text{ATP}\gamma\text{S}$ (Biolog) or bulky $\text{ATP}\gamma\text{S}$ analogs (Biolog) were used. After 30 min at 30°C, reactions were stopped by the addition of 25 μl 2x sample buffer. Thiophosphorylated samples were subsequently incubated with 2.5 mM p-nitrobenzyl alcohol (PNBM, Epitomics). This thiol-specific alkylating agent generates a bio-orthogonal thiophosphate ester that is recognized by a thiophosphate ester-specific antibody(13).

C.1.3 Western Blotting

Protein samples were separated by SDS-PAGE and transferred to nitrocellulose membrane by standard procedures. Membranes were blocked with 4% milk in Tris-buffered saline containing 1% Tween-20 (TBST) prior to incubation with the following primary antibodies in 4% milk-TBST: Mouse anti-GST (Tebu), rabbit anti-phospho Ser10 Histone H3 (Upstate), mouse anti-FLAG (Campro), rabbit anti-GFP (gift of The Netherlands Cancer Institute), mouse anti-Aurora B (Transduction), mouse anti-VSV

(Sigma), rabbit anti-thiophosphate ester (Epitomics), or anti-phospho Ser25/29 HMG2 (Acris Antibodies). After extensive washing in TBST, blots were incubated with horseradish peroxidase (HRP)- conjugated goat anti-mouse or goat anti-rabbit antibodies (DAKO) in 4% milk-TBST. Immunocomplexes were visualized using the ECL chemiluminescence detection kit from Amersham.

C.1.4 Isolation of thiophosphorylated peptides

Covalent capture of thiophosphorylated substrate proteins was performed essentially as described in Appendix A except for the following modifications. The labeled HeLa cell lysates were denatured by adding 60% by volume solid urea, 1M TCEP to 10 mM and incubating at 55°C for 1 hour. Proteins were then digested by diluting the urea to 2M by addition of 100 mM NH₄HCO₃ (pH 8), adding additional TCEP to 10 mM final, 0.5M EDTA to 1 mM, and trypsin (Promega) 1:20 by weight. The labeled lysates were digested for 16 hours at 37°C, acidified to 0.5% trifluoro acetic acid (TFA), and desalted by using a sep pak C18 column (Waters) eluting into 1 ml 50% acetonitrile 0.1%TFA. The desalted peptides were dried by using a speed vacuum to 40 µl. The pH of the peptides was adjusted by adding 40 µl of 200 mM HEPES pH7.0, 75 µl acetonitrile and brought to pH 7.0 by addition of 10% NaOH. The peptide solution was then added to 100 µl iodoacetyl beads (Pierce) pre-equilibrated with 200 mM HEPES pH7.0 and incubated with end-over-end rotation at room temperature in the dark for 16 hours. The beads were then added to small disposable columns, washed with H₂O, 5M NaCl, 50% acetonitrile, 5% formic acid, and 10 mM DTT, followed by elution with 100 µl and 200 µl (300 µl total) 1 mg/mL oxone (Sigma), desalted and concentrated on a 10 µl zip tip (Millipore)

eluting into 60 µl total volume. The resulting phosphopeptides were concentrated to 10 µl and analyzed by LC MS/MS.

C.1.5 Mass Spectrometry

The phosphopeptides resulting from oxidation promoted hydrolysis and concentration on a zip-tip were concentrated to 10 µl and separated using a 2-50% acetonitrile gradient on a NanoAcquity (Waters) reversed phase 75 micron capillary UPLC column on-line to an LTQ Velos Orbitrap mass spectrometer (Thermo-Fisher) by both ETD and HCD analysis. Peak lists were generated by using PAVA software (UCSF) and searched by batch-tag on Protein Prospector software (UCSF) for phosphopeptides with the following conditions: Taxonomy: Homo sapiens, Precursor charge range:2,3,4, monoisotopic masses. Parent mass tolerance, 20 ppm. Fragment mass tolerance (20 ppm for HCD, 0.5 Da for ETD). Digest, Trypsin. Non-specific, 0 termini. Max missed cleavages, 2. Constant mods, 0. Expectation calc method, Linear tail fit. Variable mods, Acetyl (protein N- Term), Acetyl+Oxidation (protein N-Term M) Gln→pyro-Glu (N-term Q) Met-loss (Protein N-term M) Met-loss+Acetyl (Protein N-term M) Oxidation (M) Phospho (S/T). After search, we utilized search compare with the parameters as follows: Min score protein 22, Min score peptide 15, Max E value protein 0.01, Max E value peptide 0.05, DB peptide, variable mods, protein mods, SLIP Threshold 6. Phosphosites where the SLIP score is below 6 are reported as ambiguous. Phosphosites that were identified in at least 2 experiments in the plus INCENP/AurB^{L154A/H250Y} samples (at least 2 biological replicates were performed per sample) and not in the negative controls (by XIC) were reported as putative Aurora B substrates.

5.1 References

- Adams, J.M., and Cory, S. (1998). The Bcl-2 protein family: arbiters of cell survival. *Science* *281*, 1322-1326.
- Alexander, J., Lim, D., Joughin, B.A., Hegemann, B., Hutchins, J.R., Ehrenberger, T., Ivins, F., Sessa, F., Hudecz, O., Nigg, E.A., *et al.* (2011). Spatial exclusivity combined with positive and negative selection of phosphorylation motifs is the basis for context-dependent mitotic signaling. *Sci Signal* *4*, ra42.
- Allen, J.J., Lazerwith, S.E., and Shokat, K.M. (2005). Bio-orthogonal affinity purification of direct kinase substrates. *J Am Chem Soc* *127*, 5288-5289.
- Allen, J.J., Li, M., Brinkworth, C.S., Paulson, J.L., Wang, D., Hubner, A., Chou, W.H., Davis, R.J., Burlingame, A.L., Messing, R.O., *et al.* (2007). A semisynthetic epitope for kinase substrates. *Nat Methods* *4*, 511-516.
- Arena, G., Gelmetti, V., Torosantucci, L., Vignone, D., Lamorte, G., De Rosa, P., Cilia, E., Jonas, E.A., and Valente, E.M. (2013). PINK1 protects against cell death induced by mitochondrial depolarization, by phosphorylating Bcl-xL and impairing its pro-apoptotic cleavage. *Cell Death Differ*.
- Axelrod, F.B., Liebes, L., Gold-Von Simson, G., Mendoza, S., Mull, J., Leyne, M., Norcliffe-Kaufmann, L., Kaufmann, H., and Slaugenhaupt, S.A. (2011). Kinetin improves IKBKAP mRNA splicing in patients with familial dysautonomia. *Pediatr Res* *70*, 480-483.
- Baker, P.R., Trinidad, J.C., and R.J., C. (2011). Modification site localization scoring integrated into a search engine. *Mol Cell Proteomics* *10*, M111.008078.
- Beilina, A., Van Der Brug, M., Ahmad, R., Kesavapany, S., Miller, D.W., Petsko, G.A., and Cookson, M.R. (2005). Mutations in PTEN-induced putative kinase 1 associated with recessive parkinsonism have differential effects on protein stability. *Proc Natl Acad Sci U S A* *102*, 5703-5708.
- Bichsel, S.J., Tamaskovic, R., Stegert, M.R., and Hemmings, B.A. (2004). Mechanism of activation of NDR (nuclear Dbf2-related) protein kinase by the hMOB1 protein. *The Journal of biological chemistry* *279*, 35228-35235.
- Bishop, A., Buzko, O., Heyeck-Dumas, S., Jung, I., Kraybill, B., Liu, Y., Shah, K., Ulrich, S., Witucki, L., Yang, F., *et al.* (2000a). Unnatural ligands for engineered proteins: new tools for chemical genetics. *Annu Rev Biophys Biomol Struct* *29*, 577-606.
- Bishop, A.C., Ubersax, J.A., Petsch, D.T., Matheos, D.P., Gray, N.S., Blethrow, J., Shimizu, E., Tsien, J.Z., Schultz, P.G., Rose, M.D., *et al.* (2000b). A chemical switch for inhibitor-sensitive alleles of any protein kinase. *Nature* *407*, 395-401.
- Bishop, J.D., and Schumacher, J.M. (2002). Phosphorylation of the carboxyl terminus of inner centromere protein (INCENP) by the Aurora B Kinase stimulates Aurora B kinase activity. *J Biol Chem* *277*, 27577-27580.
- Blethrow, J., Zhang, C., Shokat, K.M., and Weiss, E.L. (2004). Design and use of analog-sensitive protein kinases. *Curr Protoc Mol Biol Chapter 18*, Unit 18 11.
- Blethrow, J.D., Glavy, J.S., Morgan, D.O., and Shokat, K.M. (2008). Covalent capture of kinase-specific phosphopeptides reveals Cdk1-cyclin B substrates. *Proc Natl Acad Sci U S A* *105*, 1442-1447.

Brondyk, W.H., McKiernan, C.J., Fortner, K.A., Stabila, P., Holz, R.W., and Macara, I.G. (1995). Interaction cloning of Rabin3, a novel protein that associates with the Ras-like GTPase Rab3A. *Molecular and cellular biology* *15*, 1137-1143.

Brown, T.C., Correia, S.S., Petrok, C.N., and Esteban, J.A. (2007). Functional compartmentalization of endosomal trafficking for the synaptic delivery of AMPA receptors during long-term potentiation. *J Neurosci* *27*, 13311-13315.

Buzko, O., and Shokat, K.M. (2002). A kinase sequence database: sequence alignments and family assignment. *Bioinformatics* *18*, 1274-1275.

Castagna, M., Takai, Y., Kaibuchi, K., Sano, K., Kikkawa, U., and Nishizuka, Y. (1982). Direct activation of calcium-activated, phospholipid-dependent protein kinase by tumor-promoting phorbol esters. *J Biol Chem* *257*, 7847-7851.

Cheeseman, I.M., Anderson, S., Jwa, M., Green, E.M., Kang, J., Yates, J.R., 3rd, Chan, C.S., Drubin, D.G., and Barnes, G. (2002). Phospho-regulation of kinetochore-microtubule attachments by the Aurora kinase Ipl1p. *Cell* *111*, 163-172.

Cherukuri, S., Hock, R., Ueda, T., Catez, F., Rochman, M., and Bustin, M. (2008). Cell cycle-dependent binding of HMGN proteins to chromatin. *Mol Biol Cell* *19*, 1816-1824.

Clark, I.E., Dodson, M.W., Jiang, C., Cao, J.H., Huh, J.R., Seol, J.H., Yoo, S.J., Hay, B.A., and Guo, M. (2006). *Drosophila* pink1 is required for mitochondrial function and interacts genetically with parkin. *Nature* *441*, 1162-1166.

Cohen, P. (2001). The role of protein phosphorylation in human health and disease. The Sir Hans Krebs Medal Lecture. *Eur J Biochem* *268*, 5001-5010.

Cong, J., Geng, W., He, B., Liu, J., Charlton, J., and Adler, P.N. (2001). The furry gene of *Drosophila* is important for maintaining the integrity of cellular extensions during morphogenesis. *Development (Cambridge, England)* *128*, 2793-2802.

Conner, S.D., and Schmid, S.L. (2002). Identification of an adaptor-associated kinase, AAK1, as a regulator of clathrin-mediated endocytosis. *J Cell Biol* *156*, 921-929.

Conner, S.D., and Schmid, S.L. (2003). Differential requirements for AP-2 in clathrin-mediated endocytosis. *The Journal of cell biology* *162*, 773-779.

Cornils, H., Stegert, M.R., Hergovich, A., Hynx, D., Schmitz, D., Dirnhofer, S., and Hemmings, B.A. (2010). Ablation of the kinase NDR1 predisposes mice to the development of T cell lymphoma. *Science signaling* *3*, ra47.

De Matteis, M.A., Di Campli, A., and Godi, A. (2005). The role of the phosphoinositides at the Golgi complex. *Biochim Biophys Acta* *1744*, 396-405.

Deng, H., Dodson, M.W., Huang, H., and Guo, M. (2008). The Parkinson's disease genes pink1 and parkin promote mitochondrial fission and/or inhibit fusion in *Drosophila*. *Proc Natl Acad Sci U S A* *105*, 14503-14508.

Deng, H., Jankovic, J., Guo, Y., Xie, W., and Le, W. (2005). Small interfering RNA targeting the PINK1 induces apoptosis in dopaminergic cells SH-SY5Y. *Biochem Biophys Res Commun* *337*, 1133-1138.

Dephoure, N., Howson, R.W., Blethrow, J.D., Shokat, K.M., and O'Shea, E.K. (2005). Combining chemical genetics and proteomics to identify protein kinase substrates. *Proc Natl Acad Sci U S A* *102*, 17940-17945.

Devroe, E., Erdjument-Bromage, H., Tempst, P., and Silver, P.A. (2004). Human Mob proteins regulate the NDR1 and NDR2 serine-threonine kinases. *The Journal of biological chemistry* *279*, 24444-24451.

Ditchfield, C., Johnson, V.L., Tighe, A., Ellston, R., Haworth, C., Johnson, T., Mortlock, A., Keen, N., and Taylor, S.S. (2003). Aurora B couples chromosome alignment with anaphase by targeting BubR1, Mad2, and Cenp-E to kinetochores. *J Cell Biol* *161*, 267-280.

Emoto, K., He, Y., Ye, B., Grueber, W.B., Adler, P.N., Jan, L.Y., and Jan, Y.N. (2004). Control of dendritic branching and tiling by the Tricornered-kinase/Furry signaling pathway in *Drosophila* sensory neurons. *Cell* *119*, 245-256.

Emoto, K., Parrish, J.Z., Jan, L.Y., and Jan, Y.N. (2006). The tumour suppressor Hippo acts with the NDR kinases in dendritic tiling and maintenance. *Nature* *443*, 210-213.

Espinosa, J.S., Wheeler, D.G., Tsien, R.W., and Luo, L. (2009). Uncoupling dendrite growth and patterning: single-cell knockout analysis of NMDA receptor 2B. *Neuron* *62*, 205-217.

Ferrando, I.M., Chaerkady, R., Zhong, J., Molina, H., Jacob, H.K., Herbst-Robinson, K., Dancy, B.M., Katju, V., Bose, R., Zhang, J., *et al.* (2012). Identification of targets of c-Src tyrosine kinase by chemical complementation and phosphoproteomics. *Mol Cell Proteomics* *11*, 355-369.

Ferrer, A., Caelles, C., Massot, N., and Hegardt, F.G. (1985). Activation of rat liver cytosolic 3-hydroxy-3-methylglutaryl coenzyme A reductase kinase by adenosine 5'-monophosphate. *Biochem Biophys Res Commun* *132*, 497-504.

Fiala, J.C., Feinberg, M., Popov, V., and Harris, K.M. (1998). Synaptogenesis via dendritic filopodia in developing hippocampal area CA1. *J Neurosci* *18*, 8900-8911.

Gallegos, M.E., and Bargmann, C.I. (2004). Mechanosensory neurite termination and tiling depend on SAX-2 and the SAX-1 kinase. *Neuron* *44*, 239-249.

Gao, Y., Ge, G., and Ji, H. (2011). LKB1 in lung cancerigenesis: a serine/threonine kinase as tumor suppressor. *Protein Cell* *2*, 99-107.

Gautier, C.A., Kitada, T., and Shen, J. (2008). Loss of PINK1 causes mitochondrial functional defects and increased sensitivity to oxidative stress. *Proc Natl Acad Sci U S A* *105*, 11364-11369.

Geisler, S., Holmstrom, K.M., Treis, A., Skujat, D., Weber, S.S., Fiesel, F.C., Kahle, P.J., and Springer, W. (2010). The PINK1/Parkin-mediated mitophagy is compromised by PD-associated mutations. *Autophagy* *6*, 871-878.

Geng, W., He, B., Wang, M., and Adler, P.N. (2000). The tricornered gene, which is required for the integrity of epidermal cell extensions, encodes the *Drosophila* nuclear DBF2-related kinase. *Genetics* *156*, 1817-1828.

Gerges, N.Z., Backos, D.S., and Esteban, J.A. (2004). Local control of AMPA receptor trafficking at the postsynaptic terminal by a small GTPase of the Rab family. *The Journal of biological chemistry* *279*, 43870-43878.

Girdler, F., Gascoigne, K.E., Eysers, P.A., Hartmuth, S., Crafter, C., Foote, K.M., Keen, N.J., and Taylor, S.S. (2006). Validating Aurora B as an anti-cancer drug target. *J Cell Sci* *119*, 3664-3675.

Girdler, F., Sessa, F., Patercoli, S., Villa, F., Musacchio, A., and Taylor, S. (2008). Molecular basis of drug resistance in aurora kinases. *Chem Biol* *15*, 552-562.

Goto, H., Kiyono, T., Tomono, Y., Kawajiri, A., Urano, T., Furukawa, K., Nigg, E.A., and Inagaki, M. (2006). Complex formation of Plk1 and INCENP required for metaphase-anaphase transition. *Nat Cell Biol* *8*, 180-187.

Goto, H., Yasui, Y., Kawajiri, A., Nigg, E.A., Terada, Y., Tatsuka, M., Nagata, K., and Inagaki, M. (2003). Aurora-B regulates the cleavage furrow-specific vimentin phosphorylation in the cytokinetic process. *J Biol Chem* 278, 8526-8530.

Gregan, J., Zhang, C., Rumpf, C., Cipak, L., Li, Z., Uluocak, P., Nasmyth, K., and Shokat, K.M. (2007). Construction of conditional analog-sensitive kinase alleles in the fission yeast *Schizosaccharomyces pombe*. *Nat Protoc* 2, 2996-3000.

Gross, A., McDonnell, J.M., and Korsmeyer, S.J. (1999). BCL-2 family members and the mitochondria in apoptosis. *Genes Dev* 13, 1899-1911.

Haque, M.E., Thomas, K.J., D'Souza, C., Callaghan, S., Kitada, T., Slack, R.S., Fraser, P., Cookson, M.R., Tandon, A., and Park, D.S. (2008). Cytoplasmic Pink1 activity protects neurons from dopaminergic neurotoxin MPTP. *Proc Natl Acad Sci U S A* 105, 1716-1721.

Hardie, D.G., Ross, F.A., and Hawley, S.A. (2012). AMPK: a nutrient and energy sensor that maintains energy homeostasis. *Nat Rev Mol Cell Biol* 13, 251-262.

Harris, K.M. (1999). Structure, development, and plasticity of dendritic spines. *Current opinion in neurobiology* 9, 343-348.

Harvey, K.F., Pflieger, C.M., and Hariharan, I.K. (2003). The *Drosophila* Mst ortholog, hippo, restricts growth and cell proliferation and promotes apoptosis. *Cell* 114, 457-467.

Hattula, K., Furuholm, J., Arffman, A., and Peranen, J. (2002). A Rab8-specific GDP/GTP exchange factor is involved in actin remodeling and polarized membrane transport. *Molecular biology of the cell* 13, 3268-3280.

Hauf, S., Biswas, A., Langegger, M., Kawashima, S.A., Tsukahara, T., and Watanabe, Y. (2007). Aurora controls sister kinetochore mono-orientation and homolog bi-orientation in meiosis-I. *EMBO J* 26, 4475-4486.

Hauf, S., Cole, R.W., LaTerra, S., Zimmer, C., Schnapp, G., Walter, R., Heckel, A., van Meel, J., Rieder, C.L., and Peters, J.M. (2003). The small molecule Hesperadin reveals a role for Aurora B in correcting kinetochore-microtubule attachment and in maintaining the spindle assembly checkpoint. *J Cell Biol* 161, 281-294.

Heinis, C., Schmitt, S., Kindermann, M., Godin, G., and Johnsson, K. (2006). Evolving the substrate specificity of O6-alkylguanine-DNA alkyltransferase through loop insertion for applications in molecular imaging. *ACS Chem Biol* 1, 575-584.

Henchcliffe, C., and Beal, M.F. (2008). Mitochondrial biology and oxidative stress in Parkinson disease pathogenesis. *Nat Clin Pract Neurol* 4, 600-609.

Henderson, D.M., and Conner, S.D. (2007). A novel AAK1 splice variant functions at multiple steps of the endocytic pathway. *Molecular biology of the cell* 18, 2698-2706.

Hergovich, A., Stegert, M.R., Schmitz, D., and Hemmings, B.A. (2006). NDR kinases regulate essential cell processes from yeast to humans. *Nat Rev Mol Cell Biol* 7, 253-264.

Hertz, N.T., Wang, B.T., Allen, J.J., Zhang, C., Dar, A.C., Burlingame, A.L., and Shokat, K.M. (2010a). Chemical Genetic Approach for Kinase-Substrate Mapping by Covalent Capture of Thiophosphopeptides and Analysis by Mass Spectrometry. *Curr Prot Chem Biol* 2, 15-36.

Hertz, N.T., Wang, B.T., Allen, J.J., Zhang, C., Dar, A.C., Burlingame, A.L., and Shokat, K.M. (2010b). Chemical Genetic Approach for Kinase-Substrate Mapping by Covalent Capture of Thiophosphopeptides and Analysis by Mass Spectrometry. *Current Protocols in Chemical Biology* 2, 15-36.

Hindie, V., Stroba, A., Zhang, H., Lopez-Garcia, L.A., Idrissova, L., Zeuzem, S., Hirschberg, D., Schaeffer, F., Jorgensen, T.J., Engel, M., *et al.* (2009). Structure and allosteric effects of low-molecular-weight activators on the protein kinase PDK1. *Nat Chem Biol* 5, 758-764.

Honda, R., Korner, R., and Nigg, E.A. (2003). Exploring the functional interactions between Aurora B, INCENP, and survivin in mitosis. *Mol Biol Cell* 14, 3325-3341.

Horgan, C.P., and McCaffrey, M.W. (2009). The dynamic Rab11-FIPs. *Biochem Soc Trans* 37, 1032-1036.

Hornbeck, P.V., Chabra, I., Kornhauser, J.M., Skrzypek, E., and Zhang, B. (2004). PhosphoSite: A bioinformatics resource dedicated to physiological protein phosphorylation. *Proteomics* 4, 1551-1561.

Horton, A.C., and Ehlers, M.D. (2003). Dual modes of endoplasmic reticulum-to-Golgi transport in dendrites revealed by live-cell imaging. *J Neurosci* 23, 6188-6199.

Horton, A.C., Racz, B., Monson, E.E., Lin, A.L., Weinberg, R.J., and Ehlers, M.D. (2005). Polarized secretory trafficking directs cargo for asymmetric dendrite growth and morphogenesis. *Neuron* 48, 757-771.

Hua, Z., Leal-Ortiz, S., Foss, S.M., Waites, C.L., Garner, C.C., Voglmaier, S.M., and Edwards, R.H. (2011). v-SNARE composition distinguishes synaptic vesicle pools. *Neuron* 71, 474-487.

Huang, J., Wu, S., Barrera, J., Matthews, K., and Pan, D. (2005). The Hippo signaling pathway coordinately regulates cell proliferation and apoptosis by inactivating Yorkie, the Drosophila Homolog of YAP. *Cell* 122, 421-434.

Hummer, S., and Mayer, T.U. (2009). Cdk1 negatively regulates midzone localization of the mitotic kinesin Mklp2 and the chromosomal passenger complex. *Curr Biol* 19, 607-612.

Ishii, Y., Hori, Y., Sakai, S., and Honma, Y. (2002). Control of differentiation and apoptosis of human myeloid leukemia cells by cytokinins and cytokinin nucleosides, plant redifferentiation-inducing hormones. *Cell Growth Differ* 13, 19-26.

Ishii, Y., Sakai, S., and Honma, Y. (2003). Cytokinin-induced differentiation of human myeloid leukemia HL-60 cells is associated with the formation of nucleotides, but not with incorporation into DNA or RNA. *Biochim Biophys Acta* 1643, 11-24.

Jansen, J.M., Wanless, A.G., Seidel, C.W., and Weiss, E.L. (2009). Cbk1 regulation of the RNA-binding protein Ssd1 integrates cell fate with translational control. *Curr Biol* 19, 2114-2120.

Johnson, E.O., Chang, K.H., de Pablo, Y., Ghosh, S., Mehta, R., Badve, S., and Shah, K. (2011). PHLDA1 is a crucial negative regulator and effector of Aurora A kinase in breast cancer. *Journal of cell science* 124, 2711-2722.

Jordan, M.A., and Wilson, L. (2004). Microtubules as a target for anticancer drugs. *Nat Rev Cancer* 4, 253-265.

Kettenbach, A.N., Schweppe, D.K., Faherty, B.K., Pechenick, D., Pletnev, A.A., and Gerber, S.A. (2011). Quantitative phosphoproteomics identifies substrates and functional modules of aurora and polo-like kinase activities in mitotic cells. *Sci Signal* 4, rs5.

Kissil, J.L., Feinstein, E., Cohen, O., Jones, P.A., Tsai, Y.C., Knowles, M.A., Eydmann, M.E., and Kimchi, A. (1997). DAP-kinase loss of expression in various carcinoma and B-

cell lymphoma cell lines: possible implications for role as tumor suppressor gene. *Oncogene* 15, 403-407.

Kitada, T., Asakawa, S., Hattori, N., Matsumine, H., Yamamura, Y., Minoshima, S., Yokochi, M., Mizuno, Y., and Shimizu, N. (1998). Mutations in the parkin gene cause autosomal recessive juvenile parkinsonism. *Nature* 392, 605-608.

Klinkenberg, M., Thurrow, N., Gispert, S., Ricciardi, F., Eich, F., Prehn, J.H., Auburger, G., and Kogel, D. (2010). Enhanced vulnerability of PARK6 patient skin fibroblasts to apoptosis induced by proteasomal stress. *Neuroscience* 166, 422-434.

Koike-Kumagai, M., Yasunaga, K., Morikawa, R., Kanamori, T., and Emoto, K. (2009). The target of rapamycin complex 2 controls dendritic tiling of *Drosophila* sensory neurons through the Tricornered kinase signalling pathway. *Embo J* 28, 3879-3892.

Kondapalli, C., Kazlauskaitė, A., Zhang, N., Woodroof, H.I., Campbell, D.G., Gourlay, R., Burchell, L., Walden, H., Macartney, T.J., Deak, M., *et al.* (2012). PINK1 is activated by mitochondrial membrane potential depolarization and stimulates Parkin E3 ligase activity by phosphorylating Serine 65. *Open Biol* 2, 120080.

Konur, S., and Yuste, R. (2004). Developmental regulation of spine and filopodial motility in primary visual cortex: reduced effects of activity and sensory deprivation. *Journal of neurobiology* 59, 236-246.

Kornberg, A., Lieberman, I., and Simms, E.S. (1955). Enzymatic synthesis of purine nucleotides. *J Biol Chem* 215, 417-427.

Krishnan, P., Fu, Q., Lam, W., Liou, J.Y., Dutschman, G., and Cheng, Y.C. (2002). Phosphorylation of pyrimidine deoxynucleoside analog diphosphates: selective phosphorylation of L-nucleoside analog diphosphates by 3-phosphoglycerate kinase. *J Biol Chem* 277, 5453-5459.

Kulkarni, R.N., Bruning, J.C., Winnay, J.N., Postic, C., Magnuson, M.A., and Kahn, C.R. (1999). Tissue-specific knockout of the insulin receptor in pancreatic beta cells creates an insulin secretory defect similar to that in type 2 diabetes. *Cell* 96, 329-339.

Kuo, C.T., Zhu, S., Younger, S., Jan, L.Y., and Jan, Y.N. (2006). Identification of E2/E3 ubiquitinating enzymes and caspase activity regulating *Drosophila* sensory neuron dendrite pruning. *Neuron* 51, 283-290.

Kurischko, C., Kuravi, V.K., Wannissorn, N., Nazarov, P.A., Husain, M., Zhang, C., Shokat, K.M., McCaffery, J.M., and Luca, F.C. (2008). The yeast LATS/Ndr kinase Cbk1 regulates growth via Golgi-dependent glycosylation and secretion. *Molecular biology of the cell* 19, 5559-5578.

Kwon, S.W., Kim, S.C., Jaunbergs, J., Falck, J.R., and Zhao, Y. (2003). Selective enrichment of thiophosphorylated polypeptides as a tool for the analysis of protein phosphorylation. *Mol Cell Proteomics* 2, 242-247.

Lang, A.E., and Lozano, A.M. (1998). Parkinson's disease. First of two parts. *N Engl J Med* 339, 1044-1053.

Lens, S.M., Voest, E.E., and Medema, R.H. (2010). Shared and separate functions of polo-like kinases and aurora kinases in cancer. *Nat Rev Cancer* 10, 825-841.

Lens, S.M., Wolthuis, R.M., Klomp maker, R., Kauw, J., Agami, R., Brummelkamp, T., Kops, G., and Medema, R.H. (2003). Survivin is required for a sustained spindle checkpoint arrest in response to lack of tension. *Embo J* 22, 2934-2947.

Li, Z., Jo, J., Jia, J.M., Lo, S.C., Whitcomb, D.J., Jiao, S., Cho, K., and Sheng, M. (2010). Caspase-3 activation via mitochondria is required for long-term depression and AMPA receptor internalization. *Cell* 141, 859-871.

Lieberman, I., Kornberg, A., and Simms, E.S. (1955a). Enzymatic synthesis of nucleoside diphosphates and triphosphates. *J Biol Chem* 215, 429-440.

Lieberman, I., Kornberg, A., and Simms, E.S. (1955b). Enzymatic synthesis of pyrimidine nucleotides; orotidine-5'-phosphate and uridine-5'-phosphate. *J Biol Chem* 215, 403-451.

Liu, Y., Shah, K., Yang, F., Witucki, L., and Shokat, K.M. (1998). A molecular gate which controls unnatural ATP analogue recognition by the tyrosine kinase v-Src. *Bioorg Med Chem* 6, 1219-1226.

MacVicar, B.A., and Thompson, R.J. (2010). Non-junction functions of pannexin-1 channels. *Trends in neurosciences* 33, 93-102.

Manning, G., Whyte, D.B., Martinez, R., Hunter, T., and Sudarsanam, S. (2002). The protein kinase complement of the human genome. *Science* 298, 1912-1934.

Matsuzaki, M., Ellis-Davies, G.C., Nemoto, T., Miyashita, Y., Iino, M., and Kasai, H. (2001). Dendritic spine geometry is critical for AMPA receptor expression in hippocampal CA1 pyramidal neurons. *Nature neuroscience* 4, 1086-1092.

Mazanka, E., Alexander, J., Yeh, B.J., Charoenpong, P., Lowery, D.M., Yaffe, M., and Weiss, E.L. (2008). The NDR/LATS family kinase Cbk1 directly controls transcriptional asymmetry. *PLoS Biol* 6, e203.

McNiven, M.A., and Thompson, H.M. (2006). Vesicle formation at the plasma membrane and trans-Golgi network: the same but different. *Science* 313, 1591-1594.

Meissner, C., Lorenz, H., Weihofen, A., Selkoe, D.J., and Lemberg, M.K. (2011). The mitochondrial intramembrane protease PARL cleaves human Pink1 to regulate Pink1 trafficking. *J Neurochem* 117, 856-867.

Merrick, K.A., Wohlbold, L., Zhang, C., Allen, J.J., Horiuchi, D., Huskey, N.E., Goga, A., Shokat, K.M., and Fisher, R.P. (2011). Switching Cdk2 on or off with small molecules to reveal requirements in human cell proliferation. *Mol Cell* 42, 624-636.

Millward, T.A., Hess, D., and Hemmings, B.A. (1999). Ndr protein kinase is regulated by phosphorylation on two conserved sequence motifs. *The Journal of biological chemistry* 274, 33847-33850.

Minoshima, Y., Kawashima, T., Hirose, K., Tonozuka, Y., Kawajiri, A., Bao, Y.C., Deng, X., Tatsuka, M., Narumiya, S., May, W.S., Jr., *et al.* (2003). Phosphorylation by aurora B converts MgcRacGAP to a RhoGAP during cytokinesis. *Dev Cell* 4, 549-560.

Monaco, L., Kolthur-Seetharam, U., Loury, R., Murcia, J.M., de Murcia, G., and Sassone-Corsi, P. (2005). Inhibition of Aurora-B kinase activity by poly(ADP-ribose)ylation in response to DNA damage. *Proc Natl Acad Sci U S A* 102, 14244-14248.

Murata-Hori, M., and Wang, Y.L. (2002). The kinase activity of aurora B is required for kinetochore-microtubule interactions during mitosis. *Curr Biol* 12, 894-899.

Nakamura, K., Nemani, V.M., Azarbal, F., Skibinski, G., Levy, J.M., Egami, K., Munishkina, L., Zhang, J., Gardner, B., Wakabayashi, J., *et al.* (2011). Direct membrane association drives mitochondrial fission by the Parkinson disease-associated protein alpha-synuclein. *J Biol Chem* 286, 20710-20726.

Narendra, D., Tanaka, A., Suen, D.F., and Youle, R.J. (2008). Parkin is recruited selectively to impaired mitochondria and promotes their autophagy. *J Cell Biol* *183*, 795-803.

Narendra, D.P., Jin, S.M., Tanaka, A., Suen, D.F., Gautier, C.A., Shen, J., Cookson, M.R., and Youle, R.J. (2010). PINK1 is selectively stabilized on impaired mitochondria to activate Parkin. *PLoS Biol* *8*, e1000298.

Nelson, B., Kurischko, C., Horecka, J., Mody, M., Nair, P., Pratt, L., Zougman, A., McBroom, L.D., Hughes, T.R., Boone, C., *et al.* (2003). RAM: a conserved signaling network that regulates Ace2p transcriptional activity and polarized morphogenesis. *Molecular biology of the cell* *14*, 3782-3803.

Nemani, V.M., Lu, W., Berge, V., Nakamura, K., Onoa, B., Lee, M.K., Chaudhry, F.A., Nicoll, R.A., and Edwards, R.H. (2010). Increased expression of alpha-synuclein reduces neurotransmitter release by inhibiting synaptic vesicle reclustering after endocytosis. *Neuron* *65*, 66-79.

Niefind, K., Putter, M., Guerra, B., Issinger, O.G., and Schomburg, D. (1999). GTP plus water mimic ATP in the active site of protein kinase CK2. *Nat Struct Biol* *6*, 1100-1103.

Nishizuka, Y. (1984). The role of protein kinase C in cell surface signal transduction and tumour promotion. *Nature* *308*, 693-698.

Nunnari, J., and Suomalainen, A. (2012). Mitochondria: in sickness and in health. *Cell* *148*, 1145-1159.

Olsen, J.V., Blagoev, B., Gnäd, F., Macek, B., Kumar, C., Mortensen, P., and Mann, M. (2006). Global, in vivo, and site-specific phosphorylation dynamics in signaling networks. *Cell* *127*, 635-648.

Otsu, N. (1979). A Threshold Selection Method from Gray-Level Histograms. *EEE Transactions on Systems, Man and Cybernetics SMC-9*, 62-66.

Parkin, D.W., Leung, H.B., and Schramm, V.L. (1984). Synthesis of nucleotides with specific radiolabels in ribose. Primary ¹⁴C and secondary ³H kinetic isotope effects on acid-catalyzed glycosidic bond hydrolysis of AMP, dAMP, and inosine. *J Biol Chem* *259*, 9411-9417.

Perrera, C., Colombo, R., Valsasina, B., Carpinelli, P., Troiani, S., Modugno, M., Gianellini, L., Cappella, P., Isacchi, A., Moll, J., *et al.* (2010). Identification of Myb-binding protein 1A (MYBBP1A) as a novel substrate for aurora B kinase. *J Biol Chem* *285*, 11775-11785.

Petit, A., Kawarai, T., Paitel, E., Sanjo, N., Maj, M., Scheid, M., Chen, F., Gu, Y., Hasegawa, H., Salehi-Rad, S., *et al.* (2005). Wild-type PINK1 prevents basal and induced neuronal apoptosis, a protective effect abrogated by Parkinson disease-related mutations. *J Biol Chem* *280*, 34025-34032.

Pinsky, B.A., Kung, C., Shokat, K.M., and Biggins, S. (2006). The Ipl1-Aurora protein kinase activates the spindle checkpoint by creating unattached kinetochores. *Nat Cell Biol* *8*, 78-83.

Postnikov, Y., and Bustin, M. (2010). Regulation of chromatin structure and function by HMGN proteins. *Biochim Biophys Acta* *1799*, 62-68.

Pridgeon, J.W., Olzmann, J.A., Chin, L.S., and Li, L. (2007). PINK1 Protects against Oxidative Stress by Phosphorylating Mitochondrial Chaperone TRAP1. *PLoS Biol* *5*, e172.

Qiao, Y., Molina, H., Pandey, A., Zhang, J., and Cole, P.A. (2006). Chemical rescue of a mutant enzyme in living cells. *Science* *311*, 1293-1297.

Ray, A.S., Vela, J.E., Olson, L., and Fridland, A. (2004). Effective metabolism and long intracellular half life of the anti-hepatitis B agent adefovir in hepatic cells. *Biochem Pharmacol* *68*, 1825-1831.

Robinson, M.S. (2004). Adaptable adaptors for coated vesicles. *Trends Cell Biol* *14*, 167-174.

Rochman, M., Postnikov, Y., Correll, S., Malicet, C., Wincovitch, S., Karpova, T.S., McNally, J.G., Wu, X., Bubunenko, N.A., Grigoryev, S., *et al.* (2009). The interaction of NSBP1/HMG5 with nucleosomes in euchromatin counteracts linker histone-mediated chromatin compaction and modulates transcription. *Mol Cell* *35*, 642-656.

Ruchaud, S., Carmena, M., and Earnshaw, W.C. (2007). Chromosomal passengers: conducting cell division. *Nat Rev Mol Cell Biol* *8*, 798-812.

Rugarli, E.I., and Langer, T. (2012). Mitochondrial quality control: a matter of life and death for neurons. *EMBO J* *31*, 1336-1349.

Sabbattini, P., Canzonetta, C., Sjoberg, M., Nikic, S., Georgiou, A., Kemball-Cook, G., Auner, H.W., and Dillon, N. (2007). A novel role for the Aurora B kinase in epigenetic marking of silent chromatin in differentiated postmitotic cells. *EMBO J* *26*, 4657-4669.

Samaranch, L., Lorenzo-Betancor, O., Arbelo, J.M., Ferrer, I., Lorenzo, E., Irigoyen, J., Pastor, M.A., Marrero, C., Isla, C., Herrera-Henriquez, J., *et al.* (2010). PINK1-linked parkinsonism is associated with Lewy body pathology. *Brain* *133*, 1128-1142.

Sekiya-Kawasaki, M., Groen, A.C., Cope, M.J., Kaksonen, M., Watson, H.A., Zhang, C., Shokat, K.M., Wendland, B., McDonald, K.L., McCaffery, J.M., *et al.* (2003). Dynamic phosphoregulation of the cortical actin cytoskeleton and endocytic machinery revealed by real-time chemical genetic analysis. *J Cell Biol* *162*, 765-772.

Sessa, F., Mapelli, M., Ciferri, C., Tarricone, C., Areces, L.B., Schneider, T.R., Stukenberg, P.T., and Musacchio, A. (2005). Mechanism of Aurora B activation by INCENP and inhibition by hesperadin. *Mol Cell* *18*, 379-391.

Shah, K., Liu, Y., Deirmengian, C., and Shokat, K.M. (1997). Engineering unnatural nucleotide specificity for Rous sarcoma virus tyrosine kinase to uniquely label its direct substrates. *Proc Natl Acad Sci U S A* *94*, 3565-3570.

Shetty, R.S., Gallagher, C.S., Chen, Y.T., Hims, M.M., Mull, J., Leyne, M., Pickel, J., Kwok, D., and Slaughaupt, S.A. (2011). Specific correction of a splice defect in brain by nutritional supplementation. *Hum Mol Genet* *20*, 4093-4101.

Shin, J.H., Ko, H.S., Kang, H., Lee, Y., Lee, Y.I., Pletinkova, O., Troconso, J.C., Dawson, V.L., and Dawson, T.M. (2011). PARIS (ZNF746) repression of PGC-1alpha contributes to neurodegeneration in Parkinson's disease. *Cell* *144*, 689-702.

Song, S., Jang, S., Park, J., Bang, S., Choi, S., Kwon, K.Y., Zhuang, X., Kim, E., and Chung, J. (2013). Characterization of phosphatase and tensin homolog (PTEN)-induced putative kinase 1 (PINK1) mutations associated with Parkinson's disease in mammalian cells and *Drosophila*. *J Biol Chem*.

St John, M.A., Tao, W., Fei, X., Fukumoto, R., Carcangiu, M.L., Brownstein, D.G., Parlow, A.F., McGrath, J., and Xu, T. (1999). Mice deficient of Lats1 develop soft-tissue sarcomas, ovarian tumours and pituitary dysfunction. *Nat Genet* *21*, 182-186.

Stegert, M.R., Hergovich, A., Tamaskovic, R., Bichsel, S.J., and Hemmings, B.A. (2005). Regulation of NDR protein kinase by hydrophobic motif phosphorylation mediated by the mammalian Ste20-like kinase MST3. *Mol Cell Biol* 25, 11019-11029.

Stegert, M.R., Tamaskovic, R., Bichsel, S.J., Hergovich, A., and Hemmings, B.A. (2004). Regulation of NDR2 protein kinase by multi-site phosphorylation and the S100B calcium-binding protein. *The Journal of biological chemistry* 279, 23806-23812.

Stenmark, H. (2009). Rab GTPases as coordinators of vesicle traffic. *Nat Rev Mol Cell Biol* 10, 513-525.

Stork, O., Zhdanov, A., Kudersky, A., Yoshikawa, T., Obata, K., and Pape, H.C. (2004). Neuronal functions of the novel serine/threonine kinase Ndr2. *The Journal of biological chemistry* 279, 45773-45781.

Subramanian, M., Gonzalez, R.W., Patil, H., Ueda, T., Lim, J.H., Kraemer, K.H., Bustin, M., and Bergel, M. (2009). The nucleosome-binding protein HMGN2 modulates global genome repair. *FEBS J* 276, 6646-6657.

Toshima, J., Toshima, J.Y., Martin, A.C., and Drubin, D.G. (2005). Phosphoregulation of Arp2/3-dependent actin assembly during receptor-mediated endocytosis. *Nature cell biology* 7, 246-254.

Traub, L.M. (2009). Tickets to ride: selecting cargo for clathrin-regulated internalization. *Nat Rev Mol Cell Biol* 10, 583-596.

Trinidad, J.C., Thalhammer, A., Specht, C.G., Lynn, A.J., Baker, P.R., Schoepfer, R., and Burlingame, A.L. (2008). Quantitative analysis of synaptic phosphorylation and protein expression. *Mol Cell Proteomics* 7, 684-696.

Ubersax, J.A., Woodbury, E.L., Quang, P.N., Paraz, M., Blethrow, J.D., Shah, K., Shokat, K.M., and Morgan, D.O. (2003). Targets of the cyclin-dependent kinase Cdk1. *Nature* 425, 859-864.

Ueda, T., Catez, F., Gerlitz, G., and Bustin, M. (2008). Delineation of the protein module that anchors HMGN proteins to nucleosomes in the chromatin of living cells. *Mol Cell Biol* 28, 2872-2883.

Ultanir, S.K., and Hertz, N. T., Li, G., Ge, W.P., Burlingame, A.L., Pleasure, S.J., Shokat, K.M., Jan, L.Y., and Jan, Y.N. (2012). Chemical genetic identification of NDR1/2 kinase substrates AAK1 and Rabin8 Uncovers their roles in dendrite arborization and spine development. *Neuron* 73, 1127-1142.

Valente, E.M., Abou-Sleiman, P.M., Caputo, V., Muqit, M.M., Harvey, K., Gispert, S., Ali, Z., Del Turco, D., Bentivoglio, A.R., Healy, D.G., *et al.* (2004). Hereditary early-onset Parkinson's disease caused by mutations in PINK1. *Science* 304, 1158-1160.

Vela, J.E., Olson, L.Y., Huang, A., Fridland, A., and Ray, A.S. (2007). Simultaneous quantitation of the nucleotide analog adefovir, its phosphorylated anabolites and 2'-deoxyadenosine triphosphate by ion-pairing LC/MS/MS. *J Chromatogr B Analyt Technol Biomed Life Sci* 848, 335-343.

Vichalkovski, A., Gresko, E., Cornils, H., Hergovich, A., Schmitz, D., and Hemmings, B.A. (2008). NDR kinase is activated by RASSF1A/MST1 in response to Fas receptor stimulation and promotes apoptosis. *Curr Biol* 18, 1889-1895.

Wang, H.L., Chou, A.H., Yeh, T.H., Li, A.H., Chen, Y.L., Kuo, Y.L., Tsai, S.R., and Yu, S.T. (2007). PINK1 mutants associated with recessive Parkinson's disease are defective in inhibiting mitochondrial release of cytochrome c. *Neurobiol Dis* 28, 216-226.

Wang, X., Winter, D., Ashrafi, G., Schlehe, J., Wong, Y.L., Selkoe, D., Rice, S., Steen, J., LaVoie, M.J., and Schwarz, T.L. (2011). PINK1 and Parkin target Miro for phosphorylation and degradation to arrest mitochondrial motility. *Cell* *147*, 893-906.

Wang, Z., Edwards, J.G., Riley, N., Provance, D.W., Jr., Karcher, R., Li, X.D., Davison, I.G., Ikebe, M., Mercer, J.A., Kauer, J.A., *et al.* (2008). Myosin Vb mobilizes recycling endosomes and AMPA receptors for postsynaptic plasticity. *Cell* *135*, 535-548.

Wei, L., Gao, X., Warne, R., Hao, X., Bussiere, D., Gu, X.J., Uno, T., and Liu, Y. (2010). Design and synthesis of benzoazepin-2-one analogs as allosteric binders targeting the PIF pocket of PDK1. *Bioorg Med Chem Lett* *20*, 3897-3902.

Weiss, W.A., Taylor, S.S., and Shokat, K.M. (2007). Recognizing and exploiting differences between RNAi and small-molecule inhibitors. *Nat Chem Biol* *3*, 739-744.

Wu, S., Huang, J., Dong, J., and Pan, D. (2003). hippo encodes a Ste-20 family protein kinase that restricts cell proliferation and promotes apoptosis in conjunction with salvador and warts. *Cell* *114*, 445-456.

Xiong, H., Wang, D., Chen, L., Choo, Y.S., Ma, H., Tang, C., Xia, K., Jiang, W., Ronai, Z., Zhuang, X., *et al.* (2009). Parkin, PINK1, and DJ-1 form a ubiquitin E3 ligase complex promoting unfolded protein degradation. *J Clin Invest* *119*, 650-660.

Ye, B., Zhang, Y., Song, W., Younger, S.H., Jan, L.Y., and Jan, Y.N. (2007). Growing dendrites and axons differ in their reliance on the secretory pathway. *Cell* *130*, 717-729.

Ye, B., Zhang, Y.W., Jan, L.Y., and Jan, Y.N. (2006). The secretory pathway and neuron polarization. *J Neurosci* *26*, 10631-10632.

Youle, R.J., and Narendra, D.P. (2011). Mechanisms of mitophagy. *Nat Rev Mol Cell Biol* *12*, 9-14.

Yuste, R., and Bonhoeffer, T. (2004). Genesis of dendritic spines: insights from ultrastructural and imaging studies. *Nature reviews* *5*, 24-34.

Zhang, C., Kenski, D.M., Paulson, J.L., Bonshtien, A., Sessa, G., Cross, J.V., Templeton, D.J., and Shokat, K.M. (2005). A second-site suppressor strategy for chemical genetic analysis of diverse protein kinases. *Nat Methods* *2*, 435-441.

Zhou, Z.R., Zhang, Y.H., Liu, S., Song, A.X., and Hu, H.Y. (2012). Length of the active-site crossover loop defines the substrate specificity of ubiquitin C-terminal hydrolases for ubiquitin chains. *Biochem J* *441*, 143-149.

Adams, J.M., and Cory, S. (1998). The Bcl-2 protein family: arbiters of cell survival. *Science* *281*, 1322-1326.

Alexander, J., Lim, D., Joughin, B.A., Hegemann, B., Hutchins, J.R., Ehrenberger, T., Ivins, F., Sessa, F., Hudecz, O., Nigg, E.A., *et al.* (2011). Spatial exclusivity combined with positive and negative selection of phosphorylation motifs is the basis for context-dependent mitotic signaling. *Sci Signal* *4*, ra42.

Allen, J.J., Lazerwith, S.E., and Shokat, K.M. (2005). Bio-orthogonal affinity purification of direct kinase substrates. *J Am Chem Soc* *127*, 5288-5289.

Allen, J.J., Li, M., Brinkworth, C.S., Paulson, J.L., Wang, D., Hubner, A., Chou, W.H., Davis, R.J., Burlingame, A.L., Messing, R.O., *et al.* (2007). A semisynthetic epitope for kinase substrates. *Nat Methods* *4*, 511-516.

Arena, G., Gelmetti, V., Torosantucci, L., Vignone, D., Lamorte, G., De Rosa, P., Cilia, E., Jonas, E.A., and Valente, E.M. (2013). PINK1 protects against cell death induced by mitochondrial depolarization, by phosphorylating Bcl-xL and impairing its pro-apoptotic cleavage. *Cell Death Differ*.

Axelrod, F.B., Liebes, L., Gold-Von Simson, G., Mendoza, S., Mull, J., Leyne, M., Norcliffe-Kaufmann, L., Kaufmann, H., and Slaugenhaupt, S.A. (2011). Kinetin improves IKBKAP mRNA splicing in patients with familial dysautonomia. *Pediatr Res* *70*, 480-483.

Baker, P.R., Trinidad, J.C., and R.J., C. (2011). Modification site localization scoring integrated into a search engine. *Mol Cell Proteomics* *10*, M111.008078.

Beilina, A., Van Der Brug, M., Ahmad, R., Kesavapany, S., Miller, D.W., Petsko, G.A., and Cookson, M.R. (2005). Mutations in PTEN-induced putative kinase 1 associated with recessive parkinsonism have differential effects on protein stability. *Proc Natl Acad Sci U S A* *102*, 5703-5708.

Bichsel, S.J., Tamaskovic, R., Stegert, M.R., and Hemmings, B.A. (2004). Mechanism of activation of NDR (nuclear Dbf2-related) protein kinase by the hMOB1 protein. *The Journal of biological chemistry* *279*, 35228-35235.

Bishop, A., Buzko, O., Heyeck-Dumas, S., Jung, I., Kraybill, B., Liu, Y., Shah, K., Ulrich, S., Witucki, L., Yang, F., *et al.* (2000a). Unnatural ligands for engineered proteins: new tools for chemical genetics. *Annu Rev Biophys Biomol Struct* *29*, 577-606.

Bishop, A.C., Ubersax, J.A., Petsch, D.T., Matheos, D.P., Gray, N.S., Blethrow, J., Shimizu, E., Tsien, J.Z., Schultz, P.G., Rose, M.D., *et al.* (2000b). A chemical switch for inhibitor-sensitive alleles of any protein kinase. *Nature* *407*, 395-401.

Bishop, J.D., and Schumacher, J.M. (2002). Phosphorylation of the carboxyl terminus of inner centromere protein (INCENP) by the Aurora B Kinase stimulates Aurora B kinase activity. *J Biol Chem* *277*, 27577-27580.

Blethrow, J., Zhang, C., Shokat, K.M., and Weiss, E.L. (2004). Design and use of analog-sensitive protein kinases. *Curr Protoc Mol Biol Chapter 18*, Unit 18 11.

Blethrow, J.D., Glavy, J.S., Morgan, D.O., and Shokat, K.M. (2008). Covalent capture of kinase-specific phosphopeptides reveals Cdk1-cyclin B substrates. *Proc Natl Acad Sci U S A* *105*, 1442-1447.

Brondyk, W.H., McKiernan, C.J., Fortner, K.A., Stabila, P., Holz, R.W., and Macara, I.G. (1995). Interaction cloning of Rabin3, a novel protein that associates with the Ras-like GTPase Rab3A. *Molecular and cellular biology* *15*, 1137-1143.

Brown, T.C., Correia, S.S., Petrok, C.N., and Esteban, J.A. (2007). Functional compartmentalization of endosomal trafficking for the synaptic delivery of AMPA receptors during long-term potentiation. *J Neurosci* 27, 13311-13315.

Buzko, O., and Shokat, K.M. (2002). A kinase sequence database: sequence alignments and family assignment. *Bioinformatics* 18, 1274-1275.

Castagna, M., Takai, Y., Kaibuchi, K., Sano, K., Kikkawa, U., and Nishizuka, Y. (1982). Direct activation of calcium-activated, phospholipid-dependent protein kinase by tumor-promoting phorbol esters. *J Biol Chem* 257, 7847-7851.

Cheeseman, I.M., Anderson, S., Jwa, M., Green, E.M., Kang, J., Yates, J.R., 3rd, Chan, C.S., Drubin, D.G., and Barnes, G. (2002). Phospho-regulation of kinetochore-microtubule attachments by the Aurora kinase Ipl1p. *Cell* 111, 163-172.

Cherukuri, S., Hock, R., Ueda, T., Catez, F., Rochman, M., and Bustin, M. (2008). Cell cycle-dependent binding of HMGN proteins to chromatin. *Mol Biol Cell* 19, 1816-1824.

Clark, I.E., Dodson, M.W., Jiang, C., Cao, J.H., Huh, J.R., Seol, J.H., Yoo, S.J., Hay, B.A., and Guo, M. (2006). Drosophila pink1 is required for mitochondrial function and interacts genetically with parkin. *Nature* 441, 1162-1166.

Cohen, P. (2001). The role of protein phosphorylation in human health and disease. The Sir Hans Krebs Medal Lecture. *Eur J Biochem* 268, 5001-5010.

Cong, J., Geng, W., He, B., Liu, J., Charlton, J., and Adler, P.N. (2001). The furry gene of Drosophila is important for maintaining the integrity of cellular extensions during morphogenesis. *Development (Cambridge, England)* 128, 2793-2802.

Conner, S.D., and Schmid, S.L. (2002). Identification of an adaptor-associated kinase, AAK1, as a regulator of clathrin-mediated endocytosis. *J Cell Biol* 156, 921-929.

Conner, S.D., and Schmid, S.L. (2003). Differential requirements for AP-2 in clathrin-mediated endocytosis. *The Journal of cell biology* 162, 773-779.

Cornils, H., Stegert, M.R., Hergovich, A., Hynx, D., Schmitz, D., Dirnhofer, S., and Hemmings, B.A. (2010). Ablation of the kinase NDR1 predisposes mice to the development of T cell lymphoma. *Science signaling* 3, ra47.

De Matteis, M.A., Di Campli, A., and Godi, A. (2005). The role of the phosphoinositides at the Golgi complex. *Biochim Biophys Acta* 1744, 396-405.

Deng, H., Dodson, M.W., Huang, H., and Guo, M. (2008). The Parkinson's disease genes pink1 and parkin promote mitochondrial fission and/or inhibit fusion in Drosophila. *Proc Natl Acad Sci U S A* 105, 14503-14508.

Deng, H., Jankovic, J., Guo, Y., Xie, W., and Le, W. (2005). Small interfering RNA targeting the PINK1 induces apoptosis in dopaminergic cells SH-SY5Y. *Biochem Biophys Res Commun* 337, 1133-1138.

Dephoure, N., Howson, R.W., Blethrow, J.D., Shokat, K.M., and O'Shea, E.K. (2005). Combining chemical genetics and proteomics to identify protein kinase substrates. *Proc Natl Acad Sci U S A* 102, 17940-17945.

Devroe, E., Erdjument-Bromage, H., Tempst, P., and Silver, P.A. (2004). Human Mob proteins regulate the NDR1 and NDR2 serine-threonine kinases. *The Journal of biological chemistry* 279, 24444-24451.

Ditchfield, C., Johnson, V.L., Tighe, A., Ellston, R., Haworth, C., Johnson, T., Mortlock, A., Keen, N., and Taylor, S.S. (2003). Aurora B couples chromosome alignment with anaphase by targeting BubR1, Mad2, and Cenp-E to kinetochores. *J Cell Biol* 161, 267-280.

Emoto, K., He, Y., Ye, B., Grueber, W.B., Adler, P.N., Jan, L.Y., and Jan, Y.N. (2004). Control of dendritic branching and tiling by the Tricornered-kinase/Furry signaling pathway in *Drosophila* sensory neurons. *Cell* *119*, 245-256.

Emoto, K., Parrish, J.Z., Jan, L.Y., and Jan, Y.N. (2006). The tumour suppressor Hippo acts with the NDR kinases in dendritic tiling and maintenance. *Nature* *443*, 210-213.

Espinosa, J.S., Wheeler, D.G., Tsien, R.W., and Luo, L. (2009). Uncoupling dendrite growth and patterning: single-cell knockout analysis of NMDA receptor 2B. *Neuron* *62*, 205-217.

Ferrando, I.M., Chaerkady, R., Zhong, J., Molina, H., Jacob, H.K., Herbst-Robinson, K., Dancy, B.M., Katju, V., Bose, R., Zhang, J., *et al.* (2012). Identification of targets of c-Src tyrosine kinase by chemical complementation and phosphoproteomics. *Mol Cell Proteomics* *11*, 355-369.

Ferrer, A., Caelles, C., Massot, N., and Hegardt, F.G. (1985). Activation of rat liver cytosolic 3-hydroxy-3-methylglutaryl coenzyme A reductase kinase by adenosine 5'-monophosphate. *Biochem Biophys Res Commun* *132*, 497-504.

Fiala, J.C., Feinberg, M., Popov, V., and Harris, K.M. (1998). Synaptogenesis via dendritic filopodia in developing hippocampal area CA1. *J Neurosci* *18*, 8900-8911.

Gallegos, M.E., and Bargmann, C.I. (2004). Mechanosensory neurite termination and tiling depend on SAX-2 and the SAX-1 kinase. *Neuron* *44*, 239-249.

Gao, Y., Ge, G., and Ji, H. (2011). LKB1 in lung cancerigenesis: a serine/threonine kinase as tumor suppressor. *Protein Cell* *2*, 99-107.

Gautier, C.A., Kitada, T., and Shen, J. (2008). Loss of PINK1 causes mitochondrial functional defects and increased sensitivity to oxidative stress. *Proc Natl Acad Sci U S A* *105*, 11364-11369.

Geisler, S., Holmstrom, K.M., Treis, A., Skujat, D., Weber, S.S., Fiesel, F.C., Kahle, P.J., and Springer, W. (2010). The PINK1/Parkin-mediated mitophagy is compromised by PD-associated mutations. *Autophagy* *6*, 871-878.

Geng, W., He, B., Wang, M., and Adler, P.N. (2000). The tricornered gene, which is required for the integrity of epidermal cell extensions, encodes the *Drosophila* nuclear DBF2-related kinase. *Genetics* *156*, 1817-1828.

Gerges, N.Z., Backos, D.S., and Esteban, J.A. (2004). Local control of AMPA receptor trafficking at the postsynaptic terminal by a small GTPase of the Rab family. *The Journal of biological chemistry* *279*, 43870-43878.

Girdler, F., Gascoigne, K.E., Evers, P.A., Hartmuth, S., Crafter, C., Foote, K.M., Keen, N.J., and Taylor, S.S. (2006). Validating Aurora B as an anti-cancer drug target. *J Cell Sci* *119*, 3664-3675.

Girdler, F., Sessa, F., Patercoli, S., Villa, F., Musacchio, A., and Taylor, S. (2008). Molecular basis of drug resistance in aurora kinases. *Chem Biol* *15*, 552-562.

Goto, H., Kiyono, T., Tomono, Y., Kawajiri, A., Urano, T., Furukawa, K., Nigg, E.A., and Inagaki, M. (2006). Complex formation of Plk1 and INCENP required for metaphase-anaphase transition. *Nat Cell Biol* *8*, 180-187.

Goto, H., Yasui, Y., Kawajiri, A., Nigg, E.A., Terada, Y., Tatsuka, M., Nagata, K., and Inagaki, M. (2003). Aurora-B regulates the cleavage furrow-specific vimentin phosphorylation in the cytokinetic process. *J Biol Chem* *278*, 8526-8530.

Gregan, J., Zhang, C., Rumpf, C., Cipak, L., Li, Z., Uluocak, P., Nasmyth, K., and Shokat, K.M. (2007). Construction of conditional analog-sensitive kinase alleles in the fission yeast *Schizosaccharomyces pombe*. *Nat Protoc* 2, 2996-3000.

Gross, A., McDonnell, J.M., and Korsmeyer, S.J. (1999). BCL-2 family members and the mitochondria in apoptosis. *Genes Dev* 13, 1899-1911.

Haque, M.E., Thomas, K.J., D'Souza, C., Callaghan, S., Kitada, T., Slack, R.S., Fraser, P., Cookson, M.R., Tandon, A., and Park, D.S. (2008). Cytoplasmic Pink1 activity protects neurons from dopaminergic neurotoxin MPTP. *Proc Natl Acad Sci U S A* 105, 1716-1721.

Hardie, D.G., Ross, F.A., and Hawley, S.A. (2012). AMPK: a nutrient and energy sensor that maintains energy homeostasis. *Nat Rev Mol Cell Biol* 13, 251-262.

Harris, K.M. (1999). Structure, development, and plasticity of dendritic spines. *Current opinion in neurobiology* 9, 343-348.

Harvey, K.F., Pflieger, C.M., and Hariharan, I.K. (2003). The *Drosophila* Mst ortholog, hippo, restricts growth and cell proliferation and promotes apoptosis. *Cell* 114, 457-467.

Hattula, K., Furuholm, J., Arffman, A., and Peranen, J. (2002). A Rab8-specific GDP/GTP exchange factor is involved in actin remodeling and polarized membrane transport. *Molecular biology of the cell* 13, 3268-3280.

Hauf, S., Biswas, A., Langeegger, M., Kawashima, S.A., Tsukahara, T., and Watanabe, Y. (2007). Aurora controls sister kinetochore mono-orientation and homolog bi-orientation in meiosis-I. *EMBO J* 26, 4475-4486.

Hauf, S., Cole, R.W., LaTerra, S., Zimmer, C., Schnapp, G., Walter, R., Heckel, A., van Meel, J., Rieder, C.L., and Peters, J.M. (2003). The small molecule Hesperadin reveals a role for Aurora B in correcting kinetochore-microtubule attachment and in maintaining the spindle assembly checkpoint. *J Cell Biol* 161, 281-294.

Heinis, C., Schmitt, S., Kindermann, M., Godin, G., and Johnsson, K. (2006). Evolving the substrate specificity of O6-alkylguanine-DNA alkyltransferase through loop insertion for applications in molecular imaging. *ACS Chem Biol* 1, 575-584.

Henchcliffe, C., and Beal, M.F. (2008). Mitochondrial biology and oxidative stress in Parkinson disease pathogenesis. *Nat Clin Pract Neurol* 4, 600-609.

Henderson, D.M., and Conner, S.D. (2007). A novel AAK1 splice variant functions at multiple steps of the endocytic pathway. *Molecular biology of the cell* 18, 2698-2706.

Hergovich, A., Stegert, M.R., Schmitz, D., and Hemmings, B.A. (2006). NDR kinases regulate essential cell processes from yeast to humans. *Nat Rev Mol Cell Biol* 7, 253-264.

Hertz, N.T., Wang, B.T., Allen, J.J., Zhang, C., Dar, A.C., Burlingame, A.L., and Shokat, K.M. (2010a). Chemical Genetic Approach for Kinase-Substrate Mapping by Covalent Capture of Thiophosphopeptides and Analysis by Mass Spectrometry. *Curr Prot Chem Biol* 2, 15-36.

Hertz, N.T., Wang, B.T., Allen, J.J., Zhang, C., Dar, A.C., Burlingame, A.L., and Shokat, K.M. (2010b). Chemical Genetic Approach for Kinase-Substrate Mapping by Covalent Capture of Thiophosphopeptides and Analysis by Mass Spectrometry. *Current Protocols in Chemical Biology* 2, 15-36.

Hindie, V., Stroba, A., Zhang, H., Lopez-Garcia, L.A., Idrissova, L., Zeuzem, S., Hirschberg, D., Schaeffer, F., Jorgensen, T.J., Engel, M., *et al.* (2009). Structure and

allosteric effects of low-molecular-weight activators on the protein kinase PDK1. *Nat Chem Biol* 5, 758-764.

Honda, R., Korner, R., and Nigg, E.A. (2003). Exploring the functional interactions between Aurora B, INCENP, and survivin in mitosis. *Mol Biol Cell* 14, 3325-3341.

Horgan, C.P., and McCaffrey, M.W. (2009). The dynamic Rab11-FIPs. *Biochem Soc Trans* 37, 1032-1036.

Hornbeck, P.V., Chabra, I., Kornhauser, J.M., Skrzypek, E., and Zhang, B. (2004). PhosphoSite: A bioinformatics resource dedicated to physiological protein phosphorylation. *Proteomics* 4, 1551-1561.

Horton, A.C., and Ehlers, M.D. (2003). Dual modes of endoplasmic reticulum-to-Golgi transport in dendrites revealed by live-cell imaging. *J Neurosci* 23, 6188-6199.

Horton, A.C., Racz, B., Monson, E.E., Lin, A.L., Weinberg, R.J., and Ehlers, M.D. (2005). Polarized secretory trafficking directs cargo for asymmetric dendrite growth and morphogenesis. *Neuron* 48, 757-771.

Hua, Z., Leal-Ortiz, S., Foss, S.M., Waites, C.L., Garner, C.C., Voglmaier, S.M., and Edwards, R.H. (2011). v-SNARE composition distinguishes synaptic vesicle pools. *Neuron* 71, 474-487.

Huang, J., Wu, S., Barrera, J., Matthews, K., and Pan, D. (2005). The Hippo signaling pathway coordinately regulates cell proliferation and apoptosis by inactivating Yorkie, the Drosophila Homolog of YAP. *Cell* 122, 421-434.

Hummer, S., and Mayer, T.U. (2009). Cdk1 negatively regulates midzone localization of the mitotic kinesin Mklp2 and the chromosomal passenger complex. *Curr Biol* 19, 607-612.

Ishii, Y., Hori, Y., Sakai, S., and Honma, Y. (2002). Control of differentiation and apoptosis of human myeloid leukemia cells by cytokinins and cytokinin nucleosides, plant redifferentiation-inducing hormones. *Cell Growth Differ* 13, 19-26.

Ishii, Y., Sakai, S., and Honma, Y. (2003). Cytokinin-induced differentiation of human myeloid leukemia HL-60 cells is associated with the formation of nucleotides, but not with incorporation into DNA or RNA. *Biochim Biophys Acta* 1643, 11-24.

Jansen, J.M., Wanless, A.G., Seidel, C.W., and Weiss, E.L. (2009). Cbk1 regulation of the RNA-binding protein Ssd1 integrates cell fate with translational control. *Curr Biol* 19, 2114-2120.

Johnson, E.O., Chang, K.H., de Pablo, Y., Ghosh, S., Mehta, R., Badve, S., and Shah, K. (2011). PHLDA1 is a crucial negative regulator and effector of Aurora A kinase in breast cancer. *Journal of cell science* 124, 2711-2722.

Jordan, M.A., and Wilson, L. (2004). Microtubules as a target for anticancer drugs. *Nat Rev Cancer* 4, 253-265.

Kettenbach, A.N., Schweppe, D.K., Faherty, B.K., Pechenick, D., Pletnev, A.A., and Gerber, S.A. (2011). Quantitative phosphoproteomics identifies substrates and functional modules of aurora and polo-like kinase activities in mitotic cells. *Sci Signal* 4, rs5.

Kissil, J.L., Feinstein, E., Cohen, O., Jones, P.A., Tsai, Y.C., Knowles, M.A., Eydmann, M.E., and Kimchi, A. (1997). DAP-kinase loss of expression in various carcinoma and B-cell lymphoma cell lines: possible implications for role as tumor suppressor gene. *Oncogene* 15, 403-407.

Kitada, T., Asakawa, S., Hattori, N., Matsumine, H., Yamamura, Y., Minoshima, S., Yokochi, M., Mizuno, Y., and Shimizu, N. (1998). Mutations in the parkin gene cause autosomal recessive juvenile parkinsonism. *Nature* *392*, 605-608.

Klinkenberg, M., Thurow, N., Gispert, S., Ricciardi, F., Eich, F., Prehn, J.H., Auburger, G., and Kogel, D. (2010). Enhanced vulnerability of PARK6 patient skin fibroblasts to apoptosis induced by proteasomal stress. *Neuroscience* *166*, 422-434.

Koike-Kumagai, M., Yasunaga, K., Morikawa, R., Kanamori, T., and Emoto, K. (2009). The target of rapamycin complex 2 controls dendritic tiling of *Drosophila* sensory neurons through the Tricornered kinase signalling pathway. *Embo J* *28*, 3879-3892.

Kondapalli, C., Kazlauskaitė, A., Zhang, N., Woodroof, H.I., Campbell, D.G., Gourlay, R., Burchell, L., Walden, H., Macartney, T.J., Deak, M., *et al.* (2012). PINK1 is activated by mitochondrial membrane potential depolarization and stimulates Parkin E3 ligase activity by phosphorylating Serine 65. *Open Biol* *2*, 120080.

Konur, S., and Yuste, R. (2004). Developmental regulation of spine and filopodial motility in primary visual cortex: reduced effects of activity and sensory deprivation. *Journal of neurobiology* *59*, 236-246.

Kornberg, A., Lieberman, I., and Simms, E.S. (1955). Enzymatic synthesis of purine nucleotides. *J Biol Chem* *215*, 417-427.

Krishnan, P., Fu, Q., Lam, W., Liou, J.Y., Dutschman, G., and Cheng, Y.C. (2002). Phosphorylation of pyrimidine deoxynucleoside analog diphosphates: selective phosphorylation of L-nucleoside analog diphosphates by 3-phosphoglycerate kinase. *J Biol Chem* *277*, 5453-5459.

Kulkarni, R.N., Bruning, J.C., Winnay, J.N., Postic, C., Magnuson, M.A., and Kahn, C.R. (1999). Tissue-specific knockout of the insulin receptor in pancreatic beta cells creates an insulin secretory defect similar to that in type 2 diabetes. *Cell* *96*, 329-339.

Kuo, C.T., Zhu, S., Younger, S., Jan, L.Y., and Jan, Y.N. (2006). Identification of E2/E3 ubiquitinating enzymes and caspase activity regulating *Drosophila* sensory neuron dendrite pruning. *Neuron* *51*, 283-290.

Kurischko, C., Kuravi, V.K., Wannissorn, N., Nazarov, P.A., Husain, M., Zhang, C., Shokat, K.M., McCaffery, J.M., and Luca, F.C. (2008). The yeast LATS/Ndr kinase Cbk1 regulates growth via Golgi-dependent glycosylation and secretion. *Molecular biology of the cell* *19*, 5559-5578.

Kwon, S.W., Kim, S.C., Jaunbergs, J., Falck, J.R., and Zhao, Y. (2003). Selective enrichment of thiophosphorylated polypeptides as a tool for the analysis of protein phosphorylation. *Mol Cell Proteomics* *2*, 242-247.

Lang, A.E., and Lozano, A.M. (1998). Parkinson's disease. First of two parts. *N Engl J Med* *339*, 1044-1053.

Lens, S.M., Voest, E.E., and Medema, R.H. (2010). Shared and separate functions of polo-like kinases and aurora kinases in cancer. *Nat Rev Cancer* *10*, 825-841.

Lens, S.M., Wolthuis, R.M., Klompaker, R., Kauw, J., Agami, R., Brummelkamp, T., Kops, G., and Medema, R.H. (2003). Survivin is required for a sustained spindle checkpoint arrest in response to lack of tension. *Embo J* *22*, 2934-2947.

Li, Z., Jo, J., Jia, J.M., Lo, S.C., Whitcomb, D.J., Jiao, S., Cho, K., and Sheng, M. (2010). Caspase-3 activation via mitochondria is required for long-term depression and AMPA receptor internalization. *Cell* *141*, 859-871.

Lieberman, I., Kornberg, A., and Simms, E.S. (1955a). Enzymatic synthesis of nucleoside diphosphates and triphosphates. *J Biol Chem* *215*, 429-440.

Lieberman, I., Kornberg, A., and Simms, E.S. (1955b). Enzymatic synthesis of pyrimidine nucleotides; orotidine-5'-phosphate and uridine-5'-phosphate. *J Biol Chem* *215*, 403-451.

Liu, Y., Shah, K., Yang, F., Witucki, L., and Shokat, K.M. (1998). A molecular gate which controls unnatural ATP analogue recognition by the tyrosine kinase v-Src. *Bioorg Med Chem* *6*, 1219-1226.

MacVicar, B.A., and Thompson, R.J. (2010). Non-junction functions of pannexin-1 channels. *Trends in neurosciences* *33*, 93-102.

Manning, G., Whyte, D.B., Martinez, R., Hunter, T., and Sudarsanam, S. (2002). The protein kinase complement of the human genome. *Science* *298*, 1912-1934.

Matsuzaki, M., Ellis-Davies, G.C., Nemoto, T., Miyashita, Y., Iino, M., and Kasai, H. (2001). Dendritic spine geometry is critical for AMPA receptor expression in hippocampal CA1 pyramidal neurons. *Nature neuroscience* *4*, 1086-1092.

Mazanka, E., Alexander, J., Yeh, B.J., Charoenpong, P., Lowery, D.M., Yaffe, M., and Weiss, E.L. (2008). The NDR/LATS family kinase Cbk1 directly controls transcriptional asymmetry. *PLoS Biol* *6*, e203.

McNiven, M.A., and Thompson, H.M. (2006). Vesicle formation at the plasma membrane and trans-Golgi network: the same but different. *Science* *313*, 1591-1594.

Meissner, C., Lorenz, H., Weihofen, A., Selkoe, D.J., and Lemberg, M.K. (2011). The mitochondrial intramembrane protease PARL cleaves human Pink1 to regulate Pink1 trafficking. *J Neurochem* *117*, 856-867.

Merrick, K.A., Wohlbold, L., Zhang, C., Allen, J.J., Horiuchi, D., Huskey, N.E., Goga, A., Shokat, K.M., and Fisher, R.P. (2011). Switching Cdk2 on or off with small molecules to reveal requirements in human cell proliferation. *Mol Cell* *42*, 624-636.

Millward, T.A., Hess, D., and Hemmings, B.A. (1999). Ndr protein kinase is regulated by phosphorylation on two conserved sequence motifs. *The Journal of biological chemistry* *274*, 33847-33850.

Minoshima, Y., Kawashima, T., Hirose, K., Tonozuka, Y., Kawajiri, A., Bao, Y.C., Deng, X., Tatsuka, M., Narumiya, S., May, W.S., Jr., *et al.* (2003). Phosphorylation by aurora B converts MgcRacGAP to a RhoGAP during cytokinesis. *Dev Cell* *4*, 549-560.

Monaco, L., Kolthur-Seetharam, U., Loury, R., Murcia, J.M., de Murcia, G., and Sassone-Corsi, P. (2005). Inhibition of Aurora-B kinase activity by poly(ADP-ribose)ylation in response to DNA damage. *Proc Natl Acad Sci U S A* *102*, 14244-14248.

Murata-Hori, M., and Wang, Y.L. (2002). The kinase activity of aurora B is required for kinetochore-microtubule interactions during mitosis. *Curr Biol* *12*, 894-899.

Nakamura, K., Nemani, V.M., Azarbal, F., Skibinski, G., Levy, J.M., Egami, K., Munishkina, L., Zhang, J., Gardner, B., Wakabayashi, J., *et al.* (2011). Direct membrane association drives mitochondrial fission by the Parkinson disease-associated protein alpha-synuclein. *J Biol Chem* *286*, 20710-20726.

Narendra, D., Tanaka, A., Suen, D.F., and Youle, R.J. (2008). Parkin is recruited selectively to impaired mitochondria and promotes their autophagy. *J Cell Biol* *183*, 795-803.

Narendra, D.P., Jin, S.M., Tanaka, A., Suen, D.F., Gautier, C.A., Shen, J., Cookson, M.R., and Youle, R.J. (2010). PINK1 is selectively stabilized on impaired mitochondria to activate Parkin. *PLoS Biol* 8, e1000298.

Nelson, B., Kurischko, C., Horecka, J., Mody, M., Nair, P., Pratt, L., Zougman, A., McBroom, L.D., Hughes, T.R., Boone, C., *et al.* (2003). RAM: a conserved signaling network that regulates Ace2p transcriptional activity and polarized morphogenesis. *Molecular biology of the cell* 14, 3782-3803.

Nemani, V.M., Lu, W., Berge, V., Nakamura, K., Onoa, B., Lee, M.K., Chaudhry, F.A., Nicoll, R.A., and Edwards, R.H. (2010). Increased expression of alpha-synuclein reduces neurotransmitter release by inhibiting synaptic vesicle reclustering after endocytosis. *Neuron* 65, 66-79.

Niefind, K., Putter, M., Guerra, B., Issinger, O.G., and Schomburg, D. (1999). GTP plus water mimic ATP in the active site of protein kinase CK2. *Nat Struct Biol* 6, 1100-1103.

Nishizuka, Y. (1984). The role of protein kinase C in cell surface signal transduction and tumour promotion. *Nature* 308, 693-698.

Nunnari, J., and Suomalainen, A. (2012). Mitochondria: in sickness and in health. *Cell* 148, 1145-1159.

Olsen, J.V., Blagoev, B., Gnäd, F., Macek, B., Kumar, C., Mortensen, P., and Mann, M. (2006). Global, in vivo, and site-specific phosphorylation dynamics in signaling networks. *Cell* 127, 635-648.

Otsu, N. (1979). A Threshold Selection Method from Gray-Level Histograms. *EEE Transactions on Systems, Man and Cybernetics SMC-9*, 62-66.

Parkin, D.W., Leung, H.B., and Schramm, V.L. (1984). Synthesis of nucleotides with specific radiolabels in ribose. Primary 14C and secondary 3H kinetic isotope effects on acid-catalyzed glycosidic bond hydrolysis of AMP, dAMP, and inosine. *J Biol Chem* 259, 9411-9417.

Perrera, C., Colombo, R., Valsasina, B., Carpinelli, P., Troiani, S., Modugno, M., Gianellini, L., Cappella, P., Isacchi, A., Moll, J., *et al.* (2010). Identification of Myb-binding protein 1A (MYBBP1A) as a novel substrate for aurora B kinase. *J Biol Chem* 285, 11775-11785.

Petit, A., Kawarai, T., Paitel, E., Sanjo, N., Maj, M., Scheid, M., Chen, F., Gu, Y., Hasegawa, H., Salehi-Rad, S., *et al.* (2005). Wild-type PINK1 prevents basal and induced neuronal apoptosis, a protective effect abrogated by Parkinson disease-related mutations. *J Biol Chem* 280, 34025-34032.

Pinsky, B.A., Kung, C., Shokat, K.M., and Biggins, S. (2006). The Ipl1-Aurora protein kinase activates the spindle checkpoint by creating unattached kinetochores. *Nat Cell Biol* 8, 78-83.

Postnikov, Y., and Bustin, M. (2010). Regulation of chromatin structure and function by HMGN proteins. *Biochim Biophys Acta* 1799, 62-68.

Pridgeon, J.W., Olzmann, J.A., Chin, L.S., and Li, L. (2007). PINK1 Protects against Oxidative Stress by Phosphorylating Mitochondrial Chaperone TRAP1. *PLoS Biol* 5, e172.

Qiao, Y., Molina, H., Pandey, A., Zhang, J., and Cole, P.A. (2006). Chemical rescue of a mutant enzyme in living cells. *Science* 311, 1293-1297.

Ray, A.S., Vela, J.E., Olson, L., and Fridland, A. (2004). Effective metabolism and long intracellular half life of the anti-hepatitis B agent adefovir in hepatic cells. *Biochem Pharmacol* 68, 1825-1831.

Robinson, M.S. (2004). Adaptable adaptors for coated vesicles. *Trends Cell Biol* 14, 167-174.

Rochman, M., Postnikov, Y., Correll, S., Malicet, C., Wincovitch, S., Karpova, T.S., McNally, J.G., Wu, X., Bubunenko, N.A., Grigoryev, S., *et al.* (2009). The interaction of NSBP1/HMG5 with nucleosomes in euchromatin counteracts linker histone-mediated chromatin compaction and modulates transcription. *Mol Cell* 35, 642-656.

Ruchaud, S., Carmena, M., and Earnshaw, W.C. (2007). Chromosomal passengers: conducting cell division. *Nat Rev Mol Cell Biol* 8, 798-812.

Rugarli, E.I., and Langer, T. (2012). Mitochondrial quality control: a matter of life and death for neurons. *EMBO J* 31, 1336-1349.

Sabbattini, P., Canzonetta, C., Sjoberg, M., Nikic, S., Georgiou, A., Kembball-Cook, G., Auner, H.W., and Dillon, N. (2007). A novel role for the Aurora B kinase in epigenetic marking of silent chromatin in differentiated postmitotic cells. *EMBO J* 26, 4657-4669.

Samaranch, L., Lorenzo-Betancor, O., Arbelo, J.M., Ferrer, I., Lorenzo, E., Irigoyen, J., Pastor, M.A., Marrero, C., Isla, C., Herrera-Henriquez, J., *et al.* (2010). PINK1-linked parkinsonism is associated with Lewy body pathology. *Brain* 133, 1128-1142.

Sekiya-Kawasaki, M., Groen, A.C., Cope, M.J., Kaksonen, M., Watson, H.A., Zhang, C., Shokat, K.M., Wendland, B., McDonald, K.L., McCaffery, J.M., *et al.* (2003). Dynamic phosphoregulation of the cortical actin cytoskeleton and endocytic machinery revealed by real-time chemical genetic analysis. *J Cell Biol* 162, 765-772.

Sessa, F., Mapelli, M., Ciferri, C., Tarricone, C., Areces, L.B., Schneider, T.R., Stukenberg, P.T., and Musacchio, A. (2005). Mechanism of Aurora B activation by INCENP and inhibition by hesperadin. *Mol Cell* 18, 379-391.

Shah, K., Liu, Y., Deirmengian, C., and Shokat, K.M. (1997). Engineering unnatural nucleotide specificity for Rous sarcoma virus tyrosine kinase to uniquely label its direct substrates. *Proc Natl Acad Sci U S A* 94, 3565-3570.

Shetty, R.S., Gallagher, C.S., Chen, Y.T., Hims, M.M., Mull, J., Leyne, M., Pickel, J., Kwok, D., and Slaugenhaupt, S.A. (2011). Specific correction of a splice defect in brain by nutritional supplementation. *Hum Mol Genet* 20, 4093-4101.

Shin, J.H., Ko, H.S., Kang, H., Lee, Y., Lee, Y.I., Pletinkova, O., Troconso, J.C., Dawson, V.L., and Dawson, T.M. (2011). PARIS (ZNF746) repression of PGC-1alpha contributes to neurodegeneration in Parkinson's disease. *Cell* 144, 689-702.

Song, S., Jang, S., Park, J., Bang, S., Choi, S., Kwon, K.Y., Zhuang, X., Kim, E., and Chung, J. (2013). Characterization of phosphatase and tensin homolog (PTEN)-induced putative kinase 1 (PINK1) mutations associated with Parkinson's disease in mammalian cells and *Drosophila*. *J Biol Chem*.

St John, M.A., Tao, W., Fei, X., Fukumoto, R., Carcangiu, M.L., Brownstein, D.G., Parlow, A.F., McGrath, J., and Xu, T. (1999). Mice deficient of Lats1 develop soft-tissue sarcomas, ovarian tumours and pituitary dysfunction. *Nat Genet* 21, 182-186.

Stegert, M.R., Hergovich, A., Tamaskovic, R., Bichsel, S.J., and Hemmings, B.A. (2005). Regulation of NDR protein kinase by hydrophobic motif phosphorylation mediated by the mammalian Ste20-like kinase MST3. *Mol Cell Biol* 25, 11019-11029.

Stegert, M.R., Tamaskovic, R., Bichsel, S.J., Hergovich, A., and Hemmings, B.A. (2004). Regulation of NDR2 protein kinase by multi-site phosphorylation and the S100B calcium-binding protein. *The Journal of biological chemistry* 279, 23806-23812.

Stenmark, H. (2009). Rab GTPases as coordinators of vesicle traffic. *Nat Rev Mol Cell Biol* 10, 513-525.

Stork, O., Zhdanov, A., Kudersky, A., Yoshikawa, T., Obata, K., and Pape, H.C. (2004). Neuronal functions of the novel serine/threonine kinase Ndr2. *The Journal of biological chemistry* 279, 45773-45781.

Subramanian, M., Gonzalez, R.W., Patil, H., Ueda, T., Lim, J.H., Kraemer, K.H., Bustin, M., and Bergel, M. (2009). The nucleosome-binding protein HMGN2 modulates global genome repair. *FEBS J* 276, 6646-6657.

Toshima, J., Toshima, J.Y., Martin, A.C., and Drubin, D.G. (2005). Phosphoregulation of Arp2/3-dependent actin assembly during receptor-mediated endocytosis. *Nature cell biology* 7, 246-254.

Traub, L.M. (2009). Tickets to ride: selecting cargo for clathrin-regulated internalization. *Nat Rev Mol Cell Biol* 10, 583-596.

Trinidad, J.C., Thalhammer, A., Specht, C.G., Lynn, A.J., Baker, P.R., Schoepfer, R., and Burlingame, A.L. (2008). Quantitative analysis of synaptic phosphorylation and protein expression. *Mol Cell Proteomics* 7, 684-696.

Ubersax, J.A., Woodbury, E.L., Quang, P.N., Paraz, M., Blethrow, J.D., Shah, K., Shokat, K.M., and Morgan, D.O. (2003). Targets of the cyclin-dependent kinase Cdk1. *Nature* 425, 859-864.

Ueda, T., Catez, F., Gerlitz, G., and Bustin, M. (2008). Delineation of the protein module that anchors HMGN proteins to nucleosomes in the chromatin of living cells. *Mol Cell Biol* 28, 2872-2883.

Ultanir, S.K., and Hertz, N. T., Li, G., Ge, W.P., Burlingame, A.L., Pleasure, S.J., Shokat, K.M., Jan, L.Y., and Jan, Y.N. (2012). Chemical genetic identification of NDR1/2 kinase substrates AAK1 and Rabin8 Uncovers their roles in dendrite arborization and spine development. *Neuron* 73, 1127-1142.

Valente, E.M., Abou-Sleiman, P.M., Caputo, V., Muqit, M.M., Harvey, K., Gispert, S., Ali, Z., Del Turco, D., Bentivoglio, A.R., Healy, D.G., *et al.* (2004). Hereditary early-onset Parkinson's disease caused by mutations in PINK1. *Science* 304, 1158-1160.

Vela, J.E., Olson, L.Y., Huang, A., Fridland, A., and Ray, A.S. (2007). Simultaneous quantitation of the nucleotide analog adefovir, its phosphorylated anabolites and 2'-deoxyadenosine triphosphate by ion-pairing LC/MS/MS. *J Chromatogr B Analyt Technol Biomed Life Sci* 848, 335-343.

Vichalkovski, A., Gresko, E., Cornils, H., Hergovich, A., Schmitz, D., and Hemmings, B.A. (2008). NDR kinase is activated by RASSF1A/MST1 in response to Fas receptor stimulation and promotes apoptosis. *Curr Biol* 18, 1889-1895.

Wang, H.L., Chou, A.H., Yeh, T.H., Li, A.H., Chen, Y.L., Kuo, Y.L., Tsai, S.R., and Yu, S.T. (2007). PINK1 mutants associated with recessive Parkinson's disease are defective in inhibiting mitochondrial release of cytochrome c. *Neurobiol Dis* 28, 216-226.

Wang, X., Winter, D., Ashrafi, G., Schlehe, J., Wong, Y.L., Selkoe, D., Rice, S., Steen, J., LaVoie, M.J., and Schwarz, T.L. (2011). PINK1 and Parkin target Miro for phosphorylation and degradation to arrest mitochondrial motility. *Cell* 147, 893-906.

Wang, Z., Edwards, J.G., Riley, N., Provance, D.W., Jr., Karcher, R., Li, X.D., Davison, I.G., Ikebe, M., Mercer, J.A., Kauer, J.A., *et al.* (2008). Myosin Vb mobilizes recycling endosomes and AMPA receptors for postsynaptic plasticity. *Cell* *135*, 535-548.

Wei, L., Gao, X., Warne, R., Hao, X., Bussiere, D., Gu, X.J., Uno, T., and Liu, Y. (2010). Design and synthesis of benzoazepin-2-one analogs as allosteric binders targeting the PIF pocket of PDK1. *Bioorg Med Chem Lett* *20*, 3897-3902.

Weiss, W.A., Taylor, S.S., and Shokat, K.M. (2007). Recognizing and exploiting differences between RNAi and small-molecule inhibitors. *Nat Chem Biol* *3*, 739-744.

Wu, S., Huang, J., Dong, J., and Pan, D. (2003). hippo encodes a Ste-20 family protein kinase that restricts cell proliferation and promotes apoptosis in conjunction with salvador and warts. *Cell* *114*, 445-456.

Xiong, H., Wang, D., Chen, L., Choo, Y.S., Ma, H., Tang, C., Xia, K., Jiang, W., Ronai, Z., Zhuang, X., *et al.* (2009). Parkin, PINK1, and DJ-1 form a ubiquitin E3 ligase complex promoting unfolded protein degradation. *J Clin Invest* *119*, 650-660.

Ye, B., Zhang, Y., Song, W., Younger, S.H., Jan, L.Y., and Jan, Y.N. (2007). Growing dendrites and axons differ in their reliance on the secretory pathway. *Cell* *130*, 717-729.

Ye, B., Zhang, Y.W., Jan, L.Y., and Jan, Y.N. (2006). The secretory pathway and neuron polarization. *J Neurosci* *26*, 10631-10632.

Youle, R.J., and Narendra, D.P. (2011). Mechanisms of mitophagy. *Nat Rev Mol Cell Biol* *12*, 9-14.

Yuste, R., and Bonhoeffer, T. (2004). Genesis of dendritic spines: insights from ultrastructural and imaging studies. *Nature reviews* *5*, 24-34.

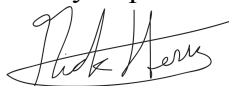
Zhang, C., Kenski, D.M., Paulson, J.L., Bonshtien, A., Sessa, G., Cross, J.V., Templeton, D.J., and Shokat, K.M. (2005). A second-site suppressor strategy for chemical genetic analysis of diverse protein kinases. *Nat Methods* *2*, 435-441.

Zhou, Z.R., Zhang, Y.H., Liu, S., Song, A.X., and Hu, H.Y. (2012). Length of the active-site crossover loop defines the substrate specificity of ubiquitin C-terminal hydrolases for ubiquitin chains. *Biochem J* *441*, 143-149.

Publishing Agreement

It is the policy of the University to encourage the distribution of all theses, dissertations, and manuscripts. Copies of all UCSF theses, dissertations, and manuscripts will be routed to the library via the Graduate Division. The library will make all theses, dissertations, and manuscripts accessible to the public and will preserve these to the best of their abilities, in perpetuity.

I hereby grant permission to the Graduate Division of the University of California, San Francisco to release copies of my thesis, dissertation, or manuscript to the Campus Library to provide access and preservation, in whole or in part, in perpetuity.



September 8, 2013

Author Signature

Date